Life of Photosynthetic Complexes in the Cyanobacterium *Synechocystis* sp. PCC 6803

by

Cheng I Daniel Yao

A Dissertation Presented in Partial Fulfillment
of the Requirements for the Degree
Doctor of Philosophy

Approved April 2011 by the
Graduate Supervisory Committee:

Wim Vermaas, Chair
Petra Fromme
Robert Roberson
Andrew Webber

ARIZONA STATE UNIVERSITY

May 2011

ABSTRACT

The cyanobacterium *Synechocystis* sp. PCC 6803 performs oxygenic photosynthesis. Light energy conversion in photosynthesis takes place in photosystem I (PSI) and photosystem II (PSII) that contain chlorophyll, which absorbs light energy that is utilized as a driving force for photosynthesis. However, excess light energy may lead to formation of reactive oxygen species that cause damage to photosynthetic complexes, which subsequently need repair or replacement. To gain insight in the degradation/biogenesis dynamics of the photosystems, the lifetimes of photosynthetic proteins and chlorophyll were determined by a combined stable-isotope (^{15}N) and mass spectrometry method. The lifetimes of PSII and PSI proteins ranged from 1-33 and 30-75 hours, respectively. Interestingly, chlorophyll had longer lifetimes than the chlorophyll-binding proteins in these photosystems. Therefore, photosynthetic proteins turn over and are replaced independently from each other, and chlorophyll is recycled from the damaged chlorophyll-binding proteins.

In *Synechocystis*, there are five small Cab-like proteins (SCPs: ScpA-E) that share chlorophyll *a/b*-binding motifs with LHC proteins in plants. SCPs appear to transiently bind chlorophyll and to regulate chlorophyll biosynthesis. In this study, the association of ScpB, ScpC, and ScpD with damaged and repaired PSII was demonstrated. Moreover, in a mutant lacking SCPs, most PSII protein lifetimes were unaffected but the lifetime of chlorophyll was decreased, and one of the nascent PSII complexes was missing. SCPs appear to bind PSII chlorophyll while PSII is repaired, and SCPs stabilize nascent PSII complexes. Furthermore, aminolevulinic acid biosynthesis, an early step of chlorophyll biosynthesis, was impaired in the absence of SCPs, so that the amount of chlorophyll in the cells was reduced.

Finally, a deletion mutation was introduced into the *sll1906* gene, encoding a member of the putative bacteriochlorophyll delivery (BCD) protein family. The Sll1906 sequence contains possible chlorophyll-binding sites, and its homolog in purple bacteria functions in proper assembly of light-harvesting complexes. However, the *sll1906* deletion did not affect chlorophyll degradation/biosynthesis and photosystem assembly. Other (parallel) pathways may exist that may fully compensate for the lack of Sll1906. This study has highlighted the dynamics of photosynthetic complexes in their biogenesis and turnover and the coordination between synthesis of chlorophyll and photosynthetic proteins.

DEDICATION

This dissertation is dedicated to my parents, An-Ni Yao and Sheng –Long Yao, and my brother, Cheng-Yu Yao,

for their support throughout all the years during my Doctoral work.

ACKNOWLEDGMENTS

Gratitude goes to my advisor Wim Vermaas

and my Committee Members Petra Fromme, Robert Roberson, and Andrew Webber.

I also thank my friends and colleagues for their supports in many aspects,

Dmitri, Sawsan, Bing, Hatem, Miguel, Christoph, Hongliang, Shuqin,

Dan Brune, Dan Jenk, Cathy, Yifei, Vicki, Ipsita, Raul, Wei, and Srini.

Special thanks to my mentor and host in Sweden, Christiane Funk, for her scientific advice.

TABLE OF CONTENTS

LIST OF TABLES

LIST OF FIGURES

Figure Page

LIST OF ABBREVIATIONS

ALA…… Aminolevulic acid

BCD……..……. Bacteriochlorophyll delivery

BN……... Blue native

Cab…….. Chlorophyll *a/b* binding protein

Cyt……. Cytochrome

DM…… β-dodecyl maltoside

DPOR…… Light-independent protochlorophyllide reductase

ETC……... Electron transfer chain

GluTR…… Glutamyl-tRNA reductase

HPLC…… High performance liquid chromatography

LAHG……..Light-activated heterotrophic growth

LHC…….Light-harvesting complex

LPOR…….. Light-dependent protochlorophyllide reductase

MALDI-TOF……...Matrix-assisted laser desorption ionization time-of-flight

MES…….. 2-[N-morpholino]ethanesulfonic acid

MS…… Mass spectrometry

OD_{730}……. Optical density at 730 nm

PAGE…… Polyacrylamide gel electrophoresis

PBG……... Porphobilinogen

POR……... Protochlorophyllide oxidoreductase

PSI……. Photosystem I

PSII…… Photosystem II

RC……. PSII reaction center-like complex

RC47……. PSII core complex lacking CP43

RCC1……. Monomeric PSII core complex

RCC2……. Dimeric PSII core complex

SDS……... Sodium dodecyl sulfate

SCPs……..…… Small Cab-like proteins

CHAPTER I. INTRODUCTION

About the cyanobacterium Synechocystis — Cyanobacteria, also called "blue-green algae", are photoautotrophic organisms capable of oxygenic photosynthesis similar to that in eukaryotic algae and plants. They are clearly separated from other bacteria, such as purple and green bacteria, because they utilize water as an electron donor for photosynthesis. Due to the ability to conduct oxygen-producing photosynthesis, it has generally been accepted that the ancestors of cyanobacteria in early stages of evolution gave rise to plastids in eukaryotes by endosymbiotic events. There are many properties, both in the structure and mechanism of photosynthesis, that are common to cyanobacteria, algae, and plants. Genetic engineering techniques facilitate studies of gene function and regulation and are applicable to cyanobacteria. Because of these factors, cyanobacteria are used as model organisms for studying photosynthesis in higher plants that have a more complex genetic system.

Synechocystis sp. PCC 6803, a member of coccus-shaped Chroococcales, is a unicellular cyanobacterium isolated from fresh water. It has been used as a model cyanobacterium in the study of photosynthesis because of two main advantages: (1) naturally transformable characteristics that permit foreign DNA to integrate into the *Synechocystis* genome by homologous recombination, and (2) the ability to perform heterotrophic growth that allows characterization of mutants that lack photosynthetic function. In 1996, *Synechocystis* sp. PCC 6803 was the first photosynthetic organism for which its entire genome sequence was determined (Kaneko *et al.*, 1996). With the DNA sequence information along with the advantages, *Synechocystis* has been studied extensively in the field of photosynthesis.

Photosystems in cyanobacteria — The signature of oxygenic photosynthesis is to extract electrons from water, producing protons and oxygen in the process. Light energy that is absorbed by chlorophylls in two pigment-binding protein complexes, photosystem I (PSI) and photosystem II (PSII), embedded in the thylakoid membrane, and by phycobilins in phycobilisomes at the periphery of the thylakoid membrane places the pigment molecules in their excited state. The excited state is transferred to an oxidizable chlorophyll in the reaction center. An electron is transferred to a nearby pigment, thereby putting into motion the light-driven electron transport chain. Then the oxidized pigment molecule is subsequently re-reduced. The electron transfer chain (ETC) in PSII consists of P680 (a special chlorophyll *a* molecule), pheophytin, plastoquinones and other components. The electron transfer is initiated with primary charge separation at P680, where the electron is extracted from, and the released electron travels along the ETC across the membrane. Oxidized P680 is re-reduced by an electron extracted from the water molecule via Tyr_z, a residue in the D1 protein (Barber, 2002). In PSI, the primary charge separation is initiated by the chlorophyll dimer P700, and electron acceptors include A_0 (Chl *a*), A_1 (phylloquinone) and F_x, F_A, and F_B, the Fe_4S_4 clusters. The electron is finally used in reduction of $NADP^+$ by ferredoxin-NADP reductase via ferredoxin. Oxidized P700 is recovered by receiving an electron from plastocyanin that carries the electron from cytochrome b_6f (cyt *b6f)* complexes. Overall, the electrons go through these two photosystem complexes via the ETC to form NADPH and to create a proton gradient that is utilized by ATP synthase to generate ATP.

The structures of both PSI and PSII have been studied in detail by several groups (Jordan *et al.*, 2001; Ferreira *et al.*, 2004; Loll *et al.*, 2005; Amunts *et al.*, 2007; Guskov *et al*., 2009). PSII in cyanobacteria consists of 20 protein subunits with 35 chlorophyll *a* molecules, 12 carotenoid molecules, 2 pheophytin molecules, 25 lipids, a heme molecule,

a chloride ion, and metal ions (Gustov *et al.*, 2007). The membrane-intrinsic part of PSII comprises the antenna proteins CP47 and CP43, the reaction center subunits D1 and D2, and 13 small subunits including cytochrome (cyt) *b*-559 (PsbE and PsbF). In addition, there are three extrinsic proteins (PsbO, PsbU, and PsbV) located at the lumenal side. The antenna proteins and reaction center proteins bind all 35 chlorophyll *a* molecules in PSII (Muh *et al.*, 2008). PSI complexes consist of 12 protein subunits and 127 cofactors including 96 chlorophylls, 2 phylloquinones, 3 Fe_4S_4 clusters, 22 carotenoids, and 4 lipids (Jordan *et al.*, 2001). The multi-protein complex is composed of nine intrinsic proteins including the two largest subunits among the photosynthetic proteins, PsaA and PsaB, and three cytosolic proteins (PsaC, PsaD, and PsaE).

Even though the PSI and PSII reaction center complexes are conserved in higher plants and cyanobacteria, their light-harvesting antennae are very different. Unlike higher plants that have integral membrane light-harvesting complexes (LHC) primarily consisting of LHC proteins containing three transmembrane helices and binding chlorophyll *a* and *b,* cyanobacteria possess water-soluble peripheral phycobilisomes as their primary light-harvesting antenna. These supramolecular complexes are primarily composed of phycobiliproteins that are covalently attached to phycobilins, open-chain tetrapyrroles derived from the heme biosynthesis pathway (Bryant, 1994). The absorption wavelengths of the phycobilins range from 565 nm (phycoerythrins), 575 nm (phycoerythrocyanins), 615 nm (phycocyanins) to 650 nm (allophycocyanins); *Synechocystis* possesses phycocyanins and allophycocyanins. The absorbed energy is transferred to the chlorophylls (absorption wavelength about 665 nm) in reaction center complexes by excitation transfer.

PSII biogenesis and repair — In oxygenic photosynthesis, PSII is easily damaged irreversibly by overexcitation; this leads to photoinhibition of PSII activity. In order to retain PSII homeostasis, PSII biogenesis and repair operate to maintain a level of functional PSII in the thylakoid membrane. The cyanobacterium *Synechocystis* sp. PCC 6803 has been used extensively to study PSII biogenesis and repair.

Upon construction and characterization of various PSII mutants lacking different sub-units of the PSII complex, a number of specific PSII sub-complexes in various PSII mutants are evidence of the stepwise assembly of PSII complexes in PSII biogenesis (Figure I-1). During PSII biogenesis, cytochrome *b-559* proteins (PsbE and PsbF) and D2 proteins (PsbD) together form a sub-complex (Komenda *et al*., 2004; Komenda *et al*., 2008). Then, this sub-complex is assembled with the pD1-PsbI sub-complex to become a PSII reaction center-like complex (RC) (Dobakova *et al.*, 2007; Komenda *et al*., 2008).

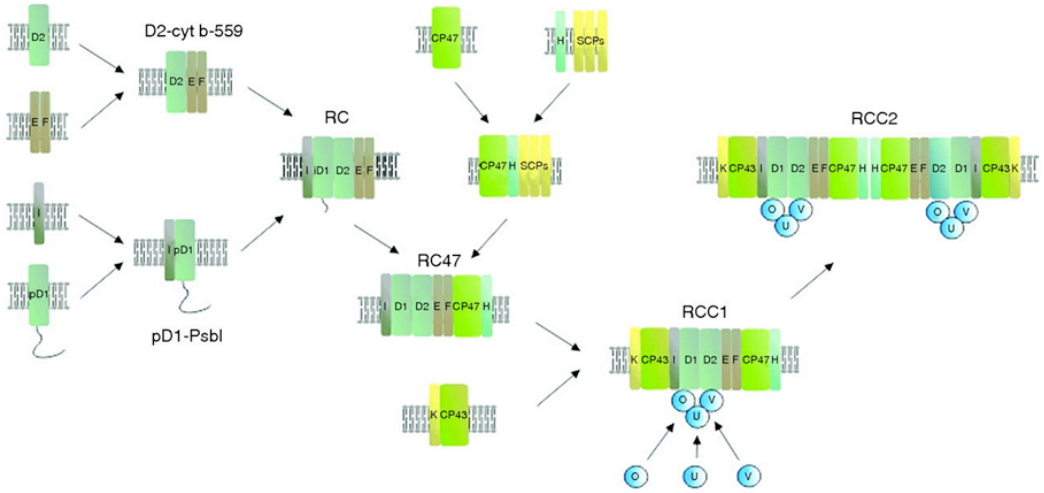

Figure I-1: Proposed scheme for assembly of the PSII complex in *Synechocystis* sp. PCC 6803. The PsbE, PsbF, PsbH, PsbI, and PsbK subunits and the extrinsic PsbO, PsbU, and PsbV subunits are designated by the appropriate upper case letter, and the small CAB-like proteins by SCPs. Cytochrome *b-559* (cyt b-559) is composed of a heterodimer of the PsbE and PsbF subunits. Types of PSII complex: RC, PSII reaction center-like complexes containing either mature D1, intermediate D1 (iD1) or precursor D1 (pD1) but lacking CP47 and CP43; RC47, PSII core complexes lacking CP43; RCC1, monomeric PSII core complex; RCC2, dimeric PSII core complex. (From Nixon *et al.*, 2010)

The D1 protein (PsbA) in the pD1-PsbI sub-complex has not yet been processed to its mature form; this precursor (pD1) carries a 16-residue extension at the C-terminus that is cleaved by CtpA to leave an intermediate eight-amino-acid extension as intermediate D1 (iD1) or to lead to mature D1 (total 344 amino acid residues) in this RC (Komenda *et al.* 2007; Inagaki *et al.*, 2001). The cleavage of the C-terminal extension of pD1 is required for assembly of a functional $CaMn_4$ cluster (Nixon *et al.*, 1992; Anbudurai *et al.*, 1994). Then, the RC-like sub-complex associates with the CP47 (PsbB)-PsbH sub-complex to form RC47. Subsequently, CP43 (PsbC) and PsbK are associated with RC47. PSII biogenesis is completed with assembly of the $CaMn_4$ cluster and attachment of the extrinsic subunits (PsbO, PsbU, and PsbV) of the oxygen-evolving complex to the PSII intrinsic protein complex. Using Blue Native/PAGE (BN/PAGE) of *Synechocystis* complexes, mature PSII is found as two forms: the PSII monomer (RCC1) and the PSII dimer (RCC2) (Herranen *et al.*, 2004).

The D1 protein is the main PSII subunit damaged during PSII photoinhibition. Rapid turnover of D1 has been observed *in vivo* in radioactive pulse-chase labeling experiments (Ohad *et al.*, 1984). In order to degrade the damaged D1 protein, partial disassembly of PSII may be required by detachment of the oxygen-evolving complex and CP43 may become loose from the PSII complex. The damaged D1 protein is likely to be degraded by members of the FtsH protease families. However, some of the FtsH proteases have shown to play a more crucial role in D1 degradation: impaired rates of D1 degradation were observed in mutants lacking FtsH2 in *Synechocystis* sp. PCC 6803 (Silva *et al.*, 2003; Komenda *et al.*, 2006) and FtsH2 and FtsH5 in *A. thaliana* (Bailey *et al.*, 2002; Kato *et al.*, 2009). After degradation of the damaged D1 protein, the replacement of the newly synthesized D1 protein occurs co-translationally into the RC47

complex (Zhang *et al.*, 1999). CP43 reattaches to form a PSII core complex, which then reassembles the $CaMn_4$ cluster and extrinsic proteins into a functional PSII.

During PSII assembly in the PSII biogenesis and repair cycle, there are PSII assembly factors that aid and/or regulate PSII assembly. These PSII assembly factors make sure that PSII assembles properly. For example, Ycf48 (Hcf136 in plants) binds to and stabilizes unassembled pD1 and aids formation of the PSII RC (Plucken *et al.*, 2002; Komenda *et al*., 2008). Psb27 is an assembly factor at the lumenal side that is mainly associated with CP47 and CP43 of monomeric PSII and non-oxygen-evolving PSII complexes and prevents binding of the oxygen-evolving complex (Kashino *et al.*, 2002; Nowaczyk *et al.*, 2006; Cormann *et al.*, 2009). Psb28 and Psb29 are important assembly factors for the CP47 protein (Dobakova *et al.*, 2009; Keren *et al.*, 2005).

Chlorophyll biosynthesis and its regulation — Chlorophyll is the most abundant cofactor in PSII complexes and may play important roles in synthesis and folding of the PSII chlorophyll-binding proteins and assembly of the PSII complexes. In a chlorophyll-depleted mutant, the PSII complex is hardly detected (Wu and Vermaas, 1995) and chlorophyll availability may be a major factor in the accumulation and assembly of PSII (Kuttkat *et al.*, 1997; Reinbothe *et al.*, 2006). The chlorophyll biosynthesis process has been studied by biochemical analyses, labeling experiments, and the use of numerous mutants lacking chlorophyll, and has been extensively reviewed (Beale, 1999; Grimm, 1999; Eckhardt *et al.,* 2004; Tanaka and Tanaka, 2007). The chlorophyll molecule is made up of chlorophyllide and phytyl groups. The phytyl tail derives from the isoprenoid biosynthetic pathway, through which also carotenoids are synthesized. Chlorophyllide, a macrocycle structure with Mg at the center, is synthesized through the tetrapyrrole biosynthesis pathway (Figure I-2).

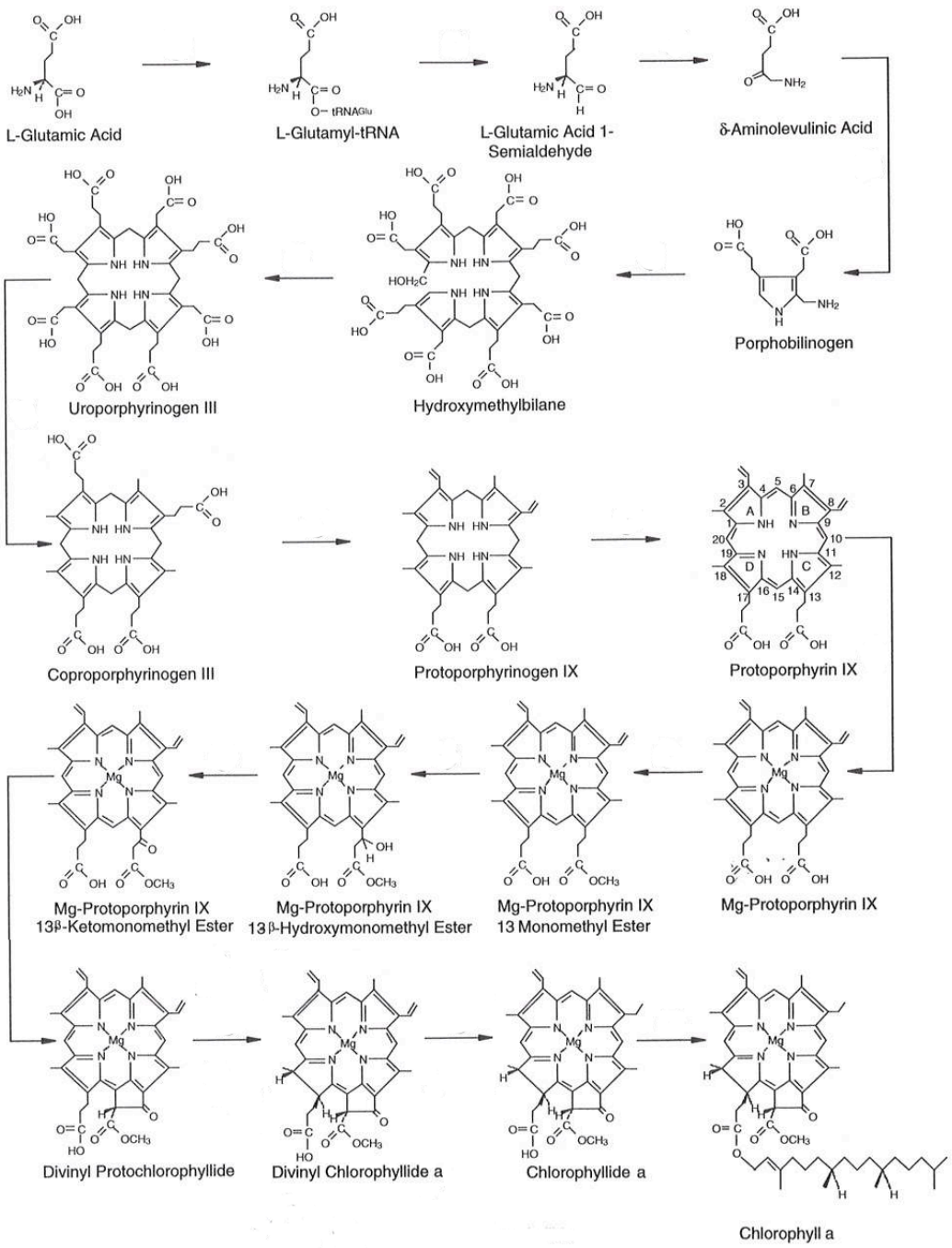

Figure I-2: Chlorophyll biosynthetic pathway. (From Blankenship, 2002)

The initial steps in tetrapyrrole biosynthesis, from the biosynthesis of 5-aminolevulinic acid (ALA) to protoporphyrinogen IX, take place in the cytosol or stroma of the plastid in plants, whereas the subsequent steps are membrane-bound (Joyard *et al.*, 2009; Mochizuki *et al.*, 2010). ALA is the first major intermediate in the tetrapyrrole biosynthetic pathway and its synthesis occurs in three enzymatic steps from glutamate (the C_5-pathway) (Beale, 1999). Glutamyl-tRNA synthetase ligates glutamate with $tRNA_{Glu}$. The reaction is followed by the one catalyzed by the glutamyl-tRNA reductase (GluTR) that reduces the carboxyl group of glutamyl-tRNA to produce glutamate-1-semialdehyde. Subsequently, glutamate-1-semialdehyde is transaminated by glutamate-1-semialdehyde aminotransferase to form ALA. ALA is a universal precursor of tetrapyrrole biosynthesis in all organisms, but this ALA biosynthetic pathway is only present in plants, algae, most bacteria including cyanobacteria, and archaea. The other eukaryotic organisms and some bacteria including non-sulfur purple bacteria have an alternative pathway (Shemin pathway) to synthesize ALA by condensation of succinyl-CoA with glycine (Mayer and Beale, 1992).

The enzymatic reactions converting ALA to protoporphyrin IX start with condensation of two ALA molecules to form a pyrrole molecule, porphobilinogen (PBG). Subsequently, four PBGs are polymerized and ligated to form the first closed tetrapyrrole ring, uroporphyrinogen III. Protoporphyrin IX is synthesized from oxidation of protoporphyrinogen IX derived from a series of decarboxylations of uroporphyrinogen III. Uroporphyrinogen III also can be utilized to produce vitamin B and siroheme via the siroheme biosynthetic branch.

Protoporphyrin IX can incorporate either Mg^{2+} or Fe^{2+}, leading molecules into the chlorophyll branch and heme branch of the tetrapyrrole biosynthesis pathway, respectively (Vavilin and Vermaas, 2002; Tanaka and Tanaka, 2007). The first step of the

chlorophyll branch is catalyzed by Mg-chelatase, a heterotrimer of three subunits, ChlH, ChlI, and ChlD, that inserts Mg^{2+} into protoporphyrin. This reaction requires ATP hydrolysis. The next couple of reactions are catalyzed by methyltransferase and cyclase to produce protochlorophyllide. Reduction of protochlorophyllide to divinyl-chlorophyllide is performed by protochlorophyllide oxidoreductase (POR). There are two types of structurally unrelated PORs, the light-dependent protochlorophyllide reductase (LPOR) and light-independent protochlorophyllide reductase (DPOR). LPOR contains only one protein subunit without a cofactor, and NADPH is required for the reaction. DPOR consists of three subunits, ChlL, ChlN, and ChlB, whose amino acid sequences show significant similarities to those of NifH, NifD, and NifK in nitrogenase, respectively (Burke *et al.*, 1993). The enzyme carries two FeS clusters, and the reduction reaction is ATP-dependent (Sarma *et al.*, 2008; Muraki *et al.*, 2010). Due to lack of DPOR in angiosperms, protochlorophyllide is accumulated when angiosperm seedlings are grown in the dark (Griffiths, 1975). The 8-vinyl group of the B ring of divinyl-chlorophyllide is reduced by divinylchlorophyllide *a* reductase to form chlorophyllide. The final step of chlorophyll *a* synthesis is to esterify chlorophyllide with phytyl pyrophosphate by chlorophyll synthase.

In order to produce a sufficient amount of chlorophyll to meet the demands of the chlorophyll-binding proteins but at the same time to prevent accumulation of excess chlorophyll and its precursors in the cell, the chlorophyll biosynthetic pathway is highly regulated. Glutamyl-tRNA reduction by GluTR in ALA synthesis is a most important regulation point in the tetrapyrrole pathway (Beale, 1990). This regulation point is reasonable because of most of the tetrapyrrole intermediates may cause damage to the cells in the light and the presence of oxygen. Controlling the GluTR activity is mainly achieved through feedback regulation by the end products such as heme, and Mg-

protoporphyrin IX and its later intermediates (Rieble and Beale, 1991). FLU has been identified as a regulatory protein to repress GluTR activity as protochlorophyllide is accumulated in higher plants (Meskauskiene *et al.*, 2001). The other regulation step is at the major branchpoint where protoporphyrin IX is directed toward either the chlorophyll or heme branches. The concentration of substrates for the formation of Mg-protoporphyrin IX such as ATP and Mg^{2+} affects Mg-chelatase activity. Also, GUN4, a regulatory protein in plants, functions in enhancing substrate binding and/or product release of Mg-chelatase (Adhikari *et al.*, 2009; Peter and Grimm, 2009). For the heme branch, an increase in ferrochelatase activity resulting in increased production of heme could inhibit synthesis of ALA (Srivastava and Beale, 2005; Beck and Grimm, 2006). However, the deletion of the C-terminal extension of ferrochelatase that contains one transmembrane helix with a CAB domain (called ScpA in *Synechocystis*) reduces its activity, which results in upregulated ALA synthesis (Sobotka *et al.*, 2008).

Chlorophyll — The chlorophyll *a* molecule contains five rings (A through E), and is classified as a chlorin rather than a porphyrin because of the reduction of ring D by protochlorophyllide reductase (Figure I-3). Chlorophyll *a* has maximal absorption at 430 (Soret), 578 (Q_x), and 662 (Q_y) nm in diethyl ether and fluoresces at 670 nm (Blankenship, 2002). All eukaryotic photosynthetic organisms and cyanobacteria have chlorophyll *a*. There are the other types of chlorophylls in photosynthetic organisms. For example, higher plants have chlorophyll *b* in their light-harvesting complexes, and purple bacteria possess bacteriochlorophylls that contain bacteriochlorins, where the B ring is reduced, instead of chlorins.

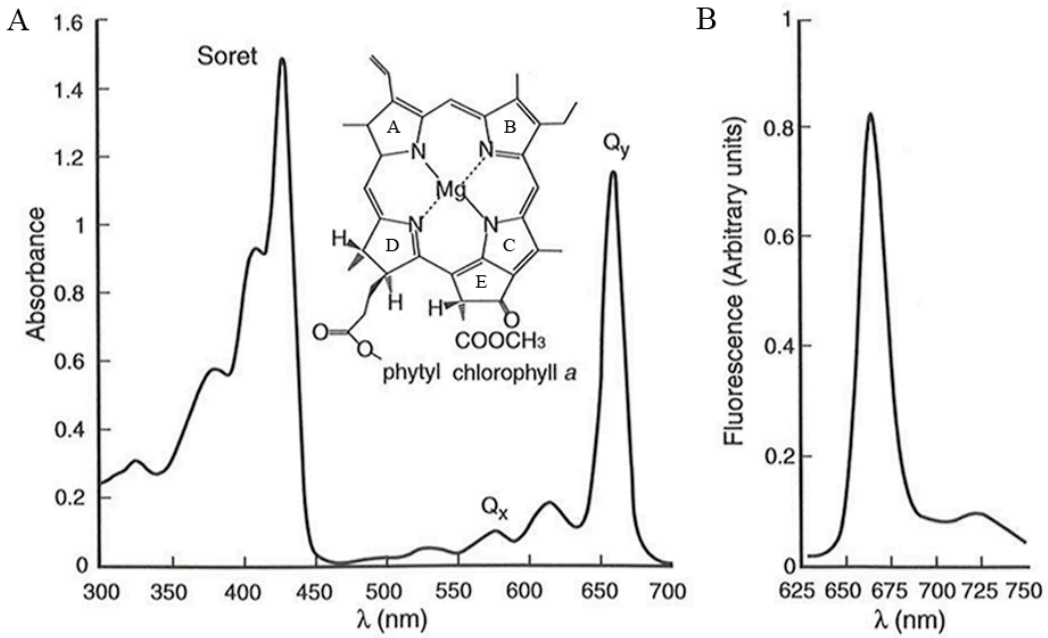

Figure I-3: Chlorophyll *a* structure and its absorption (left) and fluorescence spectra (right) in diethyl ether. (From Blankenship, 2002)

Chlorophyll is very efficient in absorbing light energy and has long-lived excited states (up to a few nanoseconds) to allow the conversion of the excitation energy into an electrochemical potential via charge separation. However, if the excitation energy is not used, the excited chlorophyll may drop its energy state to a lower-energy excited state, the chlorophyll triplet state, that has an even longer lifetime (a few μs). $^3O_2$ can react with triplet-state chlorophyll to produce $^1O_2$ that is a reactive oxygen species and can damage cells if there are no efficient quenchers nearby (Triantaphylides and Havaux, 2009). Therefore, in order to avoid the formation of $^1O_2$ generated from chlorophyll, cooperation between chlorophyll biosynthesis and synthesis of chlorophyll-binding proteins during PSII biogenesis and accommodation of chlorophyll during the PSII repair cycle are critically important as free chlorophyll in the thylakoid membrane and chlorophyll in a non-functional reaction center, where excitation energy can not be used in charge separation and where close association with a triplet quencher may not exist, are considered to be very dangerous.

Small CAB-like proteins — The cyanobacterium *Synechocystis* sp. PCC 6803 possesses five small CAB-like proteins (ScpA, ScpB, ScpC, ScpD, and ScpE; SCPs refers to all five proteins), which are predicted to have a single membrane-spanning helix. The sequence of the helices is similar to the first and third membrane-spanning region of the Cab protein family in higher plants (Dolganov *et al.*, 1995). Pigment-binding regions of Cab proteins are conserved in the SCPs, and SCPs appear to bind chlorophyll *in vitro* (Funk and Vermaas, 1999; Storm *et al.*, 2008). However, unlike CAB proteins in higher plants that function in light harvesting or photoprotection, SCPs appear to transiently bind chlorophyll in the supply of chlorophyll to photosynthetic proteins and to regulate the tetrapyrrole biosynthesis as a function of chlorophyll availability (Xu *et al.*, 2002; Xu *et al.*, 2004). Therefore, SCPs may play an important role as a bridge in communication between chlorophyll and photosynthetic proteins.

Aims of this study — Chapter II discusses the association of a member of the family of Small Cab-like Proteins (SCPs) with PSII. Because of this association, chlorophylls can be temporarily stored while PSII components are being replaced. In Chapter III, the lifetimes of PSII components are studied. The lifetime data give insight regarding the requirement and correlation between PSII protein synthesis and chlorophyll biosynthesis, and show that SCPs play important roles in reutilization of chlorophyll and in the stability of nascent PSII proteins and complexes. The SCP-less mutants also show a significant decrease in ALA biosynthesis. The fourth chapter addresses the lifetimes of PSII and PSI proteins in the wild-type strain. Based on a previous study that suggested that SCPs also stabilize the trimeric PSI complex (Wang *et al.*, 2008), the lifetime of photosynthetic proteins in the SCP-less mutant is also examined. As of results, there are no changes in

the lifetimes of most photosynthetic proteins, except the extrinsic proteins, upon removal of the SCPs. The last chapter is to characterize the *sll1906* gene that is a member of the putative bacteriochlorophyll delivery (BCD) protein. In this work, the Δ*sll1906* mutant was created. However, the chlorophyll biosynthesis/degradation and photosystem assembly are not affected in the mutant. There may be other pathways fully compensating for the lack of Sll1906.

CHAPTER II. LOCALIZATION OF THE SMALL CAB-LIKE PROTEINS IN PHOTOSYSTEM II

Abstract

The cyanobacterial SCPs consist of one-helix proteins that resemble transmembrane regions of the light-harvesting proteins of plants. To determine whether these proteins are associated with protein complexes in the thylakoid membrane, an abundant member of the SCP family, ScpD, was marked with a His tag, and proteins co-isolating with His-tagged ScpD were identified. These proteins included the major PSII components as well as FtsH, which is involved in degradation of the PSII complex. To ascertain specific interaction between ScpD and the PSII complex, the His-tagged protein fraction was subjected to two-dimensional blue native/SDS-PAGE. Again, PSII components were co-isolated with ScpD-His, and ScpD-His was found to interact most strongly with CP47. ScpD association was most prominent with the monomeric form of PSII, suggesting ScpD association with PSII that is being repaired. Using antibodies that recognize both ScpC and ScpD, we found the ScpC protein, which is very similar in primary structure to ScpD, to also co-isolate with the PSII complex. In contrast, ScpE did not co-isolate with a major protein complex in thylakoids. A fourth member of the SCP family, ScpB, could not be immunodetected, but was found by mass spectrometry in samples co-isolating with ScpD-His. Therefore, ScpB may be associated with ScpD as well. No association between SCPs and PSI could be demonstrated. On the basis of these and other data presented, we suggest that members of the SCP family can associate with damaged PSII and can serve as a temporary pigment reservoir while PSII components are being replaced.

(Published in *J. Biol. Chem.* **282**, 267-276, 2007)

Introduction

In organisms performing oxygenic photosynthesis, sunlight is absorbed by chlorophylls and other pigments, and absorbed excitation energy is transferred to the reaction centers, where the photochemical process of converting excitation energy to chemical (redox) energy takes place. These pigments are bound to proteins to keep them in their proper location and orientation so that the energy transfer is efficient and rapid and so that toxic triplet states can be quenched effectively. In plants, the vast majority of pigments, including chlorophylls *a* and *b* and various carotenoids, are bound to a family of integral membrane proteins called the light-harvesting complex (LHC). Most abundant is LHCII, the main light-harvesting complex of PS II, which has been crystallized and is known to consist of three transmembrane helices (B, C, and A), each of which is composed of 20–34 amino acids (Kuhlbrandt *et al*., 1994; Liu *et al.*, 2004). The sequences of helices A and B are very similar and comprise the CAB (chlorophyll *a*/*b*-binding) motif, which is composed of about 25 amino acid residues and includes the domain involved in chlorophyll binding (Jansson, 1999). Each individual LHCII apoprotein molecule binds an array of about eight chlorophylls *a*, six chlorophylls *b*, three to four carotenoids, and two lipids (Standfuss *et al.*, 2005). Several other closely related chlorophyll *a/b*-binding polypeptides function as light-harvesting antenna for PSII and PSI in plants. Together, these proteins are known as CAB proteins (Jansson, 1999). The CAB proteins in plants display a high degree of sequence similarity and are believed to share a common evolutionary origin (Durnford *et al.*, 1999; Heddad and Adamska, 2002). Their corresponding nuclear encoded genes belong to an extended *cab* family that includes also the genes coding for early light-inducible proteins, which are stress-induced (Adamska, 2001) and probably bind chlorophyll *a* and lutein (Adamska *et al.*, 1999). The CAB

family also includes the PsbS protein (Funk, 2001), which has an important function in non-photochemical quenching (Li *et al.*, 2000). PsbS is predicted to have four thylakoid membrane-spanning regions, and it binds chlorophylls *a* and *b* as well as carotenoids (Funk *et al.*, 1994). Moreover, related genes coding for polypeptides with one or two transmembrane α-helices have been detected in the genomes of *Arabidopsis thaliana* (Heddad and Adamska, 2000; Jansson *et al.*, 2000), rice and poplar (Klimmek *et al*. 2006), *Chlamydomonas reinhardtii* (Teramoto *et al.*, 2004), and the red alga *Cyanidioschyzon merolae* (Ohta *et al.*, 2003).

In contrast to plants, cyanobacteria lack the multihelix CAB proteins. The major peripheral LHC in some cyanobacteria is the phycobilisome, which is in the cytoplasm, is bound to the thylakoid membrane, and contributes to the deep blue-green color of cyanobacteria. However, small CAB-like proteins of <8 kDa have recently been identified in the genomes of marine and freshwater cyanobacteria (reviewed in Ref. Bhaya *et al.*, 2002). These proteins are predicted to have a single membrane-spanning α-helix, which shows significant sequence similarity to the first and third membrane-spanning regions of the green plant CAB proteins, giving them the name small CAB-like proteins (SCPs) (Funk and Vermaas, 1999). They were also designated high light-inducible proteins because their RNA level was found to increase after transfer of cells to high light and many other stress conditions (He *et al.*, 2001; Mikami *et al.*, 2002). In the small genome of the cyanobacterium *Prochlorococcus marinus* MED4, as many as 23 *scp* or *hli* genes were identified (Bhaya *et al.*, 2002), and these genes have recently been detected in the genomes of *Prochlorococcus* cyanophages (Lindell *et al.*, 2004; Sullivan *et al.*, 2005), where they are believed to maintain the photosynthetic activity of the host

during an infection (Lindell *et al.*, 2004). Although the function of the SCPs is not fully understood, these findings indicate their importance.

In the cyanobacterium *Synechocystis* sp. PCC 6803, five SCPs were identified (Funk and Vermaas, 1999); four of them (ScpB-E) encode proteins of ~ 6 kDa, whereas the fifth (ScpA) is the C-terminal extension of the ferrochelatase. The genes coding for ScpB–E are induced under various different stress conditions, including very high light intensity (>500 μmol m^{-2} s^{-1}), low temperature, and nitrogen and sulfur starvation (He *et al.*, 2001; Mikami *et al.*, 2002). A mutant with these four genes inactivated is sensitive to high intensity illumination and shows alteration in pigmentation and in the ability to perform non-photochemical dissipation of absorbed light energy (Havaux *et al.*, 2003). The enhanced expression of the *scp* genes in response to high intensity illumination is consistent with the putative function of SCPs in protection against light stress (He *et al.*, 2001). It was suggested that SCPs play a role in energy dissipation that is analogous to the process of non-photochemical quenching of higher plants (Havaux *et al.*, 2003), but the absence of *scp* genes does not affect fluorescence characteristics (Xu *et al.*, 2004). On the other hand, a carotenoid closely associated with phycobilin energy transfer is now recognized to be involved with energy transfer regulation (Mullineaux and Emlyn-Jones, 2005; Rakhimberdieva *et al.*, 2004; Wilson *et al.*, 2006). It also has been hypothesized that SCPs prevent the formation of reactive oxygen species by serving as transient carriers of chlorophyll (Xu *et al.*, 2002; Xu *et al.*, 2004).

The presence of the CAB motif in SCPs suggests that SCPs bind chlorophyll molecules in a similar way as the LHCII of plants. Furthermore, the SCPs seem to participate in tetrapyrrole biosynthesis and regulate pigment availability. The chlorophyll synthesis rates in the PSI-less/Δ*chlL*/Δ*scpB*, PSI-less/Δ*chlL*/Δ*scpE*, and PSI-less/Δ*chlL*/Δ*scpC*/Δ*scpD* strains decrease when these three mutants are transferred from

darkness to light (Xu *et al.*, 2002; Xu *et al.*, 2004). Interestingly, ScpC and ScpD seem to be functionally complementary (Xu *et al.*, 2004). These two protein sequences are most similar (87.1% identity) (He *et al.*, 2001), indicating a rather recent gene duplication (Bhaya *et al.*, 2002) or a reasonably strict primary structure requirement.

ScpD was immunologically detected in thylakoid membranes of *Synechocystis* sp. PCC 6803 (Hao *et al.*, 2001). To understand the function of this and other SCPs, it is important to know which complexes in the membrane they interact with. Here, we used His-tagged ScpD proteins to identify the main complexes with which ScpD is associated. After two-dimensional PAGE (blue native (BN) PAGE followed by SDS-PAGE), ScpD was found to be associated with monomeric PSII, its closest neighbor being CP47. CP43 and Psb28 were also found to interact with ScpD. Although ScpC could be identified in the PSII fraction and ScpB was found to co-fractionate with ScpD to some degree, ScpE was found in thylakoids, but did not seem to be associated with PSII.

Materials and Methods

Growth conditions — Synechocystis sp. PCC 6803 strains (wild-type, the PSI-less strain (Δ*psaAB*) (Shen *et al.*, 1993), the PSII-less strain (Δ*psbDIC*/Δ*psbDII*) (Carpenter *et al.*, 1990), the PSI-less/PSII-less strain (Δ*psaAB*/Δ*psbDIC*/Δ*psbDII*) (Ermakova-Gerdes *et al.*, 1996), the CP47-His-tagged HT-3 strain (Bricker *et al.*, 1998), and the ScpD-His strain (see below)) were cultivated at 30 °C in BG-11 medium (Rippka *et al.*, 1979). The PSI-less and PSII-less mutants were provided with 15 mM glucose. All strains except the PSI-less strain were grown at normal (50 μmol photons m^{-2} s^{-1}) or high (500 μmol photons m^{-2} s^{-1}) light intensity as indicated. Because of its light sensitivity, the PSI-less strain was cultured at 4 μmol photons m^{-2} s^{-1}. To induce the SCPs, the wild-type

and PSII-less strains were grown at high light intensity for 7 h. In the PSI-less/PSII-less and PSI-less strains, SCPs are induced also at light intensities of 50 and 10 μmol photons m^{-2} s^{-1}, respectively (Funk and Vermaas, 1999).

Mutant construction — To generate the ScpD-His strain, a plasmid construct was made to tag the ScpD protein in *Synechocystis* with an His_6 epitope on its N terminus and to express the corresponding gene construct under the control of the *psbAII* promoter. To construct this plasmid, the *scpD* gene was amplified by PCR using a mixture of *Taq* and *Pfu* DNA polymerases and gene-specific primers (forward, 5′-TTATACATATGCATCATCATCATCATCATGGAACTAGCCGCGGATTTCGCCT-3′; and reverse, 5′-TCGGATCCTTAGAGAGGAGAGCAACCAACCC-3′) with artificially generated restriction sites for *Nde*I and *BamH*I and containing six histidine codons (CAT) in the forward primer. After restriction, the PCR fragment was cloned into the *Nde*I and *BamH*I sites of the pPSBA plasmid; the resulting plasmid contains the *scpD*-His gene construct right behind the *psbAII* start codon (Lagarde *et al.*, 2000) and retains the upstream and downstream regions of the *Synechocystis psbAII* gene. The ligation mixture was amplified by PCR using pPSBA primers amplifying the entire *psbAII*/*scpD*-His region, and DNA of the desired size was selected. Amplification by PCR was chosen because transformation of *Escherichia coli* with the ligation mixture yielded no colonies, presumably reflecting toxicity of the plasmid to *E. coli*. The PCR product containing the *scpD*-His gene was transformed into the *Synechocystis psbAII*-KS strain, in which the *psbAII* gene was replaced with a kanamycin resistance/*sacB* cartridge (Lagarde *et al.*, 2000). The *sacB* gene codes for a levan sucrase, leading to sucrose sensitivity of this strain (Ried and Collmer, 1987). After transformation, *Synechocystis* cells were grown on BG-11 plates for 4 days. Transformants were then

transferred to plates with 5% sucrose, and sucrose-resistant colonies were checked for kanamycin sensitivity. The resulting strain expressing both wild-type and His-tagged forms of the ScpD protein was subsequently transformed with chromosomal DNA from a *scpD*$^{-}$ strain carrying a spectinomycin resistance cassette insertion (Prentki and Krisch, 1984), and spectinomycin-resistant transformants were selected (Xu *et al.*, 2002). Insertion of the *scpD*-His gene at the desired location was confirmed by DNA sequencing, and deletion of the wild-type *scpD* gene was confirmed by PCR.

Biochemical preparations — Total membranes from the different Synechocystis strains were isolated as described (Funk and Vermaas, 1999). Radioactive labeling of cells using a mixture of L-[^{35}S]methionine and L-[^{35}S]cysteine (>1000 Ci/mmol, final activity of 400 μCi/mL; Tran^{35}S-label, ICN Biomedicals) and isolation of membranes were performed as described (Komenda *et al.*, 2004). Isolated membranes were solubilized with *n*-dodecyl β-maltoside (*n*-dodecyl β-maltoside/chlorophyll ratios were 20 and 100 (w/w) in the PSI-containing and PSI-less strains, respectively), and extracted complexes were separated by BN gel electrophoresis (Schagger and von Jagow, 1991).

Isolation of His-tagged complexes — Cells from *Synechocystis* sp. PCC 6803 strains carrying a His tag were pelleted after 4 h of exposure to high light intensity (500 μmol photons m^{-2} s^{-1}), resuspended in Buffer A (50 mM MES-NaOH (pH 6.0), 10 mM $MgCl_2$, 5 mM $CaCl_2$, and 25% glycerol), and broken. Thylakoids were prepared as described (Bricker *et al.*, 1998). The cell homogenate (at 1 mg/mL chlorophyll) was brought to 1.28% β-dodecyl maltoside and incubated for 25 min at 4 °C. The sample was then loaded onto a Ni^{2+} metal affinity column. The column was washed with 9 column volumes (45 ml) of Buffer A containing 0.04% β-dodecyl maltoside and 10 mM

imidazole. Subsequently, the column was washed with 10 mL of Buffer A with 0.04% β-dodecyl maltoside and 30 mM imidazole. Bound ScpD-His was eluted with 0.04% β-dodecyl maltoside and 100 mM imidazole in Buffer A. The eluate was precipitated by the addition of an equal volume of 25% polyethylene glycol 8000 in 50 mM MES-NaOH (pH 6.0) and then resuspended in Buffer A containing 0.04% β-dodecyl maltoside.

PAGE — To the resuspended Ni^{2+} column eluate was added 0.1 volume of loading solution containing 750 mM aminocaproic acid and 5% Coomassie Brilliant Blue G-250. Protein complexes in the eluate were separated by BN-PAGE at 4 °C as described (Schagger and von Jagow, 1991) using a 5–14% polyacrylamide gradient gel. For the second dimension, the BN gel lane of interest was incubated for 20 min in a solution containing 25 mM Tris-HCl (pH 7.5) and 1% SDS and then placed on top of an SDS-12–20% polyacrylamide gel containing 7 M urea (Komenda *et al.*, 2002). After electrophoresis, gels were either stained with silver nitrate (Bjellqvist *et al.*, 1993) or transferred onto polyvinyl difluoride membrane for further analysis by Western blotting.

Immunoblotting — For immunoblotting, the proteins were transferred onto polyvinyl difluoride membrane (Towbin *et al.*, 1979). Anti-ScpC antibody raised in rabbits against residues 1–17 of the ScpC protein (MTTRGFRLDQDNRLNNF) was a gift from Dr. A. Sokolenko (University of Munich). A peptide-directed antibody against a region near the N-terminus of ScpE (ELQPNQTPVQEDPKFG) was made commercially by Innovagen AB (Lund, Sweden).

Pigment analysis — Chlorophyll content was determined in 80% acetone and was calculated as described (Porra *et al.*, 1989).

Protein analysis by matrix-assisted laser desorption ionization time-of-flight (MALDI-TOF) mass spectrometry — Protein identification by peptide mass fingerprinting and post-source decay tandem mass spectrometry (MS/MS) analysis was carried out using a Voyager-DE STR mass spectrometer (Applied Biosystems, Stockholm). In-gel digestion to produce peptides for analysis by mass spectrometry was carried out essentially as described (Shevchenko *et al.*, 1996) using sequencing-grade modified trypsin (Promega/SDS Biosciences, Falkenberg, Sweden) or sequencing-grade chymotrypsin (Roche Diagnostics, Bromma, Sweden). Silver-stained protein bands were destained prior to in-gel digestion using the method previously described (Gharahdaghi *et al.*, 1999). To analyze the in gel-digested proteins by MALDI-TOF mass spectrometry, dried droplet preparations were applied as described (Kussmann *et al.*, 1997). The matrices used were readymade solutions of α-cyano-4-hydroxycinnamic acid (G2037A) and 2,5-dihydroxybenzoic acid (G2039A) from Agilent Technologies (Stockholm). Samples were concentrated and desalted as needed using homemade Stop-and-Go extraction columns as described (Rappsilber *et al.*, 2003). Data base searches were carried out on an in-house Mascot server that was licensed to Umeå University by Matrix Science (www.matrixscience.com) using the current version of the NCBInr Database and the *Synechocystis* Protein Database of the European Bioinformatics Institute. The data bases were searched using peptide mass fingerprint spectra and post-source decay MS/MS spectra. If appropriate, proteins were identified by sequence queries that included both types of data. The search parameters restricted the error for peptide masses to 50 *ppm* and for MS/MS fragments to 0.5 Da. The instrument type specified for MS/MS ion searches was MALDI-TOF/TOF. By default, the search parameters permitted one missed

cleavage site and variable oxidation states of methionine. If appropriate, two or more missed cleavage sites were allowed.

Results

Proteins co-purifying with ScpD-His — Based on two-phase separation experiments, ScpD is a prevalent SCP member in the thylakoid membrane (Hao *et al.*, 2001), but its association with protein complexes in this membrane system remains unknown. To learn about the function of the SCPs, we decided to tag ScpD with His, to determine its interaction partners, and to analyze the SCP composition of thylakoid complexes. As described under "Materials and Methods" we created a *Synechocystis* mutant in which *scpD* had been deleted and replaced with a His-tagged *scpD* copy, the expression of which was under the control of the *psbAII* promoter. After harvesting and rupturing the cells, the total membranes were solubilized using β-dodecyl maltoside, and ScpD-His-containing complexes were isolated via nickel column chromatography (Bricker *et al.*, 1998). Subsequently, the proteins were separated by SDS-PAGE and analyzed by MALDI-TOF mass spectrometry.

To test the validity of this protocol, we also isolated PSII complexes via CP47-His using the HT-3 mutant (Bricker *et al.*, 1998) and analyzed them by SDS-PAGE (data not shown). They were composed of essentially the same subunits as shown in originally (Bricker *et al.*, 1998; Kashino *et al.*, 2002).

The SDS gel in Figure II-1 shows the washed off fractions and eventual eluate resulting from the affinity purification of the ScpD-His complex (lanes C–E) and similar fractions of a chromatography control using wild-type ScpD (lanes A and B). Although the wild-type fraction collected upon washing the column (lane A) showed no recognizable pattern, the corresponding fraction from the ScpD-His strain showed a

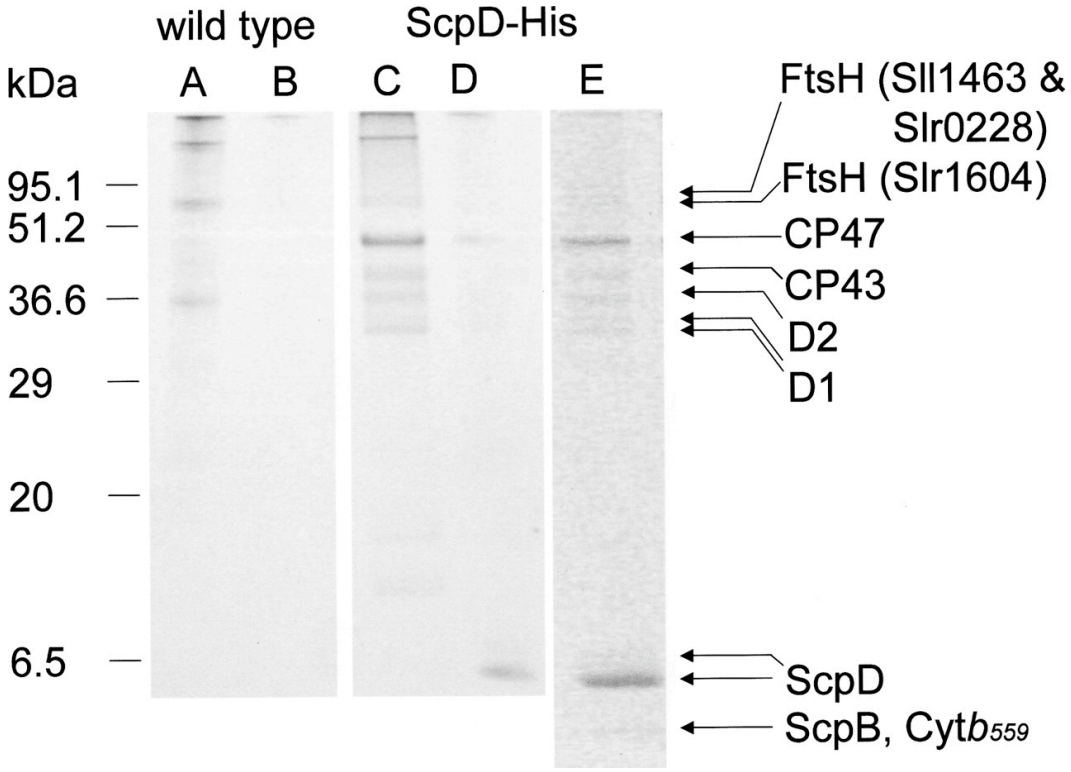

Figure II-1: Proteins co-purifying with ScpD-His. This Coomassie Blue-stained SDS-polyacrylamide gel displays total membrane fractions purified via nickel chromatography. Fractions from wild-type cells (control) are shown in lanes A and B, and fractions from the ScpD-His mutant strain are shown in lanes C–E. Lanes A and C, fractions obtained during the second washing step (0.04% β-dodecyl maltoside and 30 mM imidazole in Buffer A); lanes B, D, and E, fractions obtained in the elution step (0.04% β-dodecyl maltoside and 100 mM imidazole in Buffer A). Lanes D and E show the results of two separate experiments, and the protein bands shown in lane E were analyzed by MALDI-TOF mass spectrometry, resulting in identification as indicated to the right (also see Table II-1). Cytb559, cytochrome b_{559}.

pattern of components resembling that of PSII (lane C). Indeed, upon elution with 100 mM imidazole, such components co-eluted with ScpD-His (lanes D and E; representing results from two independent preparations). The presence of two distinct bands with apparent masses of 47.3 and 6 kDa was clearly visible in these lanes, and fainter bands migrating with apparent masses between 4 and 6, 30 and 45, and 70 and 80 kDa could be observed. The only visible differences between the PSII complexes washed off the column at 30 mM imidazole (lane C) and at 100 mM imidazole (lane D) were the

presence of ScpD-His and an enrichment of CP47 in the latter fraction. It therefore seems that most of the PSII complexes were washed off the column and that only a minor fraction was bound to ScpD. The corresponding eluent fraction from the wild-type control in lane B did not display protein bands, demonstrating the specificity of retention of the proteins in lanes D and E by ScpD-His.

To identify the proteins that co-purified with ScpD-His, the individual bands in Figure II-1 (lanes D and E) were digested with trypsin and analyzed by MALDI-TOF mass spectrometry. If the peptide mass fingerprint spectra of the individual bands were not sufficient for unequivocal protein identification, post-source decay MS/MS spectra of individual peptides were acquired for protein identification by sequence queries (Mann and Wilm, 1994; Perkins *et al.*, 1999). Table II-1 summarizes the results of this analysis. As expected, the mass spectra showed the presence of ScpD (Ssr2595) in the major band at an apparent mass of 6 kDa; ScpD was identified with high confidence by its peptide mass fingerprint spectrum in combination with an MS/MS analysis of the peptide GFRLDQDNR. The major band at an apparent mass of 47.3 kDa was found to contain CP47 (Slr0906) and the hypothetical protein Slr0909. Mass spectrometry analysis also identified CP43 (Sll0851) with an apparent mass of 39.8 kDa, and D2 (Sll0849/Slr0927) and D1 (Sll1867; two bands) with apparent masses of 36.7 kDa, 34.3 kDa, and 33.5 kDa, respectively. The band of the D2 protein also contained Slr1128, annotated as a hypothetical integral membrane protein. In the high mass range, the FtsH proteases Sll1463 and Slr0228 were present at an apparent mass of 77 kDa, and the FtsH protease slr1604 was found at an apparent mass of 71 kDa. Furthermore, Sll1021 and Slr0798 (both annotated as hypothetical proteins) were found at apparent masses of 88.1 and 95.1

Table II-1: Mass spectrometry identification of proteins apparently forming a complex with ScpD-His (data shown in Figure II-1)

Experimental /theoretical mass	ORF[a]	Gene product	Mascot search and score[b]	Sequence coverage	r.m.s. error
				%	*ppm*
95.1/76.8 kDa	Slr0798	Hypothetical protein	SQ 193	35	14
88.1/74.3 kDa	Sll1021	Hypothetical protein	PMF 249	44	7
76.7/68.1 kDa	Sll1463	FtsH	SQ 190	32	14
76.7/68.4 kDa	Slr0228	FtsH	PMF 150	39	17
70.8/67.1 kDa	Slr1604	FtsH	PMF 83	24	23
47.3/55.8 kDa	Slr0906	CP47	SQ 228	39	15
47.3/52.4 kDa	Slr0909	Hypothetical protein	SQ 142	40	11
39.8/51.8 kDa	Sll0851	CP43	SQ 143	17	25
36.7/39.4 kDa	Sll0849/Slr0927	D2	SQ 157	22	15
36.7/35.6 kDa	Slr1128	Hypothetical protein	PMF 173	51	13
34.3/39.6 kDa	Sll1867	D1	SQ 78	13	11
33.5/39.6 kDa	Sll1867	D1	SQ 132	20	10
6.9/7.7 kDa	Ssr2595	ScpD	SQ 112	50	13
6.0/7.7 kDa	Ssr2595	ScpD	SQ 131	50	32
4.8/7.7 kDa	Ssl1633	ScpB	MIS 105	18	
4.8/4.8 kDa	Smr0006	Cytochrome b_{559}	MIS 109	38	

[a] ORF, open reading frame; r.m.s., root mean square; SQ, sequence query including peptide mass fingerprint (PMF) and MS/MS ion search (MIS) data.
[b] Identified by a search in the NCBInr Database.

kDa, respectively. In the low mass range, ScpB (Ssl1633) and the small subunit of cytochrome b_{559} (Smr0006) were identified at an apparent mass of 4.8 kDa.

ScpD-His associates with PSII subunits — The composition of the affinity-purified ScpD-His complex indicated that ScpD associated with PSII components. However, fractions that are isolated by a one-step affinity purification may contain contamination by nonspecifically bound proteins. For this reason, we subjected the purified ScpD-His

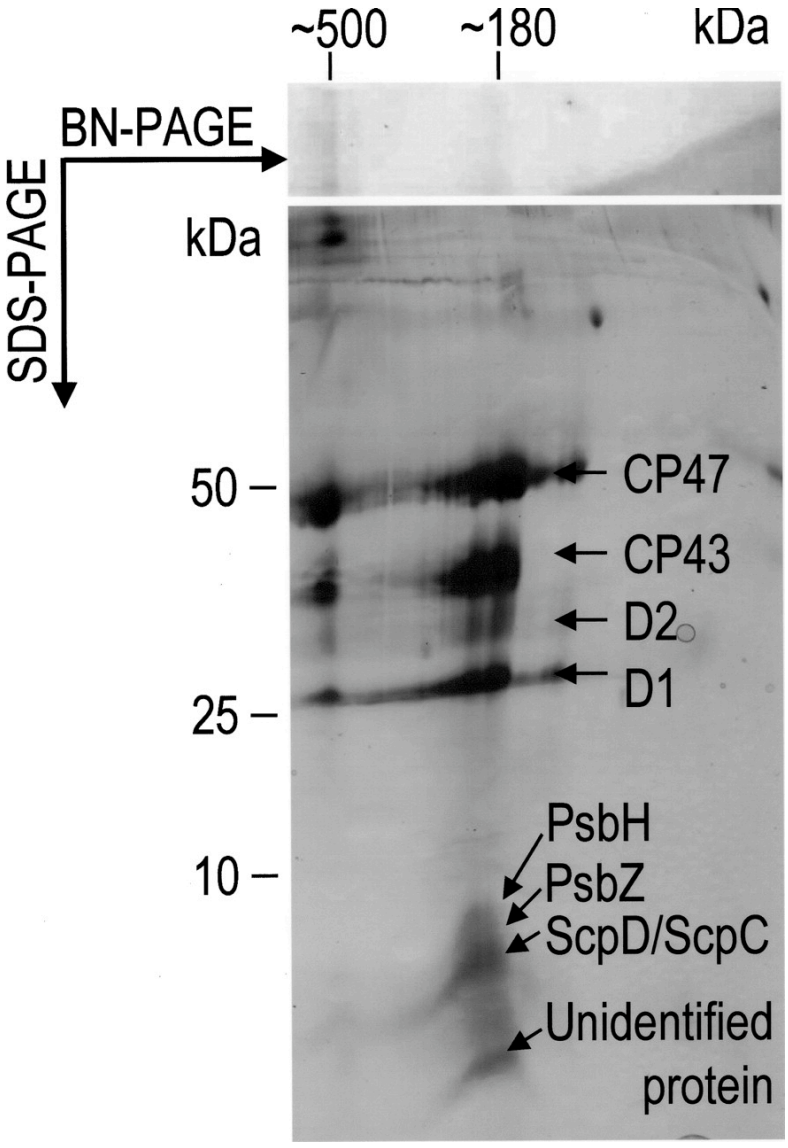

Figure II-2: ScpD-His is associated specifically with PSII. ScpD-His and copurified proteins were separated by two-dimensional BN/SDS-PAGE after nickel chromatography and solubilization with 0.04% β-dodecyl maltoside. Proteins were identified by mass spectrometry (see Table II-2).

complex to two-dimensional BN/SDS gel electrophoresis. This technique is an accepted approach to separate protein complexes and their subunits, and it has been successfully used to study protein complexes from the thylakoid membranes of higher plants (Thidholm *et al.*, 2002; Aro *et al.*, 2005). Figure II-2 shows an example for the analysis of the ScpD-His complex at ~200 kDa by two-dimensional BN/SDS gel electrophoresis.

Table II-2: Mass spectrometry identification of proteins that co-purified with ScpD-His upon separation by two-dimensional BN/SDS-PAGE after nickel chromatography and solubilization with 0.04% β-dodecyl maltoside

Experimental/ theoretical mass	ORF[a]	Gene product	Mascot search and score[b]	Sequence coverage	r.m.s. error
				%	*ppm*
52.2/55.8 kDa	Slr0906	CP47	PMF 213	38	12
38.9/51.8 kDa	Sll0851	CP43	SQ 107	15	9
33.5/39.4 kDa	Sll0849/Slr0927	D2	PMF 73[c]	20	17
27.5/39.6 kDa	Sll1867	D1	PMF 77[c]	20	20
7.8/12.2 kDa	Slr1645	PsbZ	PMF 74[c]	29	11
7.8/7.0 kDa	Ssl2598	PsbH	MIS 50	21	
7.8/7.7 kDa	Ssr2595/Ssl2542	ScpD/ScpC	MIS 24[c]	12	
5.8/7.7 kDa	Ssr2595/Ssl2542	ScpD/ScpC	MIS 25[c]	12	

[a] ORF, open reading frame; r.m.s., root mean square; SQ, sequence query including peptide mass fingerprint (PMF) and MS/MS ion search (MIS) data.

[b] Identified by a search in the NCBInr Database.

[c] Identified by a search in the *Synechocystis* sp. PCC 6803 Protein Database of the European Bioinformatics Institute.

The pattern of BN gel separation in the first dimension showed two main bands (Figure II-2). Upon SDS-PAGE in the second dimension and silver staining of the gel followed by MALDI-TOF mass spectrometry of bands, the corresponding proteins could be identified. The results are summarized in Table II-2. In the high mass region, we found the PSII core subunits CP47, CP43, D1, and D2 at apparent masses of 52, 39, 33, and 32 kDa, respectively. In the low mass region, we detected PsbH, PsbZ, and ScpC/ScpD as a broader band spanning the 6–8 kDa range. It is interesting to note that only the band with faster migration in the first dimension provided clear evidence for small subunits (Figure II-2). The slower migrating band may represent PSII dimers at 500 kDa (Thidholm *et al.*, 2002). The relatively strong affinity of the putative PSII dimer on BN gel for the dye Coomassie Blue (as seen by the intense coloration of this band relative to the more rapidly migrating PSII fraction that represents PSII monomers) was unexpected. Equally

unexpected was the depletion of ScpD and other low mass polypeptides in this fraction, as this fraction was isolated by retention on a nickel-nitrilotriacetic acid column, indicating the association with ScpD-His at the time of isolation. We hypothesize that ScpD (and possibly ScpC) is associated with monomeric PSII in a way that affects Coomassie Blue affinity (which would place the SCPs around the PSII monomer) and that the PSII monomers and dimers/multimers are in dynamic exchange. Another interesting feature of Figure II-2 is the heavy staining of low mass proteins in the more rapidly migrating band. Although quantitation of proteins based on silver staining is tenuous, the high staining intensity of these proteins suggests the association of multiple polypeptide copies with PSII.

The limited amount of the ScpD-His complex material on the BN gel shown in Figure II-2 made the analysis of the low mass proteins difficult. Although the identification of PsbH and PsbZ was unambiguous, MS/MS analysis identified the peptide GFRLDQDNR, which matches the sequence of ScpD and of its close homolog ScpC. For this reason, our mass spectrometry data do not allow us to distinguish between these two SCPs. The purification of the protein complex using His-tagged ScpD implies that ScpD is present. However, on the basis of the mass spectrometry data, we can neither confirm nor exclude the presence of ScpC.

Nearest neighbors of ScpD — The purification of ScpD-His complexes by nickel affinity chromatography and BN gel electrophoresis showed a clear association of ScpD with PSII, but did not provide evidence regarding the localization of ScpD within the PSII complex. To obtain information regarding the neighbors of ScpD-His in the PSII complex, we used a higher β-dodecyl maltoside concentration (0.8% rather than 0.04%)

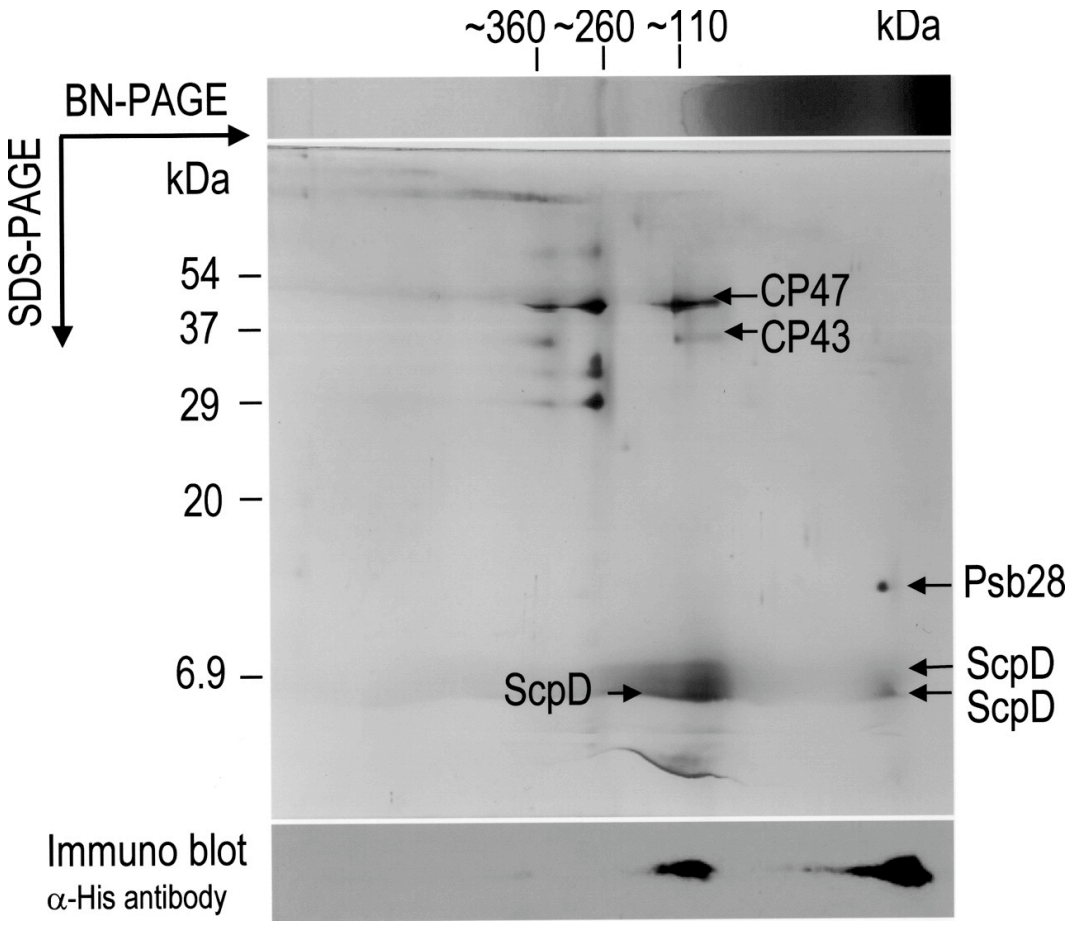

Figure II-3: Closest neighbors of ScpD. ScpD-His and co-purified proteins were separated by BN/SDS-PAGE after nickel chromatography and solubilization with 0.8% β-dodecyl maltoside. The lower panel shows immunostaining of ScpD-His after two-dimensional PAGE using an antibody directed against the His tag. Proteins were identified by mass spectrometry (see Table II-3). Note that Psb28 does not correspond to the sharp dot on the gel, but rather is an underlying band.

for solubilization of the ScpD-His complex before separation by two-dimensional BN/SDS gel electrophoresis. The BN/SDS gel in Figure II-3 shows that the stronger solubilization of the purified ScpD-His complex resulted in the formation of smaller subcomplexes. To monitor the separation of different ScpD-His complexes, the SDS gel was probed by immunoblotting using antibodies directed against the His tag. To make sure no ScpD-His was overlooked, the antibody concentration used was high, and therefore, the signal was not linear with the amount of His tag. The composition of the

ScpD-containing complexes was analyzed by MALDI-TOF mass spectrometry. Table II-3 shows the results from the analysis of two different gels and corresponds to protein bands as indicated in Figure II-3.

ScpD-His was found to be prominently associated with CP47, which was consistently detected to co-purify with ScpD-His. The weak band below that of CP47 in Figure II-3 was assigned to CP43 (Table II-3). The diffuse band in the 7–8-kDa region contained ScpD-His (see immunoblot in the lower panel of Figure II-3), and as this band was more diffuse than that of the immunoblot, it also might contain ScpC, as our mass spectra do not allow us to exclude the presence of this protein. A smaller complex toward the right in Figure II-3 clearly contained ScpD in the diffuse band in the 7–8-kDa range. In addition, we found Psb28 in a band at an apparent mass of 12.4 kDa. The distinct spot close to Psb28 is probably an artifact and does not seem to display this protein.

ScpC co-migrates with PSII — As indicated, the detected mass fragment of ScpD is exactly identical to that of ScpC. Indeed, the primary structures of ScpD and ScpC are 87% identical, and the compelling similarity between these two SCPs indicates that they may have not only a similar function, but also similar binding partners. Therefore, it was important to determine the location of ScpC in the thylakoid membrane.

Toward this goal, *Synechocystis* wild-type cells were pulse-labeled with L-[^{35}S]Met/Cys for 30 min while growing at 500 μmol photons m^{-2} s^{-1}, and subsequently, thylakoid membranes were isolated and analyzed by two-dimensional BN gel electrophoresis in combination with autoradiography. The autoradiogram of the wild-type strain in Figure II-4A (first panel) displayed a strong band in the ScpC/ScpD region at 6 kDa that was present in two complexes. The first complex, RCC1, was identified

Table II-3: Mass spectrometry identification of proteins that co-purified with ScpD-His upon separation by two-dimensional BN/SDS-PAGE after nickel chromatography and solubilization with 0.8% β-dodecyl maltoside. The results from the analysis of two different gels shown in Figure II-3 are presented. ORF, open reading frame; r.m.s., root mean square; SQ, sequence query including peptide mass fingerprint (PMF) and MS/MS ion search (MIS) data.

Experimental/ theoretical mass	ORF	Gene product	Mascot search[a]		Sequence coverage		r.m.s. error	
			Exp 1	Exp 2	Exp 1	Exp 2	Exp 1	Exp 2
							ppm	
Experiment 1								
Middle lane								
47.3/55.8 kDa	Slr0906	CP47	PMF167	PMF142	40	33	7	4
39.8/51.8 kDa	Sll0851	CP43	SQ50[b]	SQ39[b]	9	7	21	14
6.9/7.7 kDa	Ssr2595	ScpD	SQ64[b]	SQ85	50	42	20	22
Right lane								
12.4/12.5 kDa	Sll1398	Psb28	N.D.	SQ136		53		26
8.0/7.7 kDa	Ssr2595	ScpD	SQ84	MIS65	42	12	12	
7.1/7.7 kDa	Ssr2595	ScpD	SQ97	MIS72	42	12	20	

[a] Identified by a search in the NCBInr Database.

[b] Identified by a search in the Synechocystis sp. PCC 6803 Protein Database of the European Bioinformatics Institute.

previously as monomeric PSII consisting of the CP47, CP43, D2, and D1 proteins (Komenda *et al.*, 2004). The second complex, termed RC47, was smaller and was depleted in CP43. A comparison with SCP deletion mutants showed that the band with a molecular mass of 6 kDa was reduced in the Δ*scpC*/Δ*scpD* strain (second panel), but present in the Δ*scpB* and Δ*scpE* strains (third and fourth panels, respectively). These

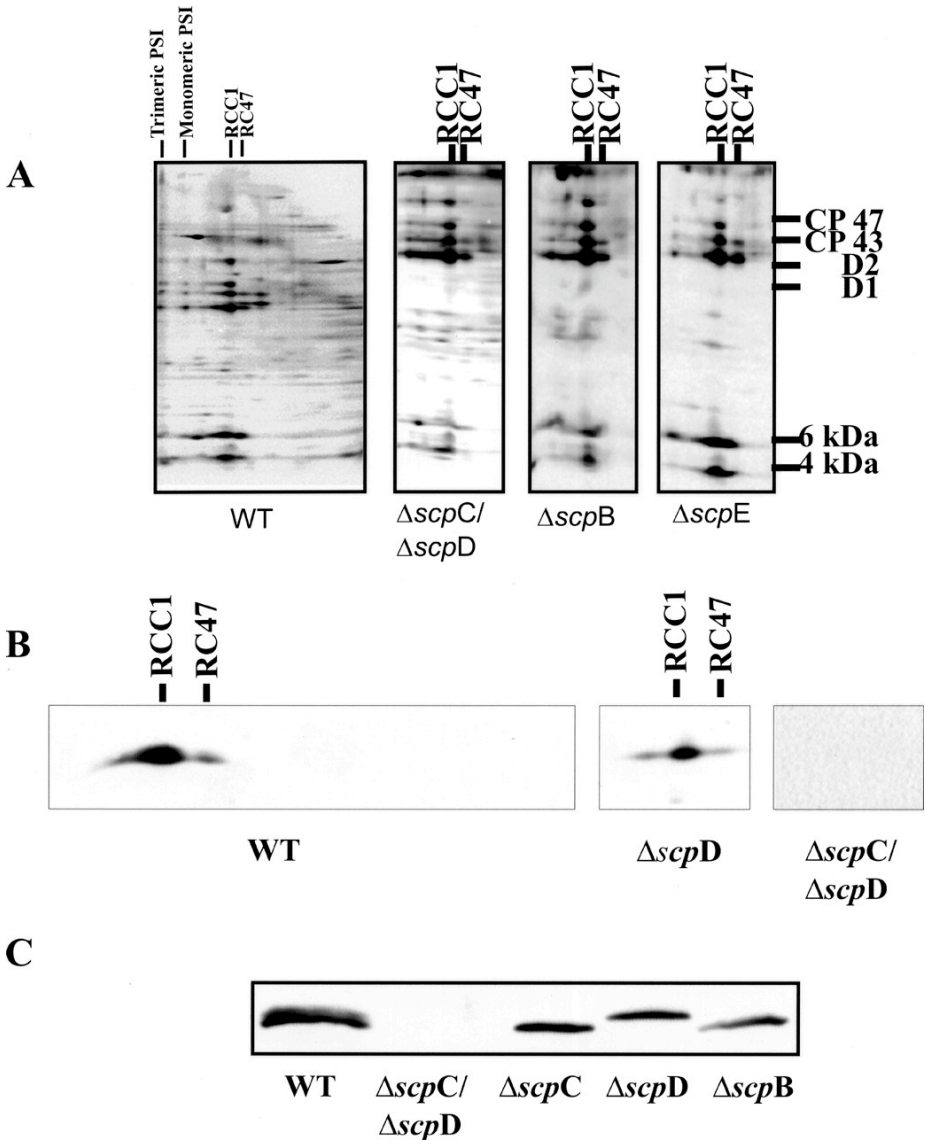

Figure II-4: ScpC co-migrates with PSII. A, autoradiograms of thylakoid membrane proteins from the high light-treated wild-type (WT) strain (whole gel) and mutant strains *ΔscpC/ΔscpD*, *ΔscpB*, and *ΔscpE* (only the PSII region is shown) after pulse radiolabeling with L-[^{35}S]Met/Cys for 30 min. Proteins were separated by two-dimensional BN/SDS-PAGE prior to autoradiography. B, immunodetection of ScpC/ScpD in the wild-type strain (whole gel) and mutant strains *ΔscpD* and *ΔscpC/ΔscpD* (only the PSII region is shown) using anti-ScpC/ScpD antibody. C, immunoblot using anti-ScpC/ScpD antibody after one-dimensional SDS-PAGE of thylakoid membrane proteins from high light-induced cells. The loaded samples contained 4 μg of chlorophyll/lane and correspond to the wild-type strain, *ΔscpC/ΔscpD*, *ΔscpC*, *ΔscpD*, and *ΔscpB* as indicated.

observations indicate that the high light-induced 6-kDa band of the RCC1 and RC47 complexes contained ScpD and/or ScpC, but most likely not ScpB or ScpE.

To distinguish between ScpD and ScpC in the 6-kDa band of the RCC1 and RC47 complexes, an antibody was raised against the N terminus of ScpC (MTTRGFRLDQDNRLNNF), which is identical to that of ScpD except for the third residue (S in ScpD). Indeed, immunostaining of high light-induced wild-type cells identified the bands in the 6-kDa region as ScpC and ScpD (Figure II-4B, left panel). The bands were absent in thylakoids of the high light-induced Δ*scpC*/Δ*scpD* strain (right panel). Therefore, the minor band with a molecular mass of 6 kDa seen in the autoradiogram of the Δ*scpC*/Δ*scpD* strain (Figure II-4A, second panel) belongs to other co-migrating proteins. In the Δ*scpD* deletion mutant, the antibody unambiguously identified ScpC co-migrating with RCC1 and RC47 (Figure II-4B, middle panel). Interestingly, after applying the same procedure to a PSII-less mutant, ScpC and ScpD were found to co-migrate with small complexes or as free proteins (data not shown), suggesting that these SCPs do not readily associate with large complexes such as PSI. Separation of thylakoid preparations from high light-induced Δ*scpC* and Δ*scpD* strains by one-dimensional SDS electrophoresis made it possible to identify the lower migrating band as ScpD (Figure II-4C, third lane) and the upper band as ScpC (fourth lane). In the wild-type strain, the ScpD protein appeared to be dominant (Figure II-4C), but the ratio between ScpC and ScpD amounts was highly variable among various strains and conditions, suggesting that ScpC and ScpD are indeed functionally equivalent. Interestingly, in the Δ*scpB* strain, the level of ScpD was decreased, and ScpC appeared to be absent altogether (fifth lane). ScpC/ScpD immunodetection by two-dimensional

BN/SDS-PAGE of extracts from the Δ*scpB* strain showed that ScpD remained associated with PSII complexes (RCC1 and RC47) as in the wild-type control (data not shown).

ScpE is not associated with PSII — Now that ScpD and ScpC have been positively correlated with PSII complexes, we set out to determine the location of the other two small SCPs as well (ScpB and ScpE; ScpA is a C-terminal extension of ferrochelatase). We were unable to generate antibodies against ScpB. However, we could elicit antibodies against the peptide ELQPNQTPVQEDPKFG, which is a sequence that is part of the N-terminal region of ScpE. These antibodies were used for detection of ScpE on SDS-polyacrylamide gels of membrane preparations from the wild-type and PSII-less strains (Vermaas *et al.*, 1990) that were grown at 500 μmol photons m^{-2} s^{-1} (high light) for 7 h to induce the expression of ScpE from the PSI-less/PSII-less strain (Ermakova-Gerdes *et al.*, 1995), in which SCPs are induced also at light intensities of 50 μmol photons m^{-2} s^{-1} (Funk and Vermaas, 1999), and from the PSI-less strain that, because of its light sensitivity, was grown at 10 μmol photons m^{-2} s^{-1}. As negative controls, membranes from the wild-type strain grown at normal light intensity (50 μmol photons m^{-2} s^{-1}) and from the Δ*scpE* strain grown at 500 μmol photons m^{-2} s^{-1} were included (Figure II-5A and D). Although no ScpE was detected in membranes from the Δ*scpE* strain or the wild-type strain grown at 50 μmol m^{-2} s^{-1}, the antibody immunostained ScpE in the other strains and in the wild-type strain grown at high light intensity.

To further localize ScpE, the total membrane fraction of the wild-type strain grown at high light intensity was separated into fractions enriched in thylakoid membranes, plasma membranes, and outer membranes using two-phase partitioning (Norling *et al.*, 1998). In these fractions, ScpE was immunodetected exclusively in the

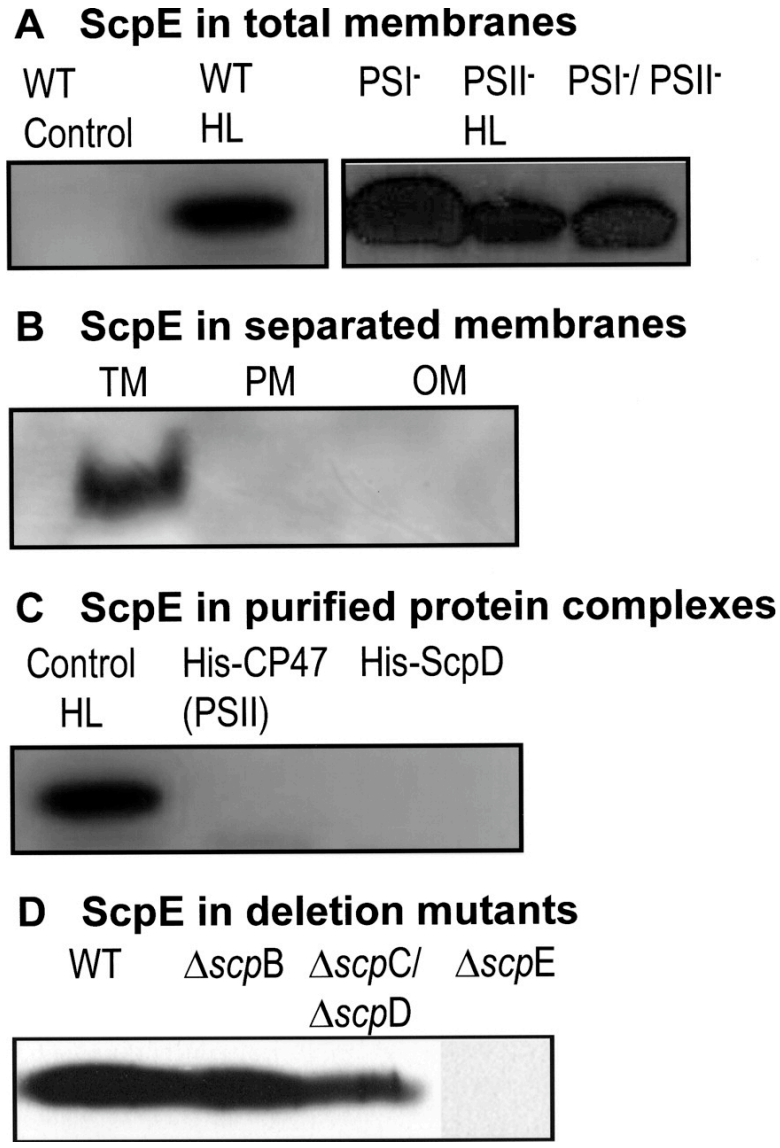

Figure II-5: ScpE is located in the thylakoid membrane. The subcellular location of ScpE was detected by immunoblotting. After breaking the cells, the total membranes were separated by one-dimensional SDS-PAGE and analyzed using anti-ScpE antibody. A, wild-type (WT), PSI-less (PSI¯), PSII-less (PSII¯), and PSI-less/PSII-less mutant cells were grown at 50 (Control), 500 (HL), and 10 (PSI-less mutant) μmol m^{-2} s^{-1}. B, thylakoid (TM), cytoplasmic (PM), and outer (OM) membranes were purified by two-phase partitioning (Aro *et al.*, 2005); separated by SDS-PAGE; and analyzed by immunoblotting using anti-ScpE antibody. C, total membranes of high light-treated wild-type and nickel chromatography-purified PSII complexes (CP47-His) (Bricker *et al.*, 1998) and ScpD-His complexes were analyzed by immunoblotting using anti-ScpE antibody. D, shown is the accumulation of ScpE in the high light-induced wild-type, *ΔscpB*, *ΔscpC/ΔscpD*, and *ΔscpE* strains. Equal amounts of cells were loaded in each lane. The proteins were separated by denaturing SDS-PAGE, transferred onto polyvinyl difluoride membrane, and probed with anti-ScpE antibody.

thylakoid membrane fraction (Figure II-5B). To investigate whether ScpE is associated with PSII, oxygen-evolving PSII was isolated from the HT-3 mutant (Bricker *et al.*, 1998), which contains a hexahistidine tag at the C terminus of the CP47 protein. Also the ScpD-His fraction eluted after nickel column purification (Figure II-1) was analyzed. Although an immunoreaction was obtained from the positive control (total membranes isolated from high light-stressed wild-type strain), ScpE could not be detected in either PSII or the ScpD-His fraction (Figure II-5C). Deletion of ScpB or ScpC and ScpD did not alter the presence of ScpE, even though the ScpE abundance was decreased in the Δ*scpC*/Δ*scpD* strain (Figure II-5D).

To determine the potential association of ScpE with membrane complexes, a two-dimensional BN/SDS-polyacrylamide gel was challenged with anti-ScpE antibodies.As indicated in Figure II-6, ScpE was not stably associated with one of the photosystems, but instead was present in small complexes and in free form in the wild-type strain as well as in the PSI-less mutant. This is in agreement with the fact that no ScpE protein was detected in isolated PSII (Figure II-5).

Discussion

In various plant genomes, one-helix proteins with high similarity to the first and third helices of the plant chlorophyll *a*/*b*-binding antenna proteins have been detected (Heddad and Adamska, 1999; Jansson *et al.*, 2000; Klimmek *et al.*, 2006; Teramoto *et al.*, 2004; Ohta *et al.*, 2003). However, their function still remains enigmatic. In this work, we have shown that ScpC–E of *Synechocystis* sp. PCC 6803 are found in thylakoid membranes. ScpC and ScpD are associated with PSII, whereas ScpE is not associated with larger membrane complexes.

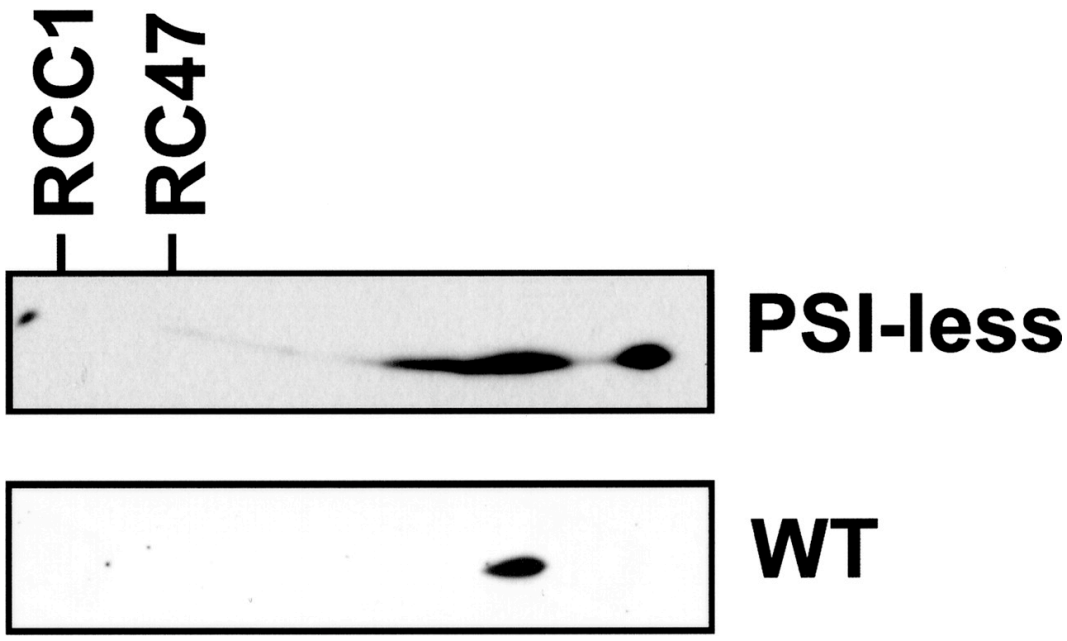

Figure II-6: ScpE is not associated with PSII. Shown is the localization of ScpE after two-dimensional BN/SDS-PAGE analysis of thylakoid membrane proteins from the PSI-less and high light-induced wild-type (WT) strains. Thylakoid membrane proteins were separated in the first dimension by BN-PAGE and in the second dimension by denaturing SDS-PAGE using a 12–20% linear gradient polyacrylamide gel, blotted onto polyvinyl difluoride membrane, and immunostained using anti-ScpE antibodies.

Plant one-helix proteins (Jansson *et al.*, 2000) are apparently involved in pigment-related processes other than light harvesting, and a light-harvesting function can also be excluded for the SCPs of *Synechocystis* sp. PCC 6803 (Xu *et al.*, 2002; Xu *et al.*, 2004). The whole *cab* gene family has been suggested to have originally evolved to serve a function in photoprotection, and the role in light harvesting may be a derived function (Jansson, 2005).

Instead, the SCPs affect steps in the chlorophyll biosynthesis pathway (Xu *et al.*, 2002) and chlorophyll stability in the cell, even in darkness (Xu *et al.*, 2004). Interestingly, the one-helix CAB-like proteins in different organisms exhibit regulatory responses opposite to those of their relatives, the light-harvesting proteins: at high light intensity, when the expression of the LHC proteins is repressed, the one-helix

proteins/SCPs are up-regulated. Also, the SCPs are up-regulated under many stress conditions (He *et al.*, 2001). This indicates a function in protection in a broad sense; they might provide either direct protection (for example, as a pigment carrier) or indirect protection by regulating pigment metabolism. From a sequence perspective, it is likely that they bind pigments (chlorophylls and carotenoids), as chlorophyll-binding residues in the CAB family are conserved in SCPs, and deletion of SCPs leads to a decrease in chlorophyll and carotenoid content of cells (Xu *et al.*, 2004).

According to the results of this study, ScpD is clearly associated with PSII. PSII core proteins co-purified with ScpD-His and formed a complex that was retained during BN-PAGE, at least when PSII was monomeric. Association of SCPs with PSII has not been observed thus far in crystallography studies of PSII (Zouni *et al.*, 2001; Kern *et al.*, 2005; Ferreira *et al.*, 2004) or in proteomic PSII association studies (Kashino *et al.*, 2002), as SCPs are apparent only under conditions of high light exposure. In PSII, ScpD seems to be associated most closely with CP47; CP47 was the most prominent band after purification of ScpD-His. However, after solubilization in the presence of increased detergent concentration, also Psb28 was detected in association with ScpD. Psb28 (Sll1398) has been found to be a substoichiometric subunit of PSII (Kashino *et al.*, 2002) and is thought to have a regulatory function. As it is considered to reside on the stromal side of PSII, it might stabilize the complex between ScpD and CP47 (Figure II-7).

Another interesting association of the light-stressed ScpD-His/PSII complex is that with several FtsH proteases. Deletion analysis of single FtsH protease in *Synechocystis* has shown that Slr1604 is crucial for the survival of cells, a phenotype that also has been observed in the deletion of Slr0228 (Nixon *et al.*, 2005). However, deletion of Sll1463 does not show a phenotype. Our mass spectrometry analysis showed

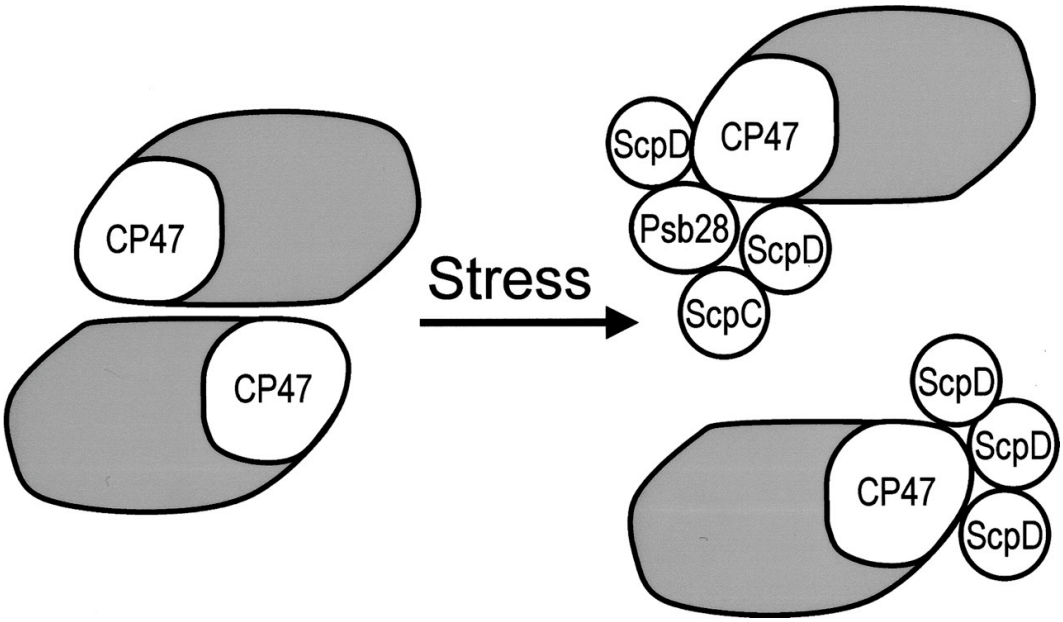

Figure II-7: Model of ScpD binding to PSII. Stress conditions cause PSII monomerization. ScpD and probably also ScpC bind to the monomers and are located close to CP47. Substoichiometric Psb28 might stabilize the binding between CP47 and ScpC/ScpD.

that this gene was expressed and that its product was apparently associated with PSII. Therefore, it is most likely involved in repair of light-stressed PSII. The co-purification of PSII and FtsH with ScpD-His suggests that ScpD is associated with the PSII repair process. This provides an explanation for the fact that ScpD was found to be associated with monomeric PSII (Figure II-2), which is often correlated with PSII repair processes. Indeed, the relatively weak Coomassie Blue staining of the monomeric PSII band suggests that ScpD forms a protective shield around PSII, most prominently interacting with the chlorophyll-binding protein CP47, which is near the periphery of the complex.

As ScpD has chlorophyll-binding potential but does not contribute to light harvesting (Xu *et al.*, 2004), an attractive hypothesis is that ScpD polypeptides serve as a chlorophyll storage device while PSII is repaired and components are replaced. Indeed, the rate of turnover of chlorophyll is much lower than that of the PSII protein

components with which it is associated (Vaviline *et al.*, 2005). Multiple ScpD and/or ScpC proteins may be associated with PSII, thus providing an explanation for the high level of SCPs relative to PSII (Figure II-2).

ScpC is part of PSII as well. Upon BN/SDS-PAGE of complexes from a PSII-less mutant, ScpC and ScpD migrated as low molecular mass complexes or as free proteins (data not shown). After denaturing PAGE, ScpC migrated at a slightly higher molecular mass compared with ScpD. ScpC and ScpD substitute for each other's function (Xu *et al.*, 2004) and have been hypothesized to form a complex (He *et al.*, 2001). Although ScpD is generally more abundant than ScpC in light-stressed wild-type cells, the ScpC/ScpD ratio may vary. ScpB was found by mass spectrometry analysis in the fraction co-isolating with ScpD-His (Figure II-1). Although this suggests that ScpB is associated with ScpD, the pulse-labeling pattern of PSII in the absence of *scpB* was similar to that of the control (Figure II-4). ScpE is present in thylakoids, but is not found to be associated with ScpD. Interestingly, ScpB and ScpE have the strongest influence on chlorophyll biosynthesis (Xu *et al.*, 2002). ScpA is the C-terminal part of ferrochelatase. In this study, we did not include ScpA, suggested to have an important function in regulating the tetrapyrrole pathway at the branch point between chlorophyll biosynthesis versus heme/phycobilin biosynthesis. It has been shown that decreased ferrochelatase activity improves photoautotrophic growth of a PSII mutant because of increased supply of chlorophyll (Sobotka *et al.*, 2005) and that the ScpA domain is important for the ferrochelatase function.

Based on the considerations provided here, the most plausible explanation regarding the function of ScpC and ScpD in light-stressed PSII is pigment storage during protein turnover. As such pigments may not be able to transfer energy to functional

photosystems and as there is no evidence for high chlorophyll fluorescence from pigments while photosystems are being repaired, excitations of pigments associated with SCPs should be quenched efficiently. However, these pigments should not be in excitation transfer contact with PSII pigments so that they do not decrease light-harvesting efficiency under conditions in which light is not in excess. There may be parallels between PSII interaction with SCPs versus the interaction between IsiA and PSI. IsiA has been found to form a ring around PSI, which is functional in light harvesting, but also empty rings that are effective energy dissipaters have been detected (Kouril *et al.*, 2005). Similarly, ScpD and ScpC may form a ring around damaged PSII centers, aid in repair, and dissipate absorbed energy as needed.

CHAPTER III. PHOTOSYSTEM II COMPONENT LIFETIMES IN THE CYANOBACTERIUM *SYNECHOCYSTIS* SP. PCC 6803: SMALL CAB-LIKE PROTEINS STABILIZE BIOSYNTHESIS INTERMEDIATES AND AFFECT EARLY STEPS IN CHLOROPHYLL SYNTHESIS

Abstract

In order to gain insight in the lifetimes of PSII chlorophyll and proteins, a combined stable-isotope labeling (^{15}N) / mass spectrometry method was used to follow both old and new pigments and proteins. PSI-less *Synechocystis* cells were grown to exponential or post-exponential phase and then diluted in BG-11 medium with ^{15}N-ammonium and ^{15}N-nitrate. PSII was isolated, and the masses of PSII protein fragments and chlorophyll were determined. Lifetimes of PSII components ranged from 1.5 h to 40 h, implying that at least some of the proteins and chlorophyll turned over independently from each other. Also, a significant amount of nascent PSII components accumulated in thylakoids when cells were in post-exponential growth phase. In a mutant lacking small Cab-like proteins (SCPs), most PSII protein lifetimes were unaffected but the lifetime of chlorophyll and the amount of nascent PSII components that accumulated were decreased. In the absence of SCPs one of the PSII biosynthesis intermediates, the monomeric PSII complex without CP43, was missing. Therefore, SCPs may stabilize nascent PSII protein complexes. Moreover, upon SCP deletion the rate of chlorophyll synthesis and the accumulation of early tetrapyrrole precursors were drastically reduced. When ^{14}N-aminolevulinic acid (ALA) was supplemented to ^{15}N-BG-11 cultures, the mutant lacking SCPs incorporated much more exogenous ALA into chlorophyll than the control demonstrating that ALA biosynthesis was impaired in the absence of SCPs. This illustrates the major effects that

non-stoichiometric PSII components such as SCPs have on intermediates and assembly, but not on the lifetime of PSII proteins.

Introduction

Cyanobacteria, algae, and plants can use sunlight and water to carry out oxygenic photosynthesis. In these organisms, linear photosynthetic electron transfer is catalyzed by the thylakoid-embedded protein complexes PSII, cyt b_6f, and PSI. Linear electron transfer provides electrons to NADP producing NADPH and transfers protons across the thylakoid membrane leading to a proton gradient that is used for ATP synthesis. NADPH and ATP can be used for carbon fixation producing organic compounds. These organic compounds, along with oxygen produced in water splitting in PSII, enable heterotrophic, aerobic life on Earth.

The photosystems are multi-protein subunits that non-covalently bind different cofactors, including chlorophyll *a*, carotenoids, quinones, lipids, and several inorganic ions. During photosynthesis, components of PSII complexes turn over rapidly, at least in comparison to PSI complexes (Powles, 1984; Sonoike, 2006). Of the proteins in the PSII complex the PsbA (D1) protein turns over most rapidly in the light (Mattoo *et al.*, 1984; Ohad *et al.,* 1984). This rapid turnover presumably is due to redox chemistry at the water-splitting complex and/or to reactive oxygen species that are generated from oxygen reacting with the triplet state chlorophyll formed upon charge recombination between the primary donor $P680^+$ and the primary acceptor pheophytin $(Phe)^-$ (Vass *et al.*, 1992; Macpherson *et al.*, 1993; Krieger-Liszkay, 2005). According to pulse-chase experiments, the D1 protein has a half time of 30 min to 1 h under intense illumination (Prasil *et al.*, 1992). However, the other PSII components appear to have a much lower turnover rate. For example, the halftime of the PsbB (CP47) protein was estimated to be about 12 h

(Schuster *et al.*, 1988; Mattoo *et al.*, 1999), and the lifetime of total chlorophyll in *Synechocystis* cells is over a week (Vavilin *et al.*, 2005). If this vast disparity in the lifetime of PSII components indeed is true, then careful orchestration of the synthesis, assembly, and repair of photosynthetic complexes is required as free chlorophyll in the cell would be harmful in the light and in the presence of oxygen and as PSII polypeptides that are not incorporated in a complex may not be stable in the membrane (Mullet *et al.*, 1990; Krieger-Liszkay, 2005; Triantaphylides and Havaux, 2009).

In the cyanobacterium *Synechocystis* sp. PCC 6803, there are five small Cab-like proteins (ScpA-E), which are single-helix membrane proteins that are located in the thylakoid membrane (Funk and Vermaas, 1999). The presence of the CAB (chlorophyll *a*/*b*-binding) motif in SCPs suggests that SCPs bind chlorophyll molecules at motifs similar to those of LHCII in plants (Jansson, 1994; Jansson *et al.*, 2000; Vavilin *et al.*, 2007; Storm *et al.*, 2008). SCPs appear to play an important role in early stages of tetrapyrrole biosynthesis and may regulate chlorophyll availability (Xu *et al.*, 2002). However, unlike CAB proteins that are associated with functional PSII in plants and are involved in light harvesting and non-photochemical quenching (NPQ), at least two of the SCPs (ScpC and ScpD) have been found to be associated with damaged and/or nascent PSII complexes (Yao *et al.*, 2007). One SCP (ScpA) is fused with ferrochelatase, suggesting a regulatory role in tetrapyrrole biosynthesis (Sobotka *et al.*, 2008). Furthermore, SCPs may prevent the formation of reactive oxygen species by serving as transient carriers of chlorophyll (Xu *et al.*, 2004), and SCPs appear to be involved in PSII re-assembly or/and repair processes by temporarily binding chlorophyll while PSII protein components are being replaced (Vavilin *et al.*, 2007).

Here we expand on the role of SCPs and show that they stabilize nascent PSII complexes and increase the presence of early chlorophyll biosynthesis precursors in the

cell. Stable-isotope labeling and mass spectroscopy allow for a detailed analysis of lifetimes of components of the PSII complex and illustrate that while different components degrade at different rates, degradation of only chlorophyll and to some degree D1 is significantly affected by SCPs.

Materials and Methods

Growth conditions — *Synechocystis* sp. PCC 6803 strains, which included the PSI-less strain (Δ*psaAB*) (Shen *et al.*, 1993), the PSI-less/SCP-less (Δ*scpABCDE*) strain (Xu *et al.*, 2002, Xu *et al.*, 2004), the CP47-His PSI-less strain carrying a His tag at the C-terminus of the CP47 (PsbB) protein (see mutant construction), and the CP47-His PSI-less/SCP-less strain, were cultivated at 30°C in BG-11 medium (Rippka *et al.*, 1979) with 5 mM glucose and buffered with 10 mM *N*-tris(hydroxymethyl)-2-aminoethanesulfonic acid (TES)-NaOH (pH 8.0). Because of the light sensitivity of PSI-less strains, cells were cultured at a light intensity of 4 μmol photons m^{-2} s^{-1}. Cell growth was monitored by measuring the optical density at 730 nm in a 1-cm cuvette using a Shimadzu UV-160 spectrophotometer.

Mutant construction — To generate strains with His-tagged PsbB (CP47), a pUC19-*psbB*-His_6-gentamycin$(Gm)^R$ plasmid was constructed. A DNA region upstream of the His_6-tag including part of *psbB* gene from the HT-3 strain (Bricker *et al.*, 1998) and a DNA region of wild-type *Synechocystis* downstream of the *psbB* gene stop codon were amplified by PCR with artificially generated restriction sites for *Eco*RI right after the stop codon of *psbB*. These two PCR fragments were digested with *Eco*RI and ligated. The ligated DNA fragment containing natural *Kpn*I sites at both ends was cloned into the *Kpn*I site of the pUC19 plasmid. The Gm^R gene from the pHP45-Gm^R plasmid was

introduced into this plasmid by using the *Eco*RI restriction site. The plasmid was introduced into the PSI-less and PSI-less/SCP-less strains to create the CP47-His PSI-less and CP47-His PSI-less/SCP-less strains. Insertion of the *psbB*-His gene at the desired location, replacing the native *psbB* gene, was confirmed by DNA sequencing, and segregation of the mutant genome in *Synechocystis* was confirmed by PCR.

Isotope labeling and isolation of His-tagged complexes — CP47-His PSI-less cultures were grown to OD_{730}~0.65 (exponential phase) or 0.9 (post-exponential phase) and were diluted four-fold in BG-11 medium containing 4.5 mM $Na^{15}NO_3$ and 2 mM $^{15}NH_4Cl$. Cell samples were collected at 1, 3, 9, 24 and 48 hours after the dilution. Cell pellets were resuspended in Buffer A (50 mM 2-(N-morpholino) ethanesulfonic acid hydrate (MES)-NaOH (pH 6.0), 10 mM $MgCl_2$, and 25% glycerol), and broken by Bead Beater (BioSpec Products, Bartlesville, OK). Cell homogenates were prepared as described (Bricker *et al.,* 1998). The cell homogenate (at 0.2 mg/mL chlorophyll) was brought to 1% β-dodecyl maltoside and incubated for 35 min at 4°C and centrifuged. The supernatant was then loaded on an affinity column with 3 ml of Ni-NTA agarose (Qiagen). The column was washed with 10 bed (Ni matrix) volumes of Buffer A containing 0.04% β-dodecyl maltoside and 10 mM imidazole. CP47-His and its associated proteins were eluted with 0.04% β-dodecyl maltoside and 100 mM imidazole in Buffer A. The eluted samples were precipitated with an equal volume of 50 mM MES-NaOH and 25% PEG 6000 (pH 6.0) and centrifuged. Isolated CP47-His complex samples were resuspended in Buffer A with 0.04% β-dodecyl maltoside.

Pigment and protein analysis — Isolated CP47-His complexes corresponding to 2 µg of chlorophyll were resuspended in 10 volumes of ice-cold 100% acetone with 0.1% NH_4Cl,

and then incubated at -80 °C for 2 h and centrifuged. Chlorophyll from the supernatant was purified by HPLC using a Waters Spherisorb S10ODS2 semi-prep column (250 X 10 mm) eluted with a water/methanol-acetone gradient, and the mass distribution was determined by MALDI-TOF (Vavilin *et al.*, 2005). The pellet, which contained proteins, was dissolved in SDS sample buffer (86 mM Tris-HCl (pH 8.0), 2.5% SDS, 20 mM dithiothreitol, and 0.25 M sucrose) and loaded on an SDS/12-20% polyacrylamide gradient gel containing 7 M urea (Komenda *et al.*, 2002). The gel was stained with 0.15% Coomassie Brilliant Blue R-250 in a solution of 50% methanol and 10% acetic acid. In-gel digestion to produce peptides for analysis by mass spectrometry (LC-MS/MS) was carried out essentially as described (Shevchenko *et al.*, 1996) using sequencing-grade modified trypsin (Promega/SDS Bioscience). For Blue Native (BN)-2D gels, isolated CP47-His complex samples corresponding to 2 μg chlorophyll were loaded. BN-PAGE was performed on a 5-14% polyacrylamide gradient gel as described (Schagger and von Jagow, 1991). For separation of proteins in the second dimension, the lanes of the BN gel were excised and incubated with 25 mM Tris/HCl, pH 7.5 containing 1% SDS (v/v) for 30 min at room temperature. The lanes were then layered onto 1.5-mm-thick SDS-PAGE gels. SDS-PAGE and gel staining were performed as described above.

Peptides in trypsin digests were separated using a Dionex Ultimate 3000 liquid chromatography system equipped with both a HPG 3400M high pressure gradient pump and a LPG 3400 MB low pressure gradient pump together with a WPS300TB autosampler and a FLM 3100B column compartment. Solvents used for peptide chromatography were X: water with 0.1% formic acid and Y: acetonitrile with 0.1% formic acid. The LPG 3400 MB pump supplied 5% Y and 95% X at a constant flow rate of 5 μL/min and was used to load 3 μL trypsin-digested samples onto a Dionex Acclaim PepMap 100 C18, 5 μm, precolumn cartridge (300 μm ID x 5 mm length). Sample

loading proceeded for 6 min, after which a valve in the column compartment placed the precolumn cartridge in line with a Dionex Acclaim PepMap 100 C18, 3 μm, capillary column (75 μm ID x 15 cm length) operated at a flow rate of 300 nL/min. Tryptic peptides were then separated using the following linear gradient: 0 to 4 min, 5% Y; 4 to 11.5 min, 5 to 20% Y; 11.5 to 51.5 min, 20 to 50% Y; 51.5 to 59 min, 50 to 65% Y; 59 to 69 min, 65 to 95% Y; 69 to 72 min, 95% Y; 72 to 74 min, 95 to 5% Y, with the remainder at each time being solvent X.

Peptides eluting from the column were analyzed using a Bruker MicrOTOF-Q mass spectrometer equipped with an online nanospray source. Calibration was performed prior to running the first sample using sodium iodide clusters sprayed from a 200 μM solution in acetone. The inlet capillary of the mass spectrometer was set at -1500 V relative to the spray needle, and nitrogen drying gas was supplied at 180 ^{o}C and a flow rate of 3 L/min. Spectra were acquired over an m/z range of 50 to 1800. Automatic MS/MS analysis with argon as the collision gas occurred at peak intensities greater than 2000 counts, with doubly charged precursors preferred. Collision energy settings for doubly charged ions were 16 eV at m/z = 350, 28 eV at m/z = 800, and 44 eV at m/z = 1200 and beyond. Collision energy settings for triply charged ions were 14 eV at m/z = 350, 24 eV at m/z = 800, and 45 eV at m/z = 1200 or greater. Data were acquired with a digitizer rate of 2 GHz with a spectra summation rate of 2 Hz. After summation of two spectra, acquisition of MS/MS spectra on each precursor was excluded for one minute.

Data analysis, including deconvolution, was performed using Bruker Data Analysis 3.4 or 4.0 software and compound mass lists exported to Biotools 3.1 as Mascot Generic (mgf) files. Peak lists were then submitted online to the Matrix Science website (www.matrixscience.com) to search databases for peptide identification using the Mascot search engine.

The percentage of unlabeled protein remaining as a function of time was corrected for growth of the culture (OD_{730}) during the time of labeling in order to be able to compare all data to those at time 0. For example, if cells doubled every 24 h and unlabeled protein at 24 h was 30% of the total intensity for that protein fragment (the remaining 70% of the protein being labeled), the % of unlabeled protein (relative to the amount at time 0) was entered as 2×30%=60% in Figure III-3 and III-4.

Chlorophyll synthesis upon illumination — PSI-less/Δ*chlL* and PSI-less/SCP-less/Δ*chlL* strains were grown in regular BG-11 medium with 5 mM glucose and 10 mM TES/NaOH (pH 8.0) in darkness for a week (Wu and Vermaas, 1995). Subsequently, cells were diluted four-fold in BG-11 medium with 5 mM glucose and 10 mM TES/NaOH (pH 8.0) and also containing 4.5 mM $Na^{15}NO_3$ and 2 mM $^{15}NH_4Cl$. Cells were then exposed to continuous illumination at an intensity of 4 μmol photons m^{-2} s^{-1}. Culture samples were collected after 1, 3, 6, 9, 12, and 24 hours. Pigments were extracted from the cells with 100% methanol. Chlorophyll was purified by HPLC and analyzed by MALDI-TOF.

Oxygen evolution — Oxygen evolution measurements were performed on intact cells at 30 °C using a Clark-type electrode (Hansatech, Cambridge, UK). Electron acceptors were 2.0 mM $K_3Fe(CN)_6$ and 0.4 mM 2,5-dimethyl-*p*-benzoquinone. The light intensity (after filtering through a water filter and a filter transmitting >550 nm light) was saturating (2,500 μmol photons m^{-2} s^{-1}).

Fluorescence spectroscopy — Fluorescence emission spectra of intact cells were measured at 77 K using a SPEX Fluorolog 2 instrument (SPEX Industries, Edison, NJ). Measurements were carried out with excitation and emission slit widths of 1 and 0.25

mm, respectively, which correspond to bandwidths of 4 and 1 nm. The excitation wavelength was 435 nm.

Aminolevulinic acid (ALA) supplementation — PSI-less and PSI-less/SCP-less strains were propagated for 2 weeks in ^{15}N BG-11 medium lacking unlabeled nitrate but containing 9 mM $Na^{15}NO_3$, 10 mM TES-NaOH (pH 8.0), and 5 mM glucose. As needed, cell cultures were diluted from OD_{730}=0.9 to an OD_{730} of about 0.3 with fresh ^{15}N BG-11 medium. After two weeks, 4 mM ALA (^{14}N) was added to the culture. After cells were grown for an additional 24 h, pigments were extracted from the cells with 100% methanol. Chlorophyll was purified by HPLC and analyzed by MALDI-TOF.

Results

Identification of PSII components — In order to determine the lifetime of PSII components, CP47-His PSI-less *Synechocystis* cells were grown in the presence of $^{15}NO_3^-$ and $^{15}NH_4^+$ for a specific time period. After harvesting and breaking the cells, the total membrane fraction was solubilized using β-dodecyl maltoside, and PSII complexes were isolated via Ni-column chromatography. Subsequently, PSII proteins were separated by SDS-PAGE and analyzed by LC-MS/MS mass spectrometry. The PsbA (D1), PsbB (CP47), PsbC (CP43), PsbD (D2), PsbE and PsbF (cytochrome b_{559}), PsbH, PsbO, and Psb27 proteins were identified in the gel (Figure III-1) and their identity was confirmed by mass spectrometry analysis. Mascot scores for PSII proteins are indicated in Table III-1. All proteins were identified reliably, but the score for PsbF was rather low as only a single peptide was identified for this component. In addition, Slr0909, a protein of unknown function whose gene is located 3.5 kbp downstream of the *psbB* gene in the *Synechocystis* genome, and the translation elongation factor Tu (Sll1099) were identified

in the fraction purified on the Ni column. The pattern of proteins co-isolating with the His-tagged CP47 was identical in the PSI-less strain and the PSI-less/SCP-less strain (Figure III-1).

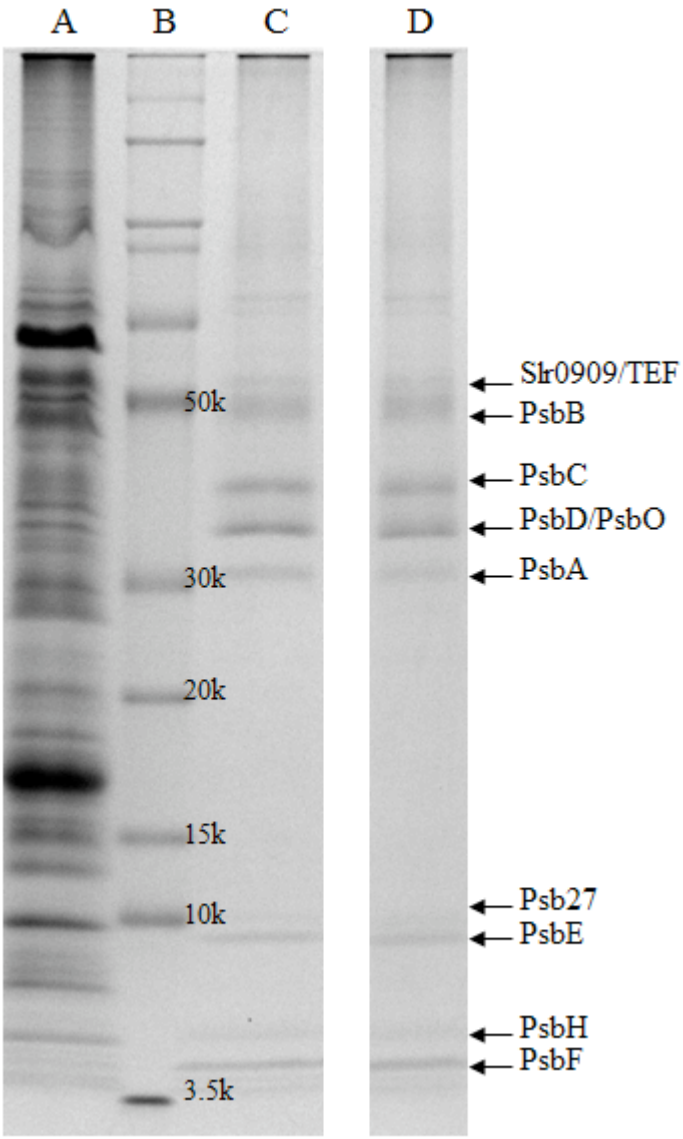

Figure III-1: CBB-stained SDS-PAGE gel of components co-isolating with CP47-His purified via nickel affinity chromatography. A. Fraction from PSI-less cells obtained during the washing step (0.04% β-dodecyl maltoside and 10 mM imidazole in Buffer A). B. Protein ladder. C and D. Fractions from PSI-less cells (C) and PSI-less/SCP-less cells (D) obtained in the elution step (0.04% β-dodecyl maltoside and 100 mM imidazole in Buffer A). Proteins were identified by LC-MS/MS. TEF (translation elongation factor-Tu, Sll1099) and Slr0909 co-purified with the PSII proteins.

Table III-1: Average Mascot scores of mass spectrometric identification of tryptic peptides of PSII proteins. The average Mascot score for each protein was calculated from the individual Mascot scores of each sample collected within 9 hours of the start of ^{15}N-labeling for all proteins except the PsbA protein; for PsbA, only samples collected within 3 hours of the start of ^{15}N-labeling were used. Longer labeling times had insufficient unlabeled peptides that are used for determining the Mascot score.

Protein	PsbA	PsbB	PsbC	PsbD	PsbE	PsbF	PsbH	PsbO	Psb27
Average Mascot Score	245±93	689±222	540±152	382±131	191±45	40±14	72±28	330±114	169±87

PSII dynamics — When using a stable isotope (^{15}N) rather than traditional pulse-chase labeling with a radiolabeled tracer, both old (unlabeled) and new (labeled) peptides can be monitored at the same time using mass spectrometry. In Figure III-2, an example of the analysis is shown for D1 and CP43 peptides. In Figure III-2A the peptides are from close to the N-terminus (residues 65-85 of D1, unlabeled base mass of 2,057; and 123-139 of CP43, unlabeled base mass of 2,052). These masses increase to 2,080 and 2,071, respectively, if these peptides are fully ^{15}N labeled. Figure III-2A shows LC-MS mass spectra of the D1 peptide after 1 h of ^{15}N-labeling and of the CP43 peptide after 9 h of labeling. The group of peaks on the left side of the spectra represents old peptides (unlabeled); slightly heavier molecules are due to natural abundance of isotopes. The group of peaks to the right side of the spectra consists of newly synthesized peptides (fully and partially ^{15}N-labeled). The *m*/*z* values are half the theoretical mass due to the double charge of the peptide: $(M+2H)^{2+}$. The spectra of these peptides at 0 h labeling time (Figure III-2, inserts) show a distribution of peaks contributed mainly by the natural abundance of ^{13}C. The distinction between peaks with ^{15}N-label and isotope peaks due to natural isotope abundance is clear (Figure III-2). By comparing the summed amplitude of

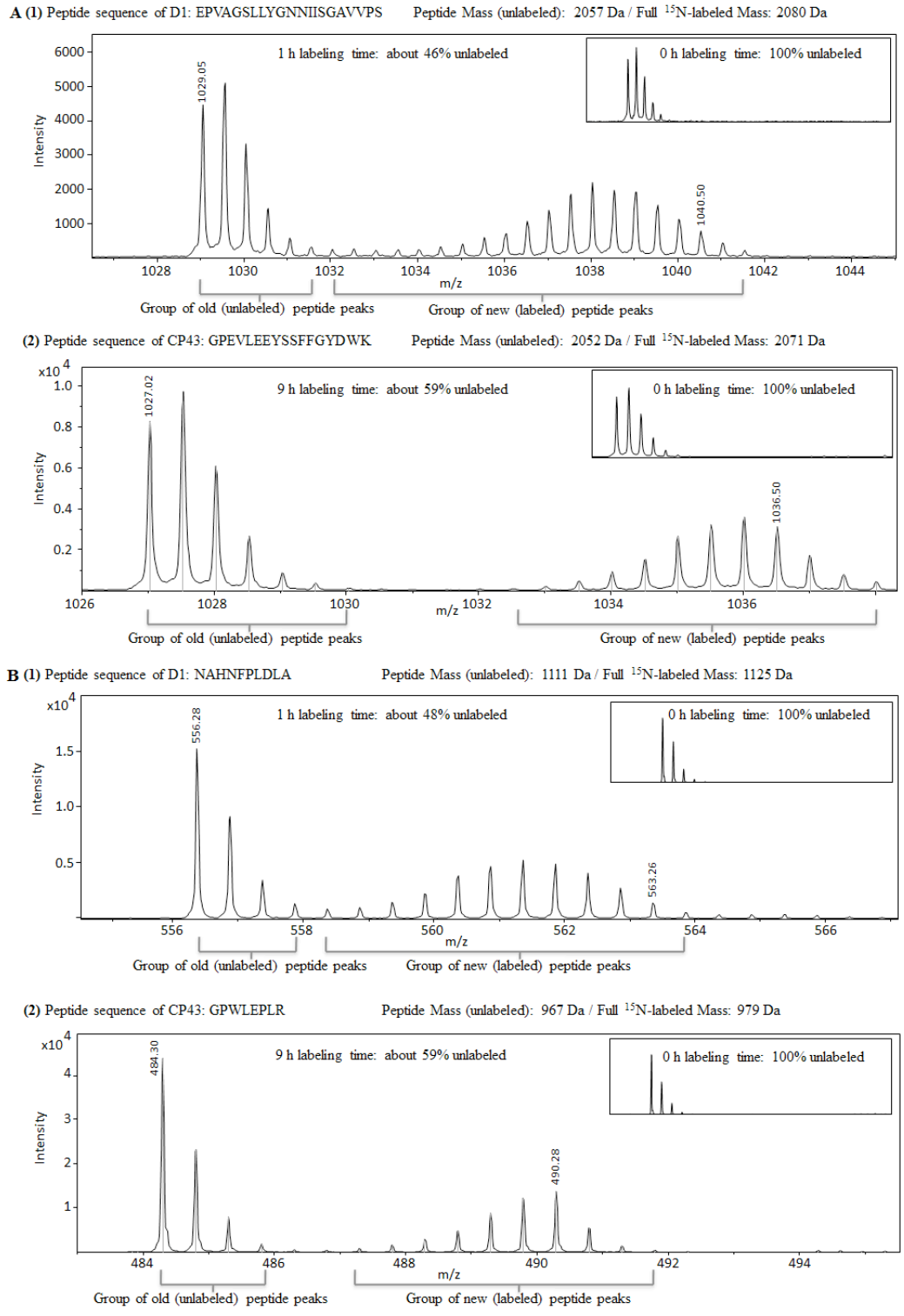

Figure III-2: LC-MS/MS spectra of peptides from near the N-terminus (A) and C-terminus (B) of PsbA (D1) that was ^{15}N-labeled for 1 h (1) and of PsbC (CP43) that was ^{15}N-labeled for 9 h (2) in PSI-less cells. The inserts show controls that were labeled for 0 h. All peptides were detected as doubly charged (z=2) molecules.

the peaks of old vs. new peptides, the ratio between the two can be determined. The N-terminal peptide of the D1 protein had only 46% unlabeled peptides left after 1 h of ^{15}N labeling, indicating rapid turnover of this protein even at low light intensity (4 μmol photons m^{-2} s^{-1}) (Figure III-2A). In contrast, CP43 peptides still were 59% unlabeled after 9 h of ^{15}N labeling (Figure III-2A).

Ribosome pausing has been postulated to occur upon translation of *psbA* message (Zhang and Aro, 2002). If so, then the labeling rate of a C-terminal region of the D1 protein is expected to have a delay relative to that of the N-terminal region. In order to test whether significant ribosome pausing occurs that would delay the labeling of C-terminal regions of the D1 protein, the labeling of a D1 peptide near the C-terminus (Figure III-2B) was compared with that shown in Figure III-2A. After 1 h of labeling the amount of labeled D1 near the C-terminus was 52%, whereas it was 54% near the N-terminus. This suggests that if ribosome pausing occurs, it is no more than a couple of minutes. A similar observation was made for labeling of a CP43 peptide near the C-terminus: after 9 h the amount of labeling (41%) was identical for a peptide near the C-terminus vs. near the N-terminus (Figure III-2).

Labeling of the PSII proteins as well as chlorophyll was followed over time (Figure III-3). The cell number increased during the ^{15}N-labeling period, and therefore the total amount of PSII proteins increased as well. What is indicated in Figure III-3A is the amount of remaining unlabeled protein in the cells over the labeling period relative to the amount of unlabeled protein at time 0. Interestingly, the amount of unlabeled material initially increased in the first 6-9 hours for many of the PSII proteins (except PsbA and PsbD) as well as for chlorophyll. This increase in the amount of unlabeled protein largely was absent in the PSI-less/SCP-less strain (Figure III-3B). The half-lives of PSII components were determined by monitoring the disappearance of old (unlabeled)

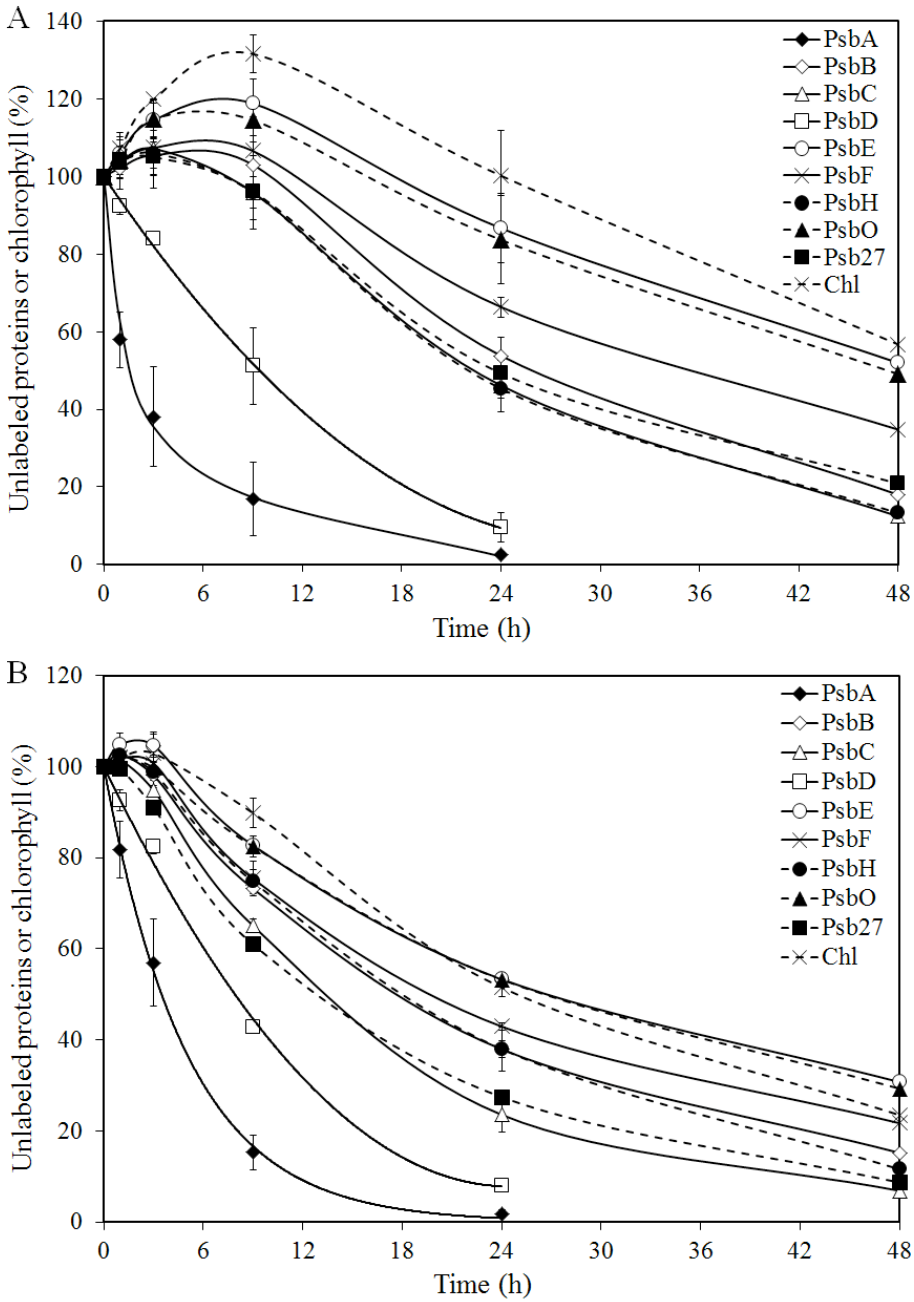

Figure III-3: Turnover of PSII components from PSI-less (A) and PSI-less/SCP-less (B) cells that were harvested in post-exponential growth phase (OD_{730}~0.9). The amount of unlabeled proteins and chlorophyll in these strains was followed during a 48-h period after the start of ^{15}N-labeling. 100% indicates the amount present at the start of labeling. PsbA: ◆ with solid line; PsbB: ◇ with solid line; PsbC: △ with solid line; PsbD: □ with solid line; PsbE: ○ with solid line; PsbF: × with solid line; PsbH: ● with dashed line; PsbO: ▲ with dashed line; Psb27: ■ with dashed line; and chlorophyll (Chl): × with dashed line. Numbers on the y-axis represent the percentage of unlabeled proteins/chlorophyll relative to time 0. Shown are the average results of two independent experiments ± S.D.

peptides in the time period between 9 and 48 hours after the start of labeling, whereas for PsbA and PsbD the time range starting at time 0 h was used (Table III-2). Table III-2 shows that the half-life time of most PSII proteins is independent of the presence of SCPs and that the various PSII proteins have greatly different lifetimes. The half-life of the D1 protein was 1.5 h in the PSI-less strain whereas the D2 protein was 5-fold more stable with a half-time of 7.5 h. The CP47 and CP43 proteins and the PsbH protein that participates in the binding of chlorophyll together with CP47 (Muh *et al.*, 2008) are about 2-fold more stable than D2, with half-times of 13-15 h. The cytochrome b_{559} proteins (PsbE and PsbF proteins), which are the anchor proteins for PSII (Stewart and Brudvig, 1998), are the most stable intrinsic PSII proteins with half times of about a day. The two luminal proteins, PsbO and Psb27, have lifetimes similar to that of some of the slower-degrading integral membrane proteins. PsbO, the Mn-stabilizing protein in the oxygen-evolving complex, has a particularly long half-life (24-33 hours), presumably because it can be dissociated from damaged PSII and reused for repaired/new PSII. The Psb27 protein, which is an assembly factor mainly associated with CP47 and CP43 of monomeric PSII and non-oxygen-evolving PSII complexes (Kashino *et al.*, 2002; Cormann *et al.*, 2009), had a 13-15 h halftime. Interestingly, in the PSI-less background strain chlorophyll had a half-life time of about 40 h, longer than any of the PSII proteins. This illustrates that chlorophyll is largely reutilized when chlorophyll-binding proteins turn over.

Absence of SCP has been shown to reduce the lifetime of chlorophylls (Vavilin *et al.*, 2007). Removal of SCPs does not greatly alter the half-life time of most PSII proteins. In the PSI-less/SCP-less mutant, the lifetimes of the CP43, PsbE, PsbF, and Psb27 proteins were slightly shorter compared to those in the PSI-less strain (Table III-1),

Table III-2: Comparison of half-lives and lag time of PSII components in PSI-less and PSI-less/SCP-less strains. The half-life times were calculated from the decrease in the percentage of unlabeled protein correcting for the increase in unlabeled protein that occurred for the longer-lived polypeptides and the chlorophyll, particularly in PSI-less cells in post-exponential phase (OD_{730}~0.9). Listed are the average results of two to five independent experiments ± S.D.

	Half-life time (h) / lag time (h)			
Strains	PSI-less		PSI-less/SCP-less	
PsbA (D1)	1.5±0.5[a]	< 1	2.5±0.5	< 1
PsbB (CP47)	15±1	6	15±2	1
PsbC (CP43)	13±1	3	11±2	1
PsbD (D2)	7.5±1	< 1	7±0.5	< 1
PsbE	28±2	7	25±2	2
PsbF	23±3	6	20±2	2
PsbH	14±1	3	15±1	1
PsbO	33±4	6	24±2	1
Psb27	15±1	3	13±1	1
Chlorophyll	40±2	9	20±1	3

[a] In exponential growth phase (OD_{730}~0.65) the half-life time of the D1 protein is 1 h. This difference is due to a small contribution of unlabeled D1 that is incorporated into PSII complexes in cells at higher density (OD_{730}~0.9).

and the PsbO lifetime seemed to have been affected a little more. However, the biggest effect of the SCP deletion was on the lifetime of chlorophyll, which was about 50% shorter relative to that in the PSI-less strain. The fact that absence of SCPs affects the lifetime of PSII-associated chlorophyll more than that of PSII proteins confirms the notion that SCPs aid in chlorophyll stabilization and recycling upon PSII degradation and reassembly (Vavilin *et al.*, 2007). However, as the chlorophyll lifetime in the PSI-less/SCP-less strain exceeds that of the main chlorophyll-binding PSII proteins, CP47 and CP43, some chlorophyll recycling occurs even in the absence of SCPs.

A pool of nascent PSII components — As indicated in Figure III-3 and Table III-2, in the PSI-less strain there was a 3 to 9 h period after the start of labeling during which the amount of unlabeled PSII proteins (except D1 and D2) as well as chlorophyll continued to increase. This cannot be due to a slow incorporation of label into amino acids as otherwise we should also have observed a significant lag for the D1 and D2 polypeptides. Our interpretation of the increase in unlabeled complexes is that there is a significant amount of PSII proteins and chlorophyll in thylakoid membranes that is not incorporated into mature PSII complexes, and that provides parts for PSII assembly and repair.

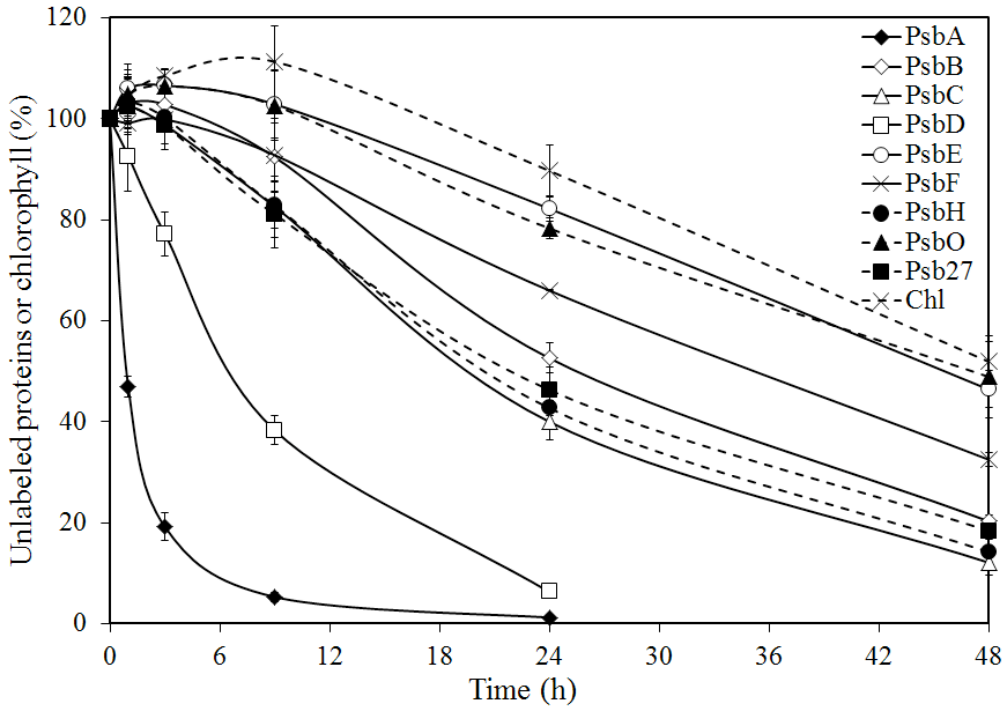

Figure III-4: Turnover of PSII components from PSI-less cells that were harvested in the exponential growth phase (OD_{730}~0.65). The amount of unlabeled proteins and chlorophyll in the strain is followed during a 48-h period after the start of ^{15}N-labeling. 100% indicates the amount present at the start of labeling. PsbA: ◆ with solid line; PsbB: ◇ with solid line; PsbC: △ with solid line; PsbD: □ with solid line; PsbE: ○ with solid line; PsbF: × with solid line; PsbH: ● with dashed line; PsbO: ▲ with dashed line; Psb27: ■ with dashed line; and chlorophyll (Chl): × with dashed line. Numbers on the y-axis represent the percentage of unlabeled proteins/chlorophyll relative to time 0. Shown are the average results of three independent experiments ± S.D.

To test our interpretation of the increase in unlabeled polypeptide being due to a reservoir of unfinished PSII complexes in the cell, the labeling experiment with PSI-less cells was repeated with cells from exponential phase (OD_{730}~0.65) instead of post-exponential phase (OD_{730}~0.9) as in exponential phase the reservoir may be expected to be smaller due to a faster de novo PSII biosynthesis (Figure III-4). The lifetimes of the PSII components were similar to those measured in cells in post-exponential phase. However, the increase in the amount of unlabeled protein is much less and the time over which an increase is observed is much shorter. These results support our interpretation and demonstrate that cells in the post-exponential growth phase tend to accumulate PSII proteins and chlorophyll to be ready for later use.

The role of SCPs — As indicated in Figure III-3B, the increase in the amount of unlabeled PSII protein in cells in the post-exponential phase is much smaller in the PSI-less/SCP-less strain relative to in the PSI-less control, whereas the half-life time of the PSII proteins is not much affected. This is very much comparable to what was shown above for cells in exponential phase. These data suggest that pools of nascent PSII proteins and protein-bound chlorophyll may be stabilized by SCPs.

In order to test the interpretation that SCPs are involved with stabilization of nascent PSII complexes and/or intermediates, isolated PSII samples from the PSI-less strain and the PSI-less/SCP-less strain were run on BN-SDS PAGE. As indicated in Figure III-5, the main difference between PSII complexes from the PSI-less and PSI-less/SCP-less strains was that the RC47(1) complex, corresponding to the PSII monomer form without the CP43 protein, was missing in the PSII preparation from the PSI-less/SCP-less strain. However, the RC47(2) band, corresponding to the RC47 dimer, was

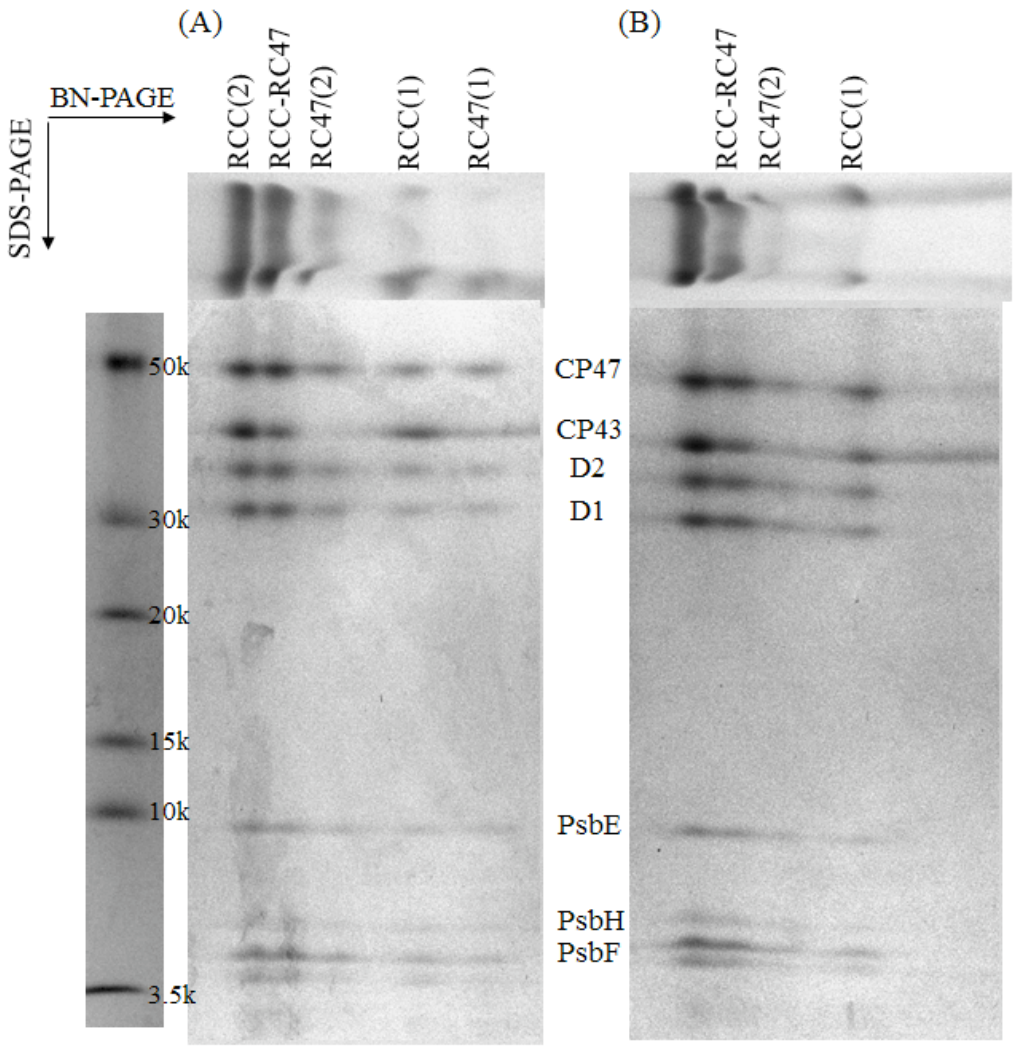

Figure III-5: BN-PAGE followed by SDS-PAGE gel for PSII complexes co-isolating with CP47-His from the PSI-less strain (A) and the PSI-less/SCP-less strain (B). The bands on BN-PAGE (top) are unstained and are colored by the native chlorophyll and Coomassie Brilliant Blue. The SDS-PAGE gel was stained with Coomassie Brilliant Blue. RCC(2): mature PSII dimer; RCC-RC47: PSII dimer lacking CP43 in one of the monomers; RC47(2): PSII dimer lacking CP43 in both monomers; RCC(1): PSII monomer; and RC47(1): PSII monomer lacking CP43.

present in preparations from both strains. In PSII biogenesis, RC47 complexes are assembled from RC complexes (D1, D2, cytb559 and PsbI proteins) and sub-CP47 complexes (CP47, PsbH and SCP proteins) (Promnares *et al.*, 2006, Nixon *et al.*, 2010). SCP association could aid the stability of the RC47 complex before dimerization occurs.

These observations suggest that our interpretation of SCPs stabilizing intermediates in formation of the mature PSII complex is reasonable.

Another role of the SCPs involves chlorophyll binding and stabilization, and earlier work has shown that deletion of SCPs in the PSI-less background strain also affects the chlorophyll content per cell and the accumulation of chlorophyll precursors (Xu *et al.*, 2002; Xu *et al.*, 2004). However, the location of this SCP effect has not yet been pinpointed. The stability of PSII is not affected by SCPs as shown in Table III-2. In line with earlier observations (Vavilin *et al.*, 2007), we do not see evidence of SCPs stably binding a large amount of chlorophyll as the oxygen evolution rate in the PSI-less strain was 2480±80 μmol O_2 (mg Chl)$^{-1}$ h^{-1} whereas in the PSI-less/SCP-less strain this rate was 2730±180 μmol O_2 (mg Chl)$^{-1}$ h^{-1}. Thus, the number of PSII reaction centers on a per-chlorophyll basis is similar regardless of the presence of SCPs.

Earlier work had indicated the lack of accumulation of chlorophyll precursors in SCP-less strains (Xu *et al.*, 2004) suggesting an early block in chlorophyll biosynthesis in the absence of SCPs. The ^{15}N-labeling approach provides an opportunity to monitor the effects of the absence of SCPs in more detail. After growth of the PSI-less/Δ*chlL* and PSI-less/SCP-less/Δ*chlL* strains in darkness for 5 days, the strains had little chlorophyll left as ChlL is required for light-independent protochlorophyllide reduction and chlorophyll synthesis (Figure III-6). After incubation in darkness, the culture was diluted four-fold with medium containing 4.5 mM $Na^{15}NO_3$ and 2 mM $^{15}NH_4Cl$ and the culture was transferred to continuous illumination at 4 μmol photons m^{-2} s^{-1}. As indicated in Figure III-6, during the first 6 hours of illumination, the PSI-less/Δ*chlL* strain synthesized primarily labeled (^{15}N) chlorophyll along with some unlabeled (^{14}N) chlorophyll. Unlabeled chlorophyll may have been synthesized in part from accumulated

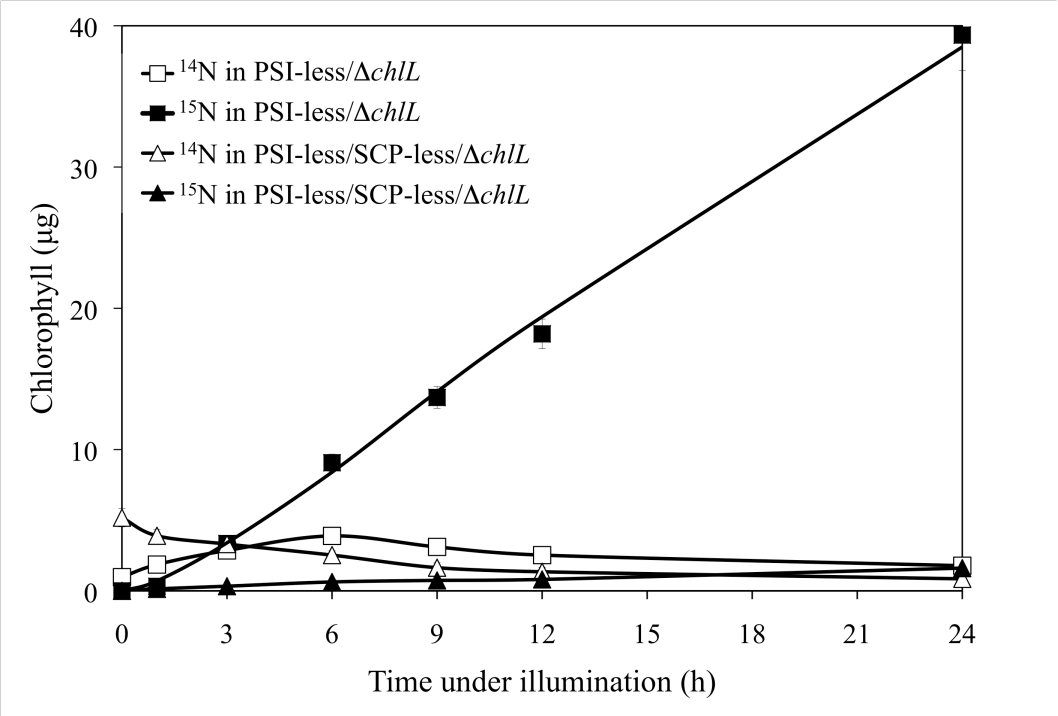

Figure III-6: Unlabeled (^{14}N) and labeled (^{15}N) chlorophyll from the PSI-less/Δ*chlL* and PSI-less/SCP-less/Δ*chlL* strains upon illumination. Cells were grown in the dark for 5 days. The cultures were illuminated after they had been diluted with three volumes of BG-11 medium containing $Na^{15}NO_3$ and $^{15}NH_4Cl$. Chlorophyll was extracted from the cells for analysis at the times indicated. Open and closed symbols represent unlabeled (^{14}N) and labeled (^{15}N) chlorophyll, respectively, in the PSI-less/Δ*chlL* (squares) and PSI-less/SCP-less/Δ*chlL* (triangles) strains. Shown are the average results of two independent experiments ± S.D.

protochlorophyllide or other available precursors. However, in the PSI-less/SCP-less/Δ*chlL* strain the amount of unlabeled chlorophyll decreased, and labeled (^{15}N) chlorophyll was synthesized very slowly (about 20-fold slower than in the PSI-less/Δ*chlL* strain). The decrease in unlabeled chlorophyll and the slow increase in labeled chlorophyll suggest that in the SCP-less mutant the amount of chlorophyll precursors is greatly diminished, and tetrapyrrole biosynthesis is impaired.

A very slow synthesis of PSII in the PSI-less/SCP-less/Δ*chlL* strain was confirmed by 77 K fluorescence emission spectra after 24 hours of illumination (Figure III-7). A peak at 695 nm corresponds to CP47-associated chlorophyll and reflects intact

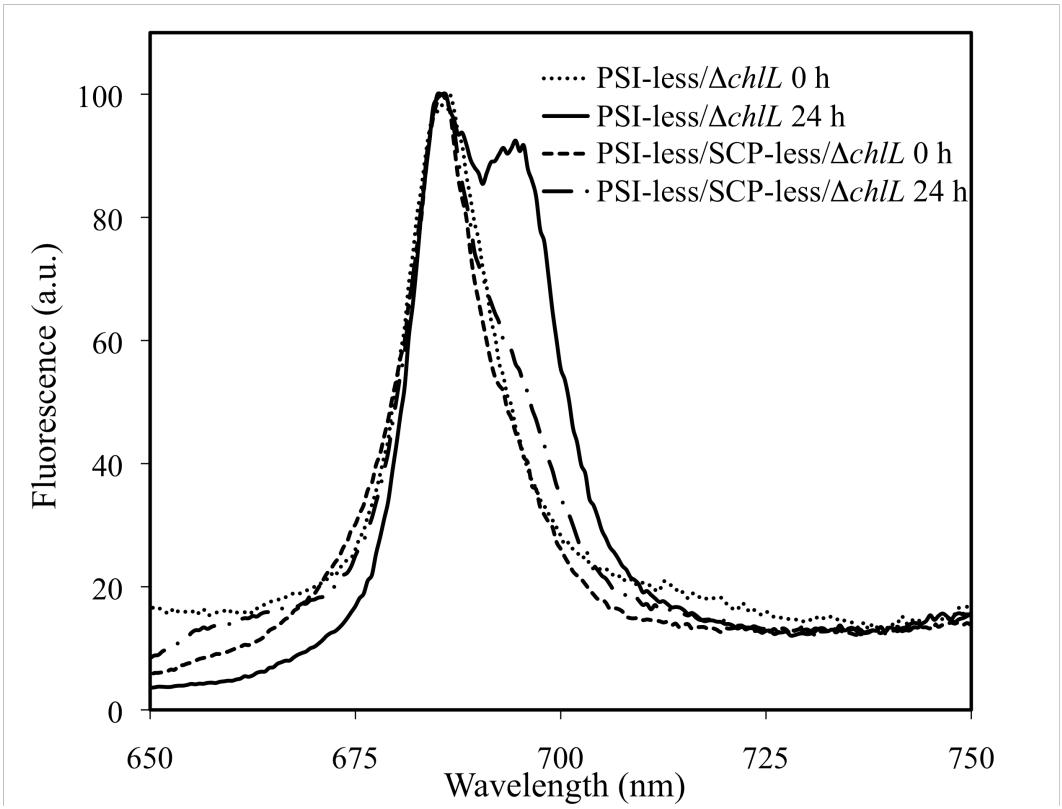

Figure III-7: 77 K fluorescence emission spectra of *Synechocystis* sp. PCC 6803 cells lacking PSI and ChlL. Cells had been grown in darkness for one week and were then transferred to continuous light (4 μmol photons m^{-2} s^{-1}) for 0 h (PSI-less/Δ*chlL*: dotted line; PSI-less/SCP-less/Δ*chlL*: dashed line) or 24 h (PSI-less/Δ*chlL* : solid line; PSI-less/SCP-less/Δ*chlL*: dashed/dotted line). The spectra were normalized to 100 at 683 nm, where phycobilisomes and some chlorophylls emit maximally. The excitation wavelength was 435 nm. a.u., arbitrary units.

PSII complexes. While in the PSI-less/Δ*chlL* strain a significant amount of PSII complexes was present after 24 h of illumination, in the PSI-less/SCP-less/Δ*chlL* strain only very little 695 nm emission was observed.

The very slow chlorophyll biosynthesis and the lack of a large amount of unlabeled chlorophyll synthesis upon illumination of the PSI-less/SCP-less/Δ*chlL* strain suggest that early intermediates in chlorophyll biosynthesis may have been depleted. Therefore, we wished to determine whether aminolevulinic acid (ALA), an early intermediate in tetrapyrrole biosynthesis, was depleted in strains lacking SCPs. As

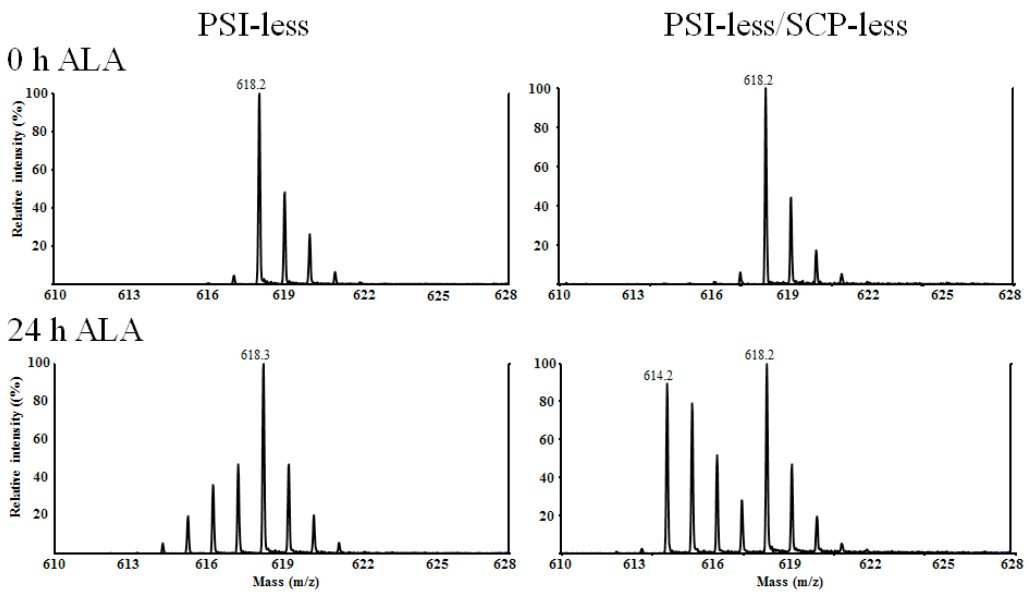

Figure III-8: MALDI-TOF mass spectra of chlorophyll isolated from ^{15}N-grown PSI-less cells with (left) or without (right) SCPs that were supplemented with ^{14}N-ALA for 0 (top) or 24 (bottom) hours. Prior to the experiment, cells were grown in ^{15}N medium, containing $Na^{15}NO_3$, for 10 days, and the culture was diluted with ^{15}N BG-11 to OD_{730}=0.35 at time 0. Unlabeled (^{14}N) aminolevulinic acid (ALA) was added at time 0 to a final concentration of 4 mM.

labeled ALA was not readily available, PSI-less and PSI-less/SCP-less strains, carrying normal ChlL, were grown in ^{15}N medium for two weeks (the culture was diluted with fresh medium as needed) so that chlorophyll in the cells was fully labeled. The cultures were then supplemented with 4 mM ^{14}N-ALA, and cells were grown for 24 hours with added ALA. If cells can readily make their own ALA, then ALA and thereby chlorophyll will be ^{15}N-labeled, whereas if cells are limited in their ALA supply and need to utilize exogenous ALA, then newly synthesized chlorophyll will be mostly unlabeled. Pigments were extracted from both strains, chlorophyll was purified by HPLC, and chlorophyll was analyzed by MALDI-TOF. As shown in Figure III-8, chlorophyll from both strains was fully ^{15}N-labeled at 0 h before the ALA supplementation, as expected. After 24 h of ALA supplementation, during which time the chlorophyll amount in the culture virtually doubled, the mass spectrum of chlorophyll from the PSI-less strain showed that the ALA

used for chlorophyll synthesis primarily was ^{15}N-ALA, which cells had synthesized themselves. In contrast, newly synthesized chlorophyll from the PSI-less/SCP-less strain was primarily unlabeled as the amounts of labeled (original) and unlabeled (newly synthesized) chlorophyll were about the same. These results suggest that the ALA amount is limiting as a consequence of the SCP deletion and that therefore SCPs appear to play an important role in the very early steps of tetrapyrrole biosynthesis (ALA formation).

Discussion

PSII protein and chlorophyll turnover — Previous work with radioisotopes had indicated that different PSII polypeptides differed in their lifetimes (Schuster *et al.*, 1988; Mattoo *et al.*, 1999), and work from our group had indicated that the chlorophyll lifetime in the cell was very long (Vavilin *et al.*, 2005; Vavilin *et al.*, 2007). It is clear that careful orchestration of the synthesis, assembly, and repair of photosynthetic complexes is required, but until now very few data were available on the lifetimes of longer-lived protein components, and there is little known about how this orchestration may occur and how it is regulated. Using stable-isotope labeling combined with mass spectrometry, both labeled (new) and unlabeled (old) peptides can be detected. The rate of disappearance of unlabeled peptides over time determines the turnover rate of the proteins, and this approach allowed an accurate and comprehensive determination of lifetimes of PSII components.

PSII complexes were isolated from PSI-less *Synechocystis* cultures grown at a light intensity of 4 μmol photons m^{-2} s^{-1}, making use of a His-tag attached to the PsbB (CP47) protein. Therefore, only polypeptides and complexes associated with PsbB with an exposed C-terminal His tag will be detected. The fraction obtained after His-tag

affinity purification contained at least nine PSII proteins (seven intrinsic proteins including the reaction center proteins PsbA and PsbD, the chlorophyll-binding proteins PsbB and PsbC, the cytochrome b_{559} proteins PsbE and PsbF, and PsbH, and two lumenal proteins (PsbO and Psb27)). Other PSII proteins may not have stained sufficiently well to be detected. Moreover, a translation elongation factor, Tu (Sll1099), and Slr0909 co-isolated with the PSII complex. In a previous study, Sll1099 was also seen from co-isolating with PSII-associated His-ScpB (Kufryk *et al.*, 2008). Slr0909 is a protein of unknown function, but it is encoded about 3 kbp downstream from *psbB* and *slr0909* could possibly be co-transcribed with *psbB* and an intervening gene of unknown function.

As indicated in Table III-2, PSII proteins have very different half-life times ranging from 1.5 hours up to 33 hours. Therefore, PSII proteins (or groups of such polypeptides) turn over and are replaced independently from each other, and remaining PSII proteins appear to be reused for assembly into a functional PSII complex. Our results confirm the radiolabeling-based interpretations of other groups (Mattoo *et al.*, 1984; Ohad *et al.*, 1984) that rapidly synthesized D1, the PSII protein with the shortest lifetime, is actually incorporated into PSII complexes. The fast turnover of D1 in the PSII complex (5 to 20 times faster than turnover rates of the other PSII proteins) poses a challenge for the PSII complex as D1 is a central rather than a peripheral part of the complex. However, the lipids around the reaction center may facilitate the replacement of damaged D1 proteins (Loll *et al.*, 2007). The other PSII proteins from the damaged complex may stay together and be re-assembled around a new D1 polypeptide, or subcomplexes may form a pool from which new complexes are formed (Smith and Howe, 1993; Zak *et al.*, 2001; Nixon *et al.*, 2005). In the latter case, PSII complexes may be assembled from "old" polypeptides originating from different PSII complexes.

The lifetime of chlorophyll in various mutant strains has been studied earlier by means of stable-isotope labeling, and because chlorophyll is much more stable than chlorophyll-binding proteins according to the lifetimes of chlorophyll-binding proteins estimated from the pulse-chase method, we have suggested that chlorophyll is recycled upon degradation of chlorophyll-binding PSII components (Vavilin *et al*., 2007). In this study, we experimentally support the earlier interpretations by comparing the half-life times of the main chlorophyll-binding proteins in PSII (D1, D2, CP47, and CP43) ($t_{1/2}$=1.5-15 h) with the half-life time of chlorophyll extracted from isolated PSII ($t_{1/2}$=40 h) (Table III-2). Therefore, chlorophyll in damaged chlorophyll-binding proteins can be re-utilized.

SCPs and chlorophyll reutilization — In cyanobacteria the SCP proteins bind chlorophyll, may associate damaged PSII centers, and serve as a temporary pigment reservoir while PSII components are being replaced (Storm *et al.*, 2008, Promnares *et al*., 2006, Yao *et al.*, 2007, Xu *et al.*, 2004). We have now analyzed how SCPs affect the lifetimes of PSII polypeptides and chlorophyll. In line with earlier observations (Vavilin *et al.*, 2007), the lifetime of PSII chlorophyll was reduced by half in the PSI-less/SCP-less strain compared to the PSI-less strain. However, the lifetimes of the chlorophyll-binding proteins in PSII (D1, D2, CP47, and CP43) and of PsbH that participates in the binding of chlorophyll remained essentially unchanged (Table III-2). This indicates that SCPs function primarily in reutilization of chlorophyll and do not affect the stability of chlorophyll-binding proteins.

Interestingly, whereas the lifetimes of PSII proteins were not changed or were decreased slightly in the SCP-less strain, the lifetime of D1 was increased (Table III-2 and Figure III-3). The longer lifetime of D1 may have been caused by slower assembly of

PSII due to the lack of chlorophyll availability, which affects D1 translation and processing in *Synechocystis* (He and Vermaas, 1998). Chlorophyll availability is thought to be lower in the absence of SCPs as the rate of chlorophyll synthesis was decreased 4-fold in the PSI-less/SCP-less strain, and the chlorophyll content per cell was almost 4-fold less than in the PSI-less strain (Figure III-6) (Vavilin *et al.*, 2007, Xu *et al.*, 2004). Therefore, during the replacement of the D1 protein in the PSII repair cycle, the proteins may be waiting for available chlorophylls to assemble PSII, which appears to take longer in the absence of SCPs.

SCPs stabilize nascent PSII protein complexes — As shown in Figure III-3, unlabeled PSII proteins (except D1 and D2) increased for the first 3 to 9 hours of ^{15}N-labeling if late-log cultures are used and SCPs are present. The D1 and D2 proteins did not show this increase in unlabeled protein, excluding the possibility that there is an extensive pool of unlabeled amino acids that remains available for many hours after the start of labeling. Instead, the most plausible explanation is that the increase in unlabeled protein originates from PSII proteins that were present at time 0 but that were not associated with PsbB with an exposed C-terminal His-tag at that time. Figure III-5 shows that the His-tag-isolated samples consist of mature PSII complexes in monomer and dimer forms as well as RC47 (PSII without CP43) dimers and RC47/mature PSII dimers. These complexes are in line with what was observed previously (Herranen *et al.*, 2004; Komenda *et al.*, 2006). However, RC47 monomers were found to occur only in the presence of SCPs, suggesting that SCPs can stabilize biosynthetic intermediates of PSII complexes. Indeed, even when cells are in late-log stage, in the PSI-less/SCP-less mutant very little synthesis of unlabeled PSII components is observed after the start of labeling (Figure III-3B),

suggesting that no significant accumulation of such PSII biosynthesis intermediates occurs if SCPs are absent.

SCPs have been found to be associated with PSII (Yao *et al.*, 2007; Kufryk *et al.*, 2008). Analysis of isolated His-tagged ScpD complexes suggests that ScpD binds to CP47 proteins in the vicinity of PsbH, and SCPs have been found to be associated with PSII throughout its biogenesis, from just CP47 proteins to monomeric PSII complexes (Promnares *et al.*, 2006; Yao *et al.*, 2007). Therefore, even though SCPs do not stabilize PSII components in mature PSII complexes (Table III-2), there is significant SCP-induced stabilization of nascent PSII complexes.

SCPs and ALA biosynthesis — In addition, SCPs also appear to be involved, directly or indirectly, in ALA biosynthesis. This effect results in slow chlorophyll biosynthesis in the absence of SCPs (Figure III-6) and in slow generation of PSII complexes (Figure III-7). In contrast to the PSI-less strain that does not use much exogenous ALA and that therefore can generate and utilize sufficient internal ALA, the PSI-less/SCP-less mutant readily uses exogenous ALA for chlorophyll biosynthesis (Figure III-8). The most straightforward interpretation of these results is that deletion of SCPs in the PSI-less background strain severely impairs the ALA biosynthesis pathway. However, ALA synthesis is thought to occur in the cytoplasm (Joyard *et al.*, 2009), and SCPs are transmembrane proteins located in thylakoid membranes. This suggests that the SCP-mediated regulation of ALA synthesis is not a direct effect but rather may be influenced by intermediate events.

ALA synthesis is a tightly regulated step that is negatively regulated by, for example, protochlorophyllide that accumulates in darkness in plants (Richter *et al.*, 2010). However, based on results of earlier studies, there is no accumulation of

protochlorophyllide or earlier intermediates such as Mg-protoporphyrin IX in PSI-less and PSI-less/SCP-less strains if chlorophyll biosynthesis has not been impaired (Xu *et al.*, 2004). However, chlorophyllide, which is chlorophyll without the phytyl tail, accumulates as the chlorophyll biosynthesis rate and chlorophyll content per cell decrease in the PSI-less/SCP-less strain (Xu *et al.*, 2004). It is possible that chlorophyllide, which is more hydrophilic than chlorophyll, may serve as a signal for ALA biosynthesis enzymes to negatively regulate the output of ALA, thus reducing overall chlorophyll biosynthesis in the PSI-less/SCP-less strain (Figure III-8). Indeed, in plants reduced expression and activity of chlorophyll synthase also has been shown to cause a feedback-controlled inactivation of ALA synthesis (Shalygo *et al.*, 2009).

In conclusion, stable-isotope labeling (^{15}N), mass spectrometry and well-defined mutants are a powerful combination to provide insights in assembly and synthesis of PSII polypeptides and associated cofactors; chlorophyll already is associated with subcomplexes that are intermediates in PSII synthesis. SCPs aid the stability of nascent PSII complexes in PSII biogenesis and also affect the flux from ALA through the tetrapyrrole biosynthesis pathway to chlorophyll. This work illustrates the multiple levels of control and regulation that pigments and SCPs have in PSII synthesis and assembly.

CHAPTER IV. LIFETIMES OF PHOTOSYSTEM I AND PHOTOSYSTEM II PROTEINS IN THE CYANOBACTERIUM *SYNECHOCYSTIS* SP. PCC 6803

Abstract

In order to study the dynamics of photosystem II (PSII) and photosystem I (PSI), the lifetimes of photosynthetic proteins were determined by a combined stable-isotope labeling (^{15}N) / mass spectrometry method. Upon labeling, newly synthesized proteins and chlorophyll were heavier due to isotope incorporation, and old and new pew proteins in the two photosystems could be distinguished. The lifetimes of PSI and PSII proteins ranged from 30 to 75 h and from less than 1 h to 11 h, respectively, and nascent PSI proteins accumulate in the thylakoid membrane. PSI complexes indeed were much more stable than PSII complexes, and the lifetimes of PSII proteins at higher light intensity were decreased from those determined at lower light intensity in a previous study. However, the lifetime of chlorophyll was longer than that of chlorophyll-binding proteins, implying that chlorophyll is recycled. Moreover, the dynamics of PSI and PSII complexes showed that the interchange between monomeric and multimeric forms of PSI and PSII, if multimers indeed are not artifacts, occurs on a timescale of about an hour or less. In the SCP-less mutant, the lifetimes of most PSI proteins and the amount of nascent PSI proteins in the membrane were not affected. Also, from an earlier study, the rate of chlorophyll biosynthesis and the lifetime of chlorophyll did not change. These results indicate that the function of SCPs might not involve the PSI complex and its proteins.

Introduction

Oxygenic photosynthesis in cyanobacteria, algae, and plants is catalyzed mainly by two multisubunit complexes, photosystem I (PSI) and photosystem II (PSII). PSI and PSII are embedded in the thylakoid membrane and are composed of multiple protein subunits that bind chlorophyll, carotenoids, and other cofactors. Electrons provided by PSII originate from water, and PSI provides additional energy from light to produce NADPH. A proton gradient established across the thylakoid membrane upon electron transfer is used for ATP synthesis, and NAPDH is utilized for cellular processes including carbon fixation leading to the synthesis of organic compounds.

In cyanobacteria, the PSII complex consists of 20 protein subunits, together binding 35 chlorophylls; moreover, extrinsic proteins are located on the lumenal side (Guskov *et al*., 2009). According to BN gel results and PSII crystal structures, cyanobacterial PSII complexes are present in dimeric and monomeric forms (Guskov *et al.*, 2009; Herranen *et al.*, 2004). However, the composition and structure of PSI complexes is very different than that of PSII complexes. Compared with PSII, PSI has less protein subunits (12 of them) but a lot more chlorophyll (96 of them), and its extrinsic proteins are located on the cytosolic side (Jordan *et al.*, 2001). Cyanobacterial PSI complexes were found in trimeric and monomeric forms *in vitro* (Herranen *et al.*, 2004; Jordan *et al.*, 2001), but trimeric PSI was never observed in the crystal structure and BN protein gels so far in plants (Jensen *et al.*, 2003; Amunts *et al.*, 2007). However, the most interesting difference between the two photosystems is their stability. The major challenge that PSII complexes face is the photodamage that is caused by oxidizing species. Some components of PSII complexes show a high turnover rate; in particular the D1 protein that binds many cofactors including part of P680 turns over on the timescale

of about an hour (Ohad *et al.*, 1984). In contrast to PSII, PSI is more stable. Therefore, the dynamics of PSII and PSI complexes may be different.

From previous studies, in the cyanobacterium *Synechocystis* sp. PCC 6803 the lifetimes of PSII components at low light intensity (4 μmol photons m^{-2} s^{-1}) had been determined to range from 1.5 h for the D1 protein up to 40 h for PSII-associated chlorophyll (Yao *et al.*, submitted). However, the lifetime of chlorophyll extracted from whole cells in wild type is over 200 h (Vavilin *et al.*, 2007). As most chlorophyll is associated with PSI in cyanobacteria (Guskov *et al.*, 2009; Jordan *et al.*, 2001), this would suggest that PSI-associated chlorophyll is more stable than PSII chlorophyll. In order to gain comprehensive knowledge in the lifetimes of PSI and PSII proteins and their associated chlorophyll, stable-isotope labeling (^{15}N), BN/SDS-PAGE, and mass spectrometry were applied to monitor the fate of old and newly synthesized proteins over time. In addition, Small Cab-like proteins (SCPs), single transmembrane helix proteins, have shown to be involved in PSII chlorophyll recycling. There is also evidence that SCPs stabilize PSI complexes (Wang *et al.*, 2008). In this study, the lifetimes of PSII and PSI proteins and chlorophyll will be determined with and without SCPs, and the dynamics of PSII and PSI complexes between their different forms will be discussed.

Materials and Methods

Strains and growth conditions — The wild-type (WT) and Δ*scpABCDE* (SCP-less) strains (Xu *et al.*, 2002, Xu *et al.*, 2004) of *Synechocystis* sp. PCC 6803 were grown photoautotropically in liquid BG-11 medium (Rippka *et al.*, 1979) at 30 °C at a light intensity of 75 μmol photons m^{-2} s^{-1}. Cell growth was monitored by measuring the optical density at 730 nm in a 1-cm cuvette using a Shimadzu UV-160 spectrophotometer.

Isotope labeling and membrane preparation — Cell cultures were grown to an OD_{730}~0.65 and were diluted four-fold in BG11 medium containing 4.5 mM $Na^{15}NO_3$ and 2 mM $^{15}NH_4Cl$. Cell samples were collected at 3, 9, 24 and 48 hours after the dilution. Cell pellets were resuspended in a mixture of 50 mM 2-(N-morpholino) ethanesulfonic acid hydrate (MES)-NaOH (pH 6.0), 10 mM $MgCl_2$, and 25% glycerol, and broken by Bead Beater (BioSpec Products, Bartlesville, OK). Cell membranes were prepared exactly as described (Bricker *et al.,* 1998) and were stored at -80°C.

PAGE — Wild type and SCP-less membrane samples corresponding to 10 µg of chlorophyll were solubilized in 1% β-dodecyl maltoside for 45 min on ice in darkness; subsequently 0.1 volume of loading solution containing 750 mM aminocaproic acid and 5% Coomassie Brilliant Blue G-250 were added. Protein complexes in the membrane were separated in the first dimension by blue-native (BN) electrophoresis at 4 °C in a 5-14% polyacrylamide gel according to Schagger and von Jagow (1991). For the second dimension, the BN gel lanes were incubated for 45 min at room temperature in a solution containing 25 mM Tris-HCl (pH 7.5), 2% SDS, and 10% mercaptoethanol. The lanes were then layered onto a 1.5-mm-thick SDS/12-20% polyacrylamide gradient gel containing 7 M urea (Komenda *et al.*, 2002). The gel was stained with 0.15% CBB R-250 in a solution of 50% methanol and 10% acetic acid. In-gel digestion to produce peptides for analysis by mass spectrometry (LC-MS/MS) was carried out essentially as described (Shevchenko *et al.*, 1996) using sequencing-grade modified trypsin (Promega/SDS Bioscience).

Protein analysis — Peptides in trypsin digests were separated using a Dionex Ultimate 3000 liquid chromatography system equipped with both a HPG 3400M high pressure

gradient pump and a LPG 3400 MB low pressure gradient pump together with a WPS300TB autosampler and a FLM 3100B column compartment. A Bruker MicrOTOF-Q mass spectrometer equipped with an online nanospray source was used for protein identification. Instrumental setups for HPLC and mass spectrometer and data analysis were described earlier (Yao *et al.*, submitted)

Results

Identification of photosynthetic protein complexes and photosynthetic proteins — Membrane protein complexes from wild-type *Synechocystis* sp. PCC 6803 cells were separated by blue native (BN)-PAGE and then proteins from each individual protein complex were separated by SDS-PAGE (Figure IV-1). Various PSI complexes (PSI supercomplex, and trimeric and monomeric PSI complexes) and PSII complexes (dimeric and monomeric complete PSII complexes, and the CP43-less PSII monomer (RC47)) were identified in membranes from both the wild-type and SCP-less strains. Protein complexes other than photosynthetic complexes, such as NDH complexes, were seen as well. The profile of membrane proteins and complexes were very similar to that in a study from Herranen *et al.* (2001). In order to determine the lifetimes of PSII and PSI proteins, 2D BN/SDS-PAGE as performed with membrane protein samples from wild-type and SCP-less cells grown in the presence of $^{15}NO_3^-$ and $^{15}NH_4^+$ for a specific time period (0 h, 3 h, 9 h, 24 h, and 48 h). PsaA, PsaB, PsaD, PsaF, PsaL, and PsaE from protein spot 1-6 (respectively) in trimeric PSI and PsbB, PsbC, PsbD, and PsbA from protein spot 11-14 (respectively) in monomeric PSII were identified and used to determine their labeling.

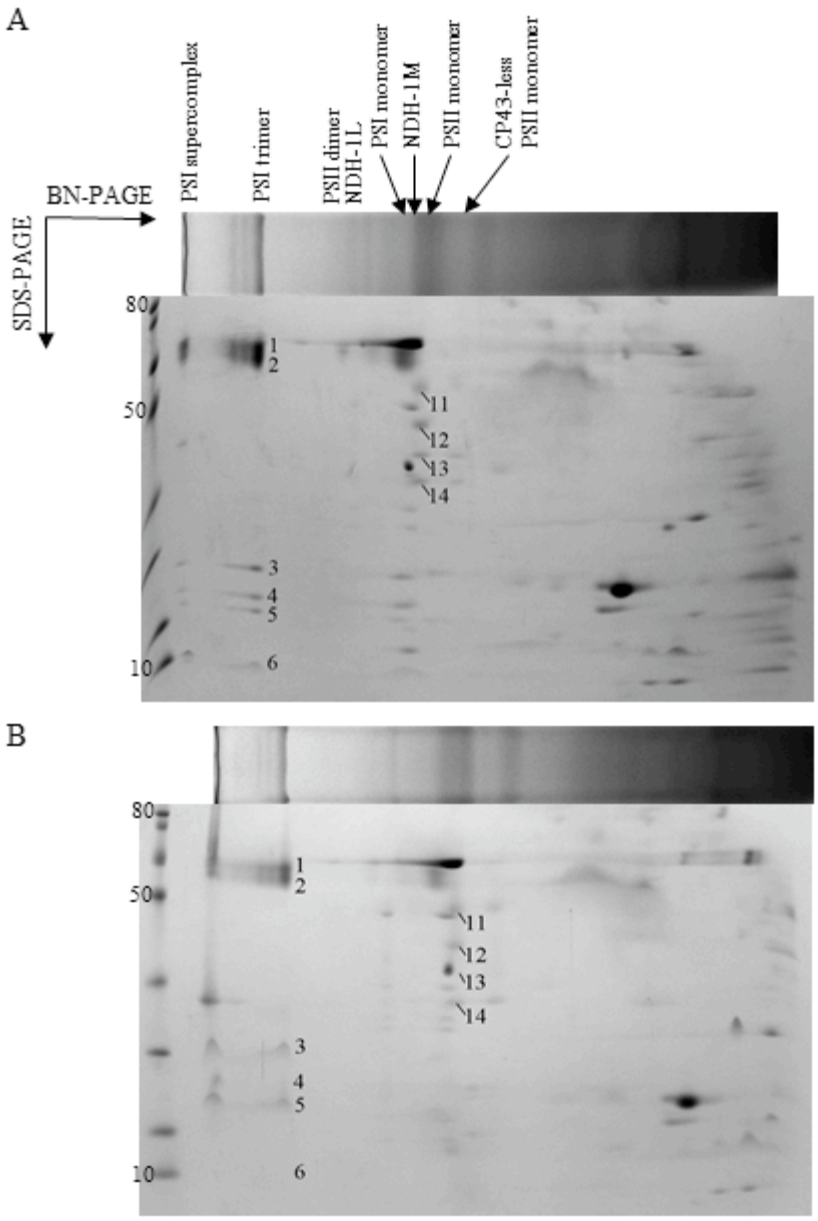

Figure IV-1: BN-PAGE followed by SDS-PAGE gel using membrane proteins from the wild-type (A) and SCP-less (B) strains. The bands on BN-PAGE were visualized by the native chlorophyll and Coomassie Brilliant Blue. SDS-PAGE was stained with Coomassie Brilliant Blue. Protein spots 1-6 were due to the PSI proteins: PsaA, PsaB, PsaD, PsaF, PsaL, and PsaE, respectively, and spots 11-14 were due to the PSII proteins: PsbB, PsbC, PsbD, and PsbA, respectively. The proteins were identified by LC-MS/MS. Marker proteins are to the left. Protein ladder is in kDa.

Dynamics of photosystem I and photosystem II — Labeling and disapprearance of unlabeled PSI and PSII proteins were followed over time (Figure IV-2). The cell number

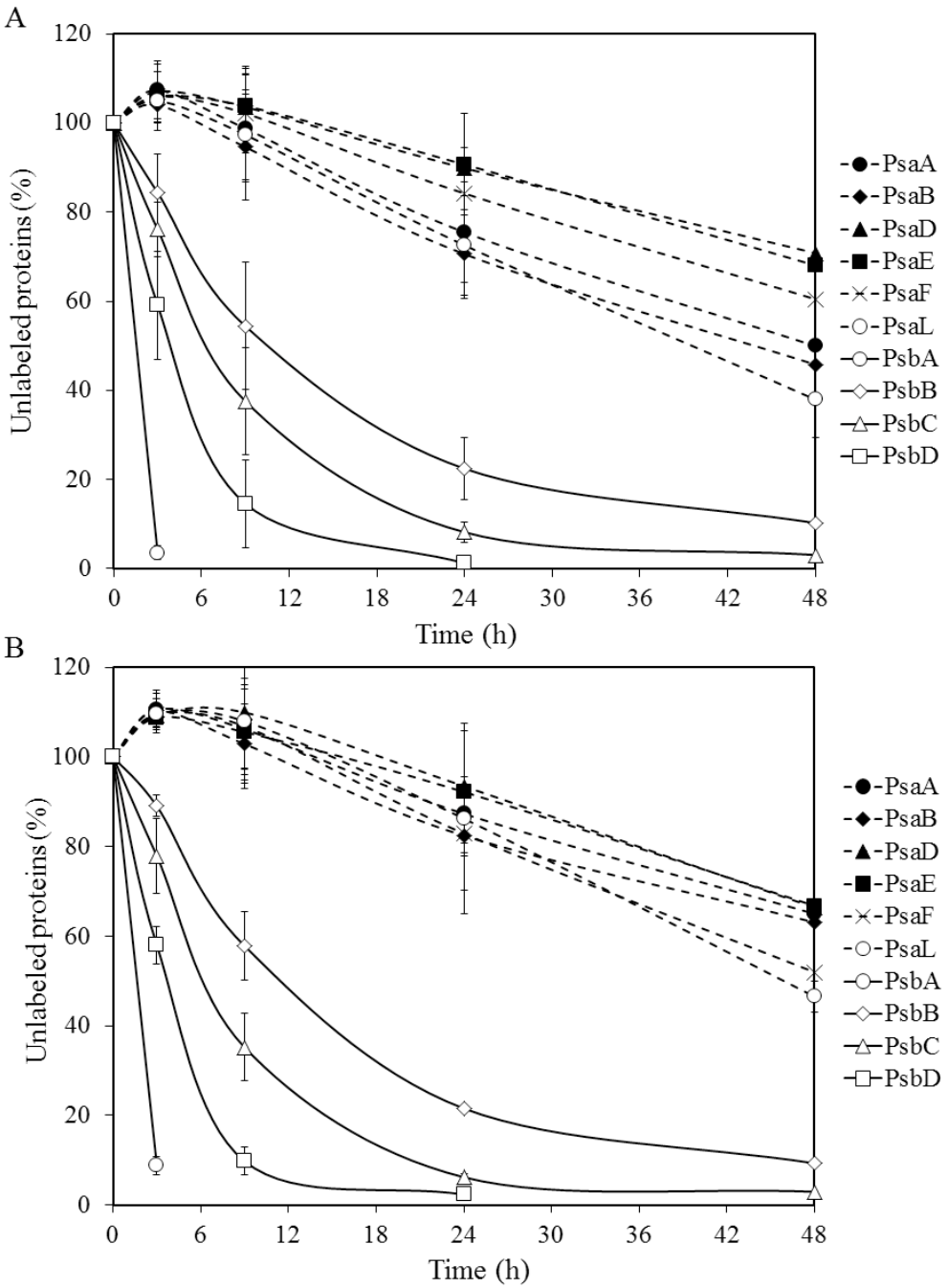

Figure IV-2: Turnover of photosynthetic proteins from the wild-type (A) and SCP-less (B) cells. The amount of unlabeled proteins in the wild-type strain is followed during a 48-h period after the start of ^{15}N-labeling. 100% indicates the amount present at the start of labeling. PSI proteins are in dashed line, and PSII proteins are in solid line. PsaA: ● with dashed line; PsaB: ◆ with dashed line; PsaD: ▲ with dashed line; PsaE: ■ with dashed line; PsaF: × with dashed line; PsaL: ○ with dashed line; PsbA: ○ with solid line; PsbB: ◇ with solid line; PsbC: △ with solid line; and PsbD: □ with solid line. Numbers on the y-axis represent the percentage of unlabeled proteins/chlorophyll relative to time 0. Shown are the average results of two independent experiments ± error.

increased during the ^{15}N-labeling period, and therefore the total amount of proteins increased as well. What is indicated in Figure IV-2A is the amount of unlabeled protein in the culture volume relative to the amount in the same volume at time 0. Interestingly, the amount of unlabeled material increases initially in the first 3 hours for all of the PSI proteins (Figure IV-2A dashed lines) in the wild-type strain. In contrast to PSI proteins, PSII reaction center proteins (D1 and D2) do not show such an increase, and PSII antenna proteins (CP47 and CP43) have a minor lag in the exponential decrease of unlabeled protein (Figure IV-2A solid lines). The half-lives of PSI and PSII components (Table IV-1) were determined by monitoring the disappearance of old (unlabeled) peptides in the time period between 9 and 48 hours after the start of labeling, whereas for PSII proteins PsbA and PsbD half-lives were calculated from time 0 and for PsbB and PsbC starting at 3 hours after labeling. In wild type, the half-lives of PSI reaction center proteins (PsaA and PsaB) are 40 h whereas the other intrinsic PSI proteins, PsaF, which is involved in docking of plastocyanin, and PsaL, which plays a role in formation of the PSI trimer in cyanobacteria (Chitnis and Chitnis, 1993; Fischer *et al.*, 1998; Karapetyan *et al.*, 1999), have half-life times of 50 and 30 h, respectively. The extrinsic proteins (PsaD and PsaE) have longer half-lives (70-75 h) presumably because they can be dissociated from damaged PSI and be reused for repaired or new PSI. The fact that extrinsic proteins have longer half-lives than the intrinsic proteins also has been seen for PSII (Yao *et al.*, submitted). PSII proteins have much shorter half-lives than PSI proteins. Compared with the lifetimes of PSII proteins in the earlier study (Yao *et al.*, submitted), the lifetimes of PSII proteins are much shorter in this experiment, presumably due to the higher light intensity during culture conditions. The unlabeled D1 protein had largely disappeared at the 3-h timepoint. The D2 protein was more stable but had a halftime of a little over 3 h.

Table IV-1: Comparison of half-lives of PSI and PSII components in the wild-type and SCP-less strains. The half-life times were calculated from the decrease in the percentage of unlabeled protein correcting for the increase in unlabeled protein that occurred for the longer-lived polypeptides. Listed are the average results of two independent experiments ± error.

	Half-life time (h)	
Strains	Wild-type	SCP-less
PsaA	40±7	50±4
PsaB	40±7	50±4
PsaD	75±7	50±7
PsaE	70±7	53±4
PsaF	50±7	40±2
PsaL	30±1	30±6
PsbA (D1)	< 1	< 1
PsbB (CP47)	11±2.5	10.5±1
PsbC (CP43)	6.5±1.5	6±0.5
PsbD (D2)	3.3±1	3±0.3

The CP43 and CP47 proteins, the chlorophyll-binding proteins, have halftimes of 6.5 and 11 h, respectively. These results are in line with the concept that PSII complexes turn over much faster than PSI complexes.

As indicated in Figure IV-2A, in the wild-type strain there was a 3 h period after the start of labeling during which the amount of unlabeled PSI proteins continued to increase. This cannot be due to a slow incorporation of label into amino acids as D1 polypeptides were almost fully labeled after 3-h period. Therefore, our interpretation of the increase in unlabeled complexes is that there are nascent PSI proteins in thylakoid membranes that are not incorporated into mature PSI complexes. For the PSII proteins, the PsbB and PsbC proteins show only very small lags in the exponential decrease of unlabeled proteins 3 hours after the start of labeling.

Table IV-2: Comparison of percentage of unlabeled PSI proteins in trimeric and monomeric forms and PSII proteins in dimeric and monomeric forms at 3, 9, 24, and 48 h of labeling. Listed are the average results of one to ten peptides.

		3 h	9 h	24 h	48 h
PsaA	Trimer	96±1	78±2	46±3	14±1.5
	Monomer	95±1	78±1	46±2	13±0.5
PsaB	Trimer	91±1	75±2	43±2	13±1.5
	Monomer	91±2	74±2	43±1	
PsaE	Trimer	94±1	80±1	55±1	18.5±0.1
	Monomer	92±1	78±1	57±1	
PsaF	Trimer	94±0	79±3	51±2	16.5±1.5
	Monomer	93±2	78±3	54±2	11.5
PsaL	Trimer	94±1	76±2	45±1	10±0.5
	Monomer	93±1	78±1		
PsbA	Dimer	2.5			
	Monomer	4.0±1.5			
PsbB	Dimer	80±2	50±3	16±2	3.0±1.5
	Monomer	77±1	47±1	15±2	3.5±1.0
PsbC	Dimer	72±2	37±1	5.5±0.5	1.1±0.2
	Monomer	69±2	34±1	5.5±0.5	1.1±0.1
PsbD	Dimer	59	16±2	0.9±0.1	
	Monomer	58±2	16±1	0.8±0.1	

PSI is thought to exist in both trimeric and monomeric forms, and PSII is thought to exist in dimeric and monomeric forms, based on results of crystal structures and separation of isolated complexes under non-denaturing conditions. In order to get insights in the conversion dynamics of PSI between trimeric and monomeric forms and of PSII between dimeric and monomeric forms, the percentage of labeled and unlabeled PSI and PSII proteins from different forms was monitored upon different times of labeling. Table IV-2 shows the percentage of unlabeled proteins at different times of labeling. Each PSI or PSII protein had a similar lifetime when the complex was in monomeric vs. multimeric

form. These results demonstrate that the different forms of PSI or PSII, if relevant under *in vivo* conditions, are in equilibrium, and the dynamics of PSI and PSII switching between the different forms occurs on a timescale of about an hour or less.

Role of SCPs in the photosystems — In a previous study (Yao *et al.*, submitted), deletion of SCPs in a PSI-less background strain did not change the lifetimes of PSII proteins except of the PsbO protein. This is consistent with current results showing that deletion of SCPs in the wild-type background strain had little effect on the lifetimes of the PSII proteins (Table IV-1, Figure IV-2B solid lines). The half-life time of the intrinsic PSI proteins was not much affected by removal of the SCPs either while the half-life time of the extrinsic PSI proteins (PsaD and PsaE) decreased (Table IV-1). Also, the amount of nascent PSI proteins accumulating in the membrane was not significantly changed upon the removal of SCPs (Figure IV-2). These results indicate that SCPs might not influence the PSI proteins.

Discussion

Pulse-chase methods using radioisotopes have been widely used to estimate the lifetimes of polypeptides. However, this method is difficult for relatively stable proteins as other proteins may be labeled much faster and more intensely. PSI proteins were known to be long-lived proteins, but their lifetimes have not been specifically determined. Using stable-isotope labeling combined with mass spectrometry, we can determine the lifetimes of PSI (long-lived) and PSII (short-lived) proteins in parallel.

Turnover of PSII and PSI proteins — Photosystem complexes and proteins were separated by the BN/SDS-PAGE and identified by LC-MS/MS (Figure IV-1). The

lifetimes of PSII proteins including the reaction center proteins D1 and D2 and the chlorophyll-binding proteins CP47 and CP43 were determined (Table IV-1). However, compared with the lifetime of the PSII proteins in the PSI-less background strain grown at 4 μmol photons m^{-2} s^{-1} in a previous study (Yao *et al.*, submitted), the lifetimes of the PSII proteins in the wild-type strain were decreased by 50% except for the CP47 protein whose lifetime was only decreased by 30%. In the current experiments, the wild-type strain was cultured at a light intensity that was almost 20 times stronger than that used for the PSI-less strain in the previous study. Light intensity is a main factor to determine the length of the lifetimes of PSII core proteins although PSII in the PSI-less strain may easily occur in the acceptor side of photoinhibition under the same light condition compared with the wild-type strain because of over-reduction of plastoquinone pool due to the lack in PSI complexes. The lifetimes of four PSII core proteins showed a logical progression: the D1 protein, where the processes of water oxidation and charge separation take place, appears to experience the most photodamage (Aro *et al.*, 1993); the further the other PSII proteins are from the D1 protein, the longer is their lifetime.

In contrast to PSII proteins, PSI proteins are stable. PsaA and PsaB, the reaction center proteins, had similar lifetimes to the other intrinsic proteins, PsaF and PsaL (Table IV-1). This result demonstrates that the processes of charge separation and electron transport in PSI are very stable and do not rapidly induce protein damage. The PSI extrinsic proteins, PsaD and PsaE, exhibit longer lifetimes than the PSI intrinsic proteins. This phenomenon has also been seen in PSII in a previous study (Yao *et al.*, submitted) as PsbO had a longer lifetime than any of the PSII intrinsic proteins. Extrinsic proteins presumably can be easily dissociated from damaged photosystems and reused for repaired/new photosystems.

As indicated in Table IV-2, the PSI and PSII proteins have the same percentage of unlabeled peptides in the monomeric vs. multimeric form of the photosystems throughout the period of the labeling. These results support the notion that the PSI and PSII complexes dynamically interchange between monomers and multimers. Although the PSII and PSI complexes in X-ray crystals always show up as multimers in cyanobacteria (Jordan *et al.*, 2001; Ferreira *et al.*, 2004; Loll *et al.*, 2005; Guskov *et al.*, 2009), BN gels show both multimers and monomers of PSI and PSII complexes (Herranen *et al.*, 2004), and freeze-fractured micrograph of plant thyakoids reveals PSII dimers and monomers in stacked and non-stacked regions of grana, respectively (Staehelin, 1976; Staehelin, 2003). A possible explanation is that the exchange between monomers and multimers in the thylakoid membrane may be highly dynamic *in vivo*.

Chlorophyll in the photosystems — In the cyanobacterium *Synechocystis* sp. PCC 6803, PSI is an abundant membrane protein complex in the thylakoid membrane binding over 90% of the chlorophyll in cells. Previous studies with ^{15}N-labeling had demonstrated that the lifetime of chlorophyll in the wild-type cells was very long (>200 h), whereas it was much shorter (80 h) in PSI-less cells (Vavilin *et al.*, 2007). This suggests that PSI-associated chlorophyll has a long lifetime. Indeed, PSI proteins have a relatively long lifetime as well (Table IV-1). However, the lifetime of chlorophyll is more than 5 times longer than that of the PSI chlorophyll-binding proteins (PsaA and PsaB). This suggests that chlorophyll is recycled upon degradation of PSI chlorophyll-binding proteins and can be reincorporated into new or existing complexes. The recycling of chlorophyll is also seen in PSII (Vavilin *et al.*, 2007; Yao *et al.*, submitted).

SCPs, chlorophyll, and photosynthetic proteins — Based on previous studies (Vavilin *et al.*, 2007; Yao *et al.*, submitted), the lifetime of PSII chlorophyll is reduced in the PSI-less/SCP-less strain. SCPs function in reutilization of PSII chlorophyll while PSII components are being replaced, and do not affect the lifetimes of PSII chlorophyll-binding proteins. As shown in Table IV-1, the lifetimes of PSI chlorophyll-binding proteins were not affected by removal of SCPs either. In addition, the lifetime of chlorophyll in PSI-containing strains did not change or decreased slightly upon deletion of SCPs (Vavilin *et al.*, 2007). As PSI complexes contain most of chlorophyll in *Synechocystis* cells, SCPs do not appear to play an important role in recycling of chlorophyll from PSI.

The absence of SCPs led to a significant decrease in the amount of nascent PSII proteins/complexes in the PSI-less background strain (Yao *et al.*, submitted). The loss of nascent PSII proteins in the PSI-less/SCP-less strain was interpreted to be due to decrease in the supply of chlorophyll and the reduction of the amount of the PSII complexes. However, as shown in Figure IV-2, there is a small increase in the amount of unlabeled PsbB proteins in the SCP-less strain relative to in the wild type. As SCPs stabilize the nascent PSII complexes such as RC47 complexes (Yao *et al.*, submitted), the increase in unlabeled PsbB proteins in the thylakoid membrane may come from the destabilization of nascent PSII complexes in the SCP-less strain. However, the amount of nascent PSI proteins did not change much upon removal of SCPs as PSI proteins are predominant photosynthetic proteins in wild-type *Synechocystis* cells. Additionally, the lifetimes of PSI proteins and chlorophyll were not affected. SCPs may not function to stabilize nascent PSI proteins and complexes.

In conclusion, the lifetimes of PSI proteins are much longer than the lifetimes of PSII proteins. However, recycling of chlorophyll occurs in both photosystems. PSII and

PSI complexes dynamically exchange between monomeric and multimeric complexes, if multimeric complexes indeed exist *in vivo*, on the order of an hour or less. Upon the removal of SCPs, SCPs have no effects on the lifetimes of most of the photosynthetic proteins, and the lifetime of chlorophyll is mostly unaffected as SCPs only recycle PSII chlorophyll but not PSI chlorophyll. Overall, SCPs do not seem to play an important role in PSI complexes and their components.

CHAPTER V. FUNCTION OF SLL1906, A MEMBER OF THE BACTERIOCHLOROPHYLL DELIVERY FAMILY, IN THE CYANOBACTERIUM *SYNECHOCYSTIS* SP. PCC 6803

Abstract

A deletion mutation was introduced into the *sll1906* gene in the cyanobacterium *Synechocystis* sp. PCC 6803 to examine the function of Sll1906, the corresponding member of the bacteriochlorophyll delivery (BCD) family. The Sll1906 sequence contains possible chlorophyll-binding sites. The pigment profile indicated that the chlorophyll and carotenoids contents were not altered in the mutant, and no chlorophyll precursors accumulated. According to the oxygen evolution and 77 K fluorescence emission spectra, the PSII activity and PSII/PSI ratio remained the same upon deletion of the gene. The *sll1906* deletion was also introduced into the Δ*chlL* background mutant strain, in which chlorophyll is synthesized in the light only. When grown in light-activated heterotrophic growth (LAHG) conditions, the rate of chlorophyll degradation in the Δ*chlL*/Δ*sll1906* mutant was similar to that in the Δ*chlL* background strain. When cells were returned to continuous illumination after a week of growth under LAHG conditions, both the rate of chlorophyll synthesis and chlorophyll-dependent photosystem biogenesis were monitored. The deletion of the *sll1906* gene affected neither. Although *sll1906* deletion did not affect chlorophyll degradation/biosynthesis and photosystem assembly, Sll1906 could still be involved in these processes as other pathways may compensate in the absence of Sll1906.

(In press, *Proc. Photosynth. Congress in Beijing 2010*)

Introduction

Chlorophyll is a key pigment in the process of photosynthesis and chlorophyll *a* is present in all oxygenic phototrophs. However, in the light chlorophyll may give rise to harmful reactive oxygen species if chlorophyll excitation would not be quenched efficiently. Therefore, the concentration of free chlorophyll (not bound to proteins and not close to carotenoids) is minimized in the cell. This is achieved by highly regulating chlorophyll synthesis in conjunction with synthesis of photosynthetic proteins. However, even though chlorophyll biosynthesis has been well studied, it is unknown how, for example, chlorophyll delivery from chlorophyll synthase to chlorophyll-binding proteins occurs. The existence of chlorophyll transfer proteins in oxygenic phototrophs may be expected but has not been demonstrated. However, members of a putative BCD family have been identified in purple bacteria (Saier *et al.*, 1999). The BCD proteins have 12 putative transmembrane segments and exhibit similar topological features. The topology of the PucC protein with 12 membrane-spanning segments has been examined in *Rhodobacter capsulatus*; both the N and C termini of the protein are located in the cytoplasm (LeBlanc and Beatty, 1996). The function of PucC is thought to be a shepherding activity that allows the light-harvesting complex (LH) 1 and 2 to assemble properly; the N terminus of the protein is important for its function (Jaschke et al, 2008; LeBlanc and Beatty, 1996). In the cyanobacterium *Synechocystis* sp. PCC 6803, a PucC homolog is found. This homolog, Sll1906, is also a member of the BCD family. In this work, the Δ*sll1906* mutant was created and analyzed in terms of chlorophyll transfer potential.

Materials and Methods

Growth conditions — *Synechocystis* sp. PCC 6803 wild type and mutant strains were grown photoautotrophically with air bubbling at 30 °C in BG-11 medium at a light intensity of 40 μmol photons m^{-2} s^{-1}. When the strains were grown in liquid culture under light-activated heterotrophic growth (LAHG) conditions, cells were kept in complete darkness except for one 15-min light period (white light at 20 μmol photons m^{-2} s^{-1}) every 24 h, and the cultures were supplemented with 5 mM glucose. Cell growth was monitored by measuring the optical density at 730 nm in a 1-cm cuvette using a Shimadzu UV-160 spectrophotometer.

Construction of mutants and transformation of Synechocystis sp. PCC 6803 — *Synechocystis* sp. PCC 6803 Δ*sll1906* mutants were generated by transformation of *Synechocystis* cells with a plasmid containing the *sll1906* gene with the section from 25 bp (*Bam*HI) downstream of the start codon to 306 bp (*Bcl*I) upstream of the stop codon replaced by a kanamycin (Km) resistance cassette from pUC4K. Transformants were selected by screening for kanamycin resistance and subcultured at increasing concentrations of antibiotics to allow segregation of wild-type and mutant genome copies to occur, thus leading to homozygous strains. Segregation was confirmed by PCR using *Synechocystis* sp. PCC 6803 DNA from transformants as a template and one forward primer (CTTACAACAGGCCCTACAAG) and two reverse primers: one is CATCGGATACGTCCACCAAG that hybridizes to the *sll1906* gene, and the other is CATGAGTGACGACTGAATCC that is used to check insertion of the Km^r gene. Construction of the Δ*chlL* mutant was described earlier (Wu and Vermaas, 1995).

Pigments analysis — Pigments were extracted from *Synechocystis* cells with 100% methanol with 0.1% NH_4OH. Chlorophyll content of the cells was measured by a Shimadzu UV-160 spectrophotometer. Total pigment content was analyzed by HPLC using a Waters Spherisorb S10ODS2 (250 mm × 10 mm) Semi-Prep column. The column was eluted with H_2O, methanol, and acetone at a flow rate of 2.0 mL/min using the following gradient program: 0 to 1 min, 90% of methanol in water; 1 to 6 min, 90 to 100% of methanol in water; 6 to 10 min, 0 to 25 % of acetone in methanol; 10-12 min, 25 to 60% of acetone in methanol; 12 to 21 min, 60 to 100% of acetone in methanol; and 21 to 25 min, 100% acetone.

Oxygen evolution — Oxygen evolution measurements were performed at 30 °C using a Clark-type electrode (Hansatech, Cambridge, UK). Intact cells were used, and 2.0 mM $K_3Fe(CN)_6$ and 0.4 mM 2,5-dimethyl-*p*-benzoquinone were used as electron acceptors. The light intensity (after filtering through a water filter and a filter transmitting >550 nm light) was saturating (2500 μmol photons m^{-2} s^{-1}).

Fluorescence spectroscopy — Fluorescence emission spectra of intact cells were measured at 77 K using a SPEX Fluorolog 2 instrument (SPEX Industries, Edison, NJ). Measurements were carried out with excitation and emission slit widths of 1 and 0.25 mm, respectively, which correspond to bandwidths of 4 and 1 nm. The excitation wavelength was 435 nm.

Results

Construction and characteristics of sll1906 deletion mutants — In order to examine the function of Sll1906, a Δ*sll1906* mutant was generated with an insertional deletion in the

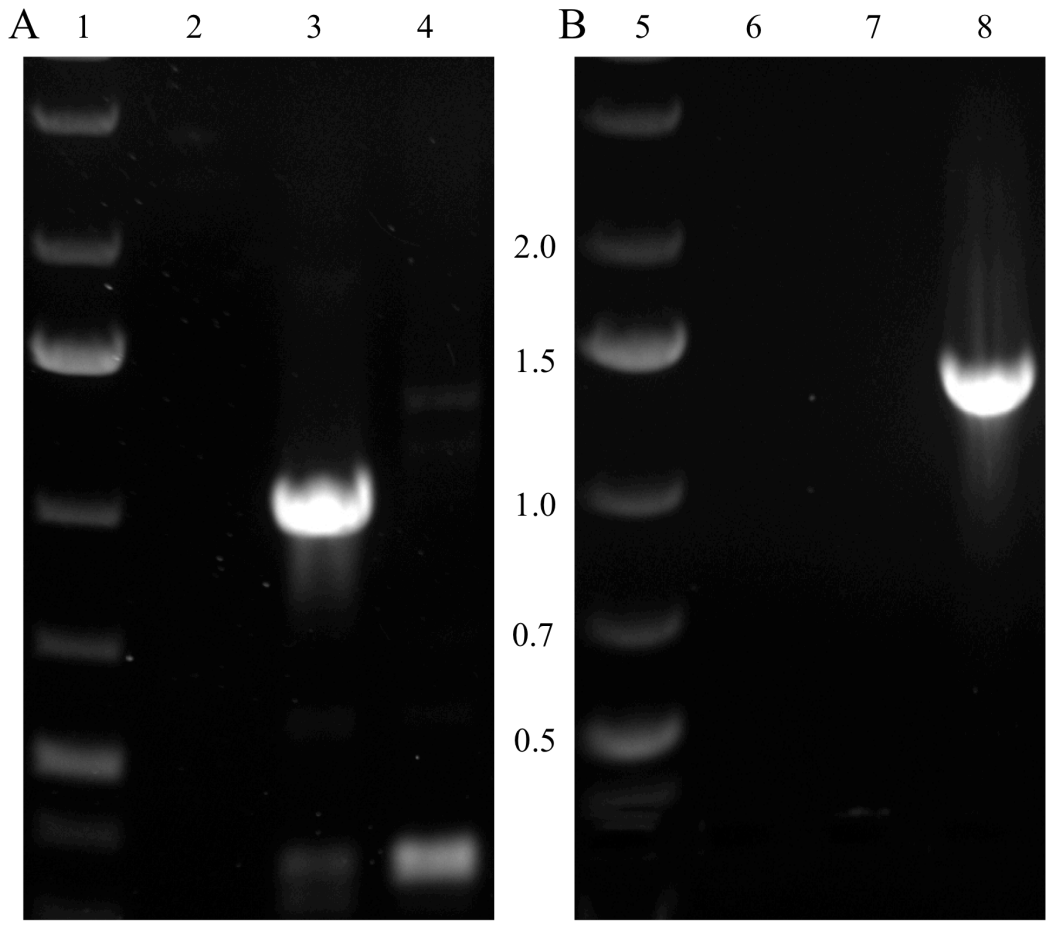

Figure V-1: Segregation of the Δ*sll1906* strain of *Synechocystis* sp. PCC 6803. PCR samples applied in A were amplified from the primers for confirmation of existence of the native *sll1906* gene (PCR product of about 1 kbp), and those in B were amplified from the primers indicating the insertion of the Kanamycin cassette. PCR products from wild type are in lanes 3 and 7, and from the Δ*sll1906* strain in lane 4 and 8. The results indicate complete segregation of the Δ*sll1906* strain. Lanes 1 and 5 are DNA ladders (sizes in kbp are indicated), and 2 and 6 are negative controls where no DNA was added in the PCR.

sll1906 open reading frame. A kanamycin cassette was inserted in the *sll1906* gene, and 77% of *sll1906* were replaced with the antibiotic resistance cassette. Complete segregation of the Δ*sll1906* mutant was achieved and was verified by PCR. Figure V-1 illustrates the results for the Δ*sll1906* strain in comparison with the wild type.

Table V-1: Effects of the *sll1906* deletion mutation on doubling time, chlorophyll content, and oxygen evolution rates of wild type and Δ*chlL* cells. Listed are the average results of two or three independent experiments ± S.D. ND: Not determined.

Strain	Cell doubling time (h)	Chlorophyll content (μg chl/(ml·OD_{730}))	Oxygen evolution (μmol O_2/(mg chl·h)
Wild type	12±2	3.55±0.21	424±36
Δ*sll1906*	13±2	3.63±0.25	442±31
Δ*chlL*	12±1	2.60±0.14	ND
Δ*chlL*/Δ*sll1906*	13±1	2.65±0.21	ND

Deletion of Sll1906 was found to have no significant impact on photoautotrophic growth, the amount of chlorophyll per cell, and PSII-driven oxygen evolution (Table V-1). This lack of a significant difference between strains with or without the *sll1906* gene was found also at a higher light intensity (110 μmol photons m^{-2} s^{-1}) (data not shown) and in Δ*chlL* background (Δ*chlL*) strains.

Pigment composition of the mutants — To determine the effect of deletion of Sll1906 in wild-type strains in terms of their content of pigments such as chlorophyll, chlorophyll precursors, and carotenoids, cells were extracted with 100% methanol, and the extracts were subjected to HPLC analysis. Chlorophyll and chlorophyll precursors such as Mg-protoporphyrin IX, Mg-protoporphyrin 13-monomethyl ester, and protochlorophyllide would have been detected by HPLC by means of 410 nm absorbance if such precursors accumulated (Figure V-2A). However, no chlorophyll precursors accumulated in either strain. The chlorophyll (C) content was similar in the wild type and Δ*sll1906* mutant, consistent with the results reported in Table V-1. Pheophytin *a* (P) was found in both strains at equally low levels. As shown in Figure V-2B, there is no change in the

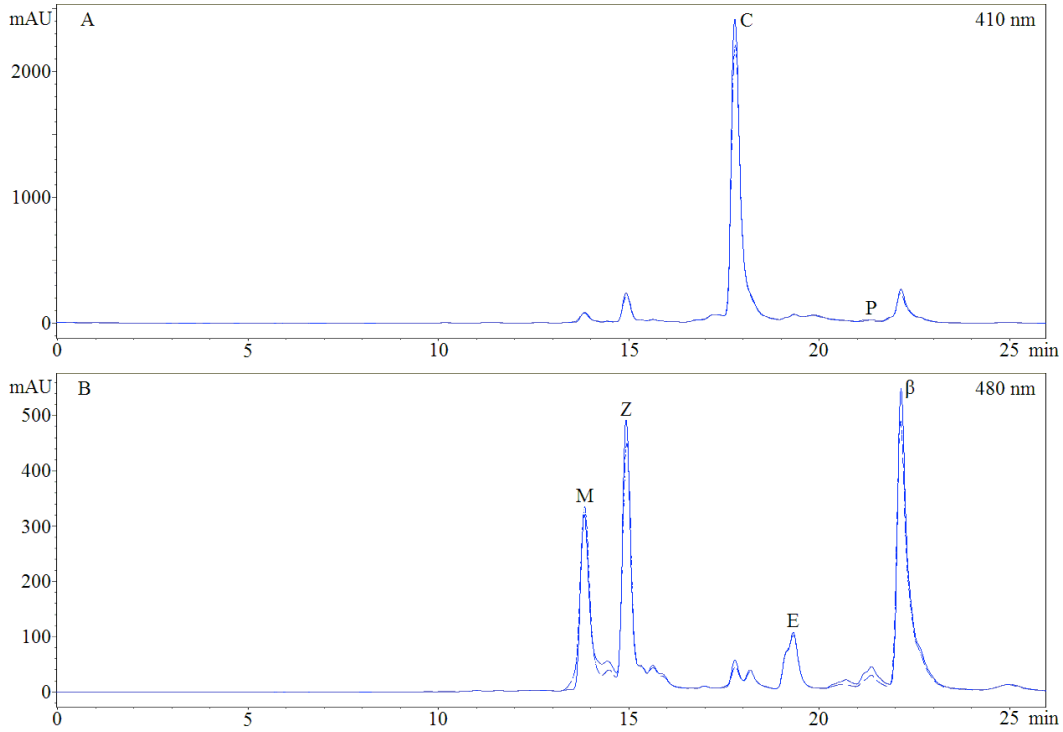

Figure V-2: HPLC spectra of cyanobacterial pigments. Each spectrum showed both wild type (solid line) and Δ*sll1906* (dashed line) samples that were extracted by 100% methanol from an equal amount of cells. Spectra were essentially overlapping. The absorption was monitored at 410 nm (A) and 480 nm (B) to indicate the presence and amount of chlorophyll (C), myxoxanthophyll (M), zeaxanthin (Z), echinenone (E), β-carotene (β), and pheophytin (P).

composition of carotenoids either. The amount of all four major carotenoids zeaxanthin (Z), echinenone (E), β-carotene (β), and myxoxanthophyll (M) were within 10% between the wild-type and Δ*sll1906* strains.

Chlorophyll degradation and synthesis — In cyanobacteria, both LPOR and DPOR are present that convert protochlorophyllide to chlorophyllide, an immediate precursor of chlorophyll. When Δ*chlL* cells that have lost DPOR function were grown in darkness or under LAHG conditions, chlorophyll synthesis was inhibited, and existing chlorophyll was degraded or diluted by growth of the culture. Figure V-3A upon growth in LAHG

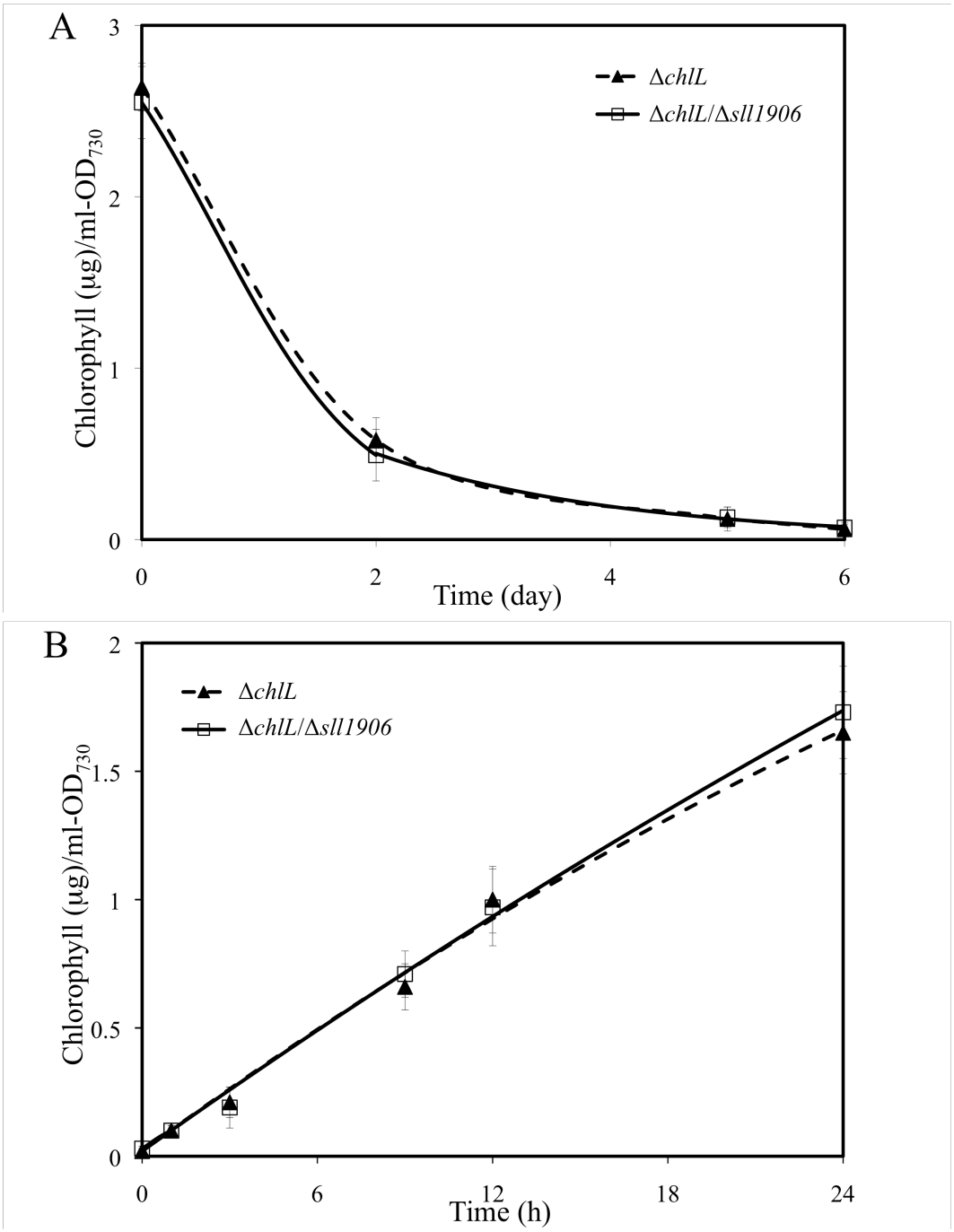

Figure V-3: Chlorophyll degradation and light-dependent chlorophyll synthesis. Chlorophyll levels (μg/ml-OD_{730}) were monitored in the Δ*chlL* (triangle with dashed line) and Δ*chlL*/Δ*sll1906* (open square with solid line) strains upon transfer to LAHG conditions at time 0 (A) or upon transfer to continuous illumination (40 μmol photons m^{-2} s^{-1}) at time 0 after cells had been grown under LAHG conditions for 2 weeks (B).
shows the chlorophyll content in the Δ*chlL* strains with and without the *sll1906* gene

conditions for 6 days. No significant difference in chlorophyll degradation was observed. To examine whether the chlorophyll biosynthesis rate was affected by Sll1906, the cells were grown in LAHG conditions for at least about a week until the amount of chlorophyll was minimal, and subsequently the rate of synthesis of chlorophyll was determined upon continuous illumination at 40 μmol photons m^{-2} s^{-1}. As shown in Figure V-3B, the Δ*sll1906* mutant exhibited the same rate of chlorophyll synthesis as the wild type. Therefore, deletion of Sll1906 did not affect the process of chlorophyll degradation and synthesis.

Photosystem biogenesis — In order to study the effects of deletion of Sll1906 on PSI and PSII, 77 K fluorescence emission spectra of whole cells were measured upon excitation at 435 nm. A major peak at 725 nm is characteristic for PSI-associated chlorophyll, and two smaller peaks at 685 and 695 nm correspond to phycobilisomes and chlorophylls, and CP47-associated chlorophyll, respectively (Figure V-4). Deletion of Sll1906 did not change the PSII/PSI ratio regardless of wild-type or *chlL*$^-$ backgrounds (Figure V-4A). However, the PSII/PSI ratio increased in the *chlL*$^-$ mutants. According to Table V-1, the chlorophyll content was reduced about 25% upon deletion of *chlL*. Therefore, it most likely is a decrease in amount of PSI that caused the increase of the PSII/PSI ratio.

To see whether the absence of Sll1906 affected the biogenesis of PSII and PSI upon chlorophyll synthesis, the Δ*chlL* and Δ*chlL*/Δ*sll1906* strains were monitored by 77 K fluorescence emission spectra at different stages of greening after a week of culturing under LAHG conditions. At time 0, there were no peaks at 695 and 725 nm, which means that very little or no PSII and PSI was present (Figure V-4B). During 24 hours of illumination, deletion of Sll1906 did not have an impact on the rate of PSII and PSI

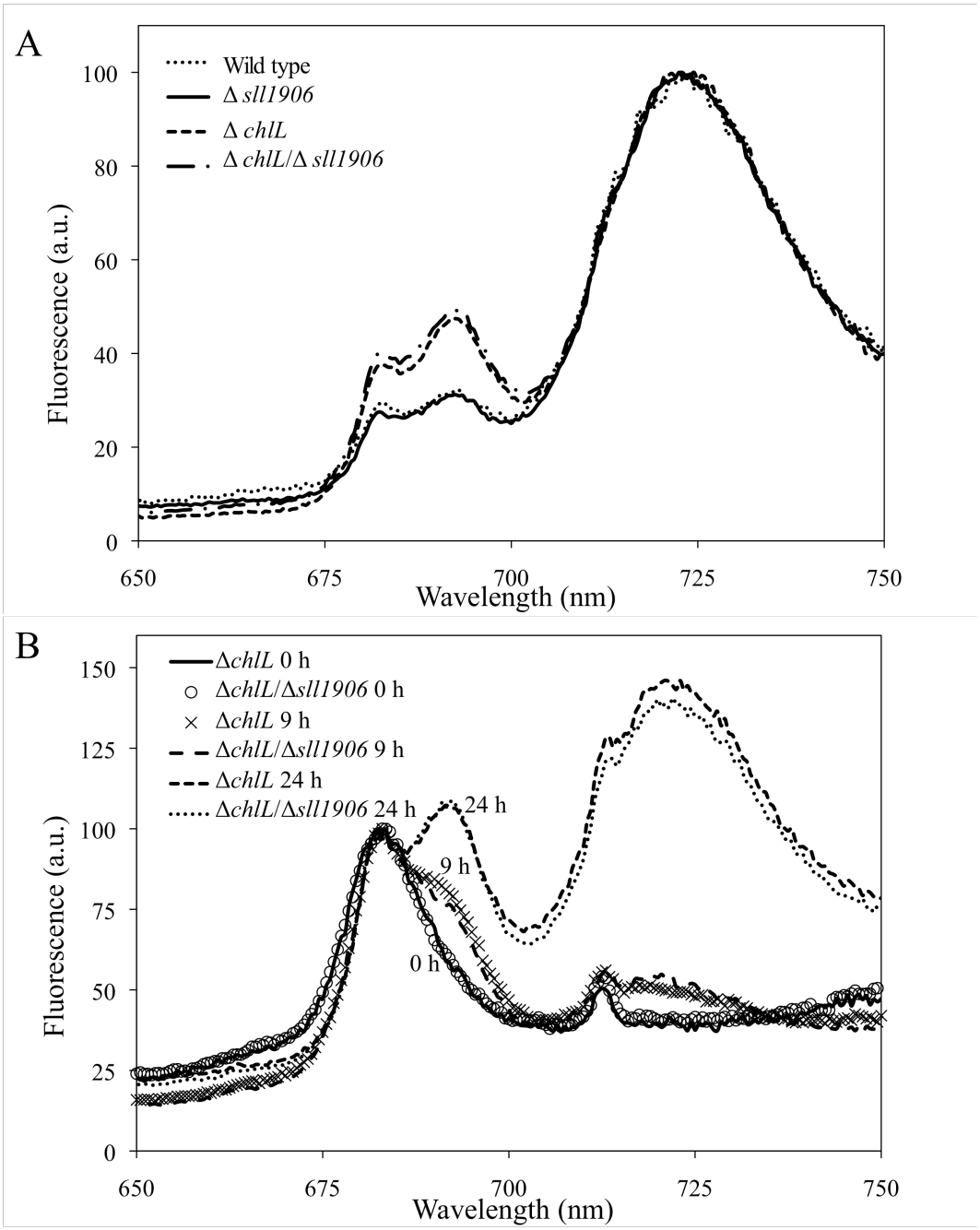

Figure V-4: 77 K fluorescence emission spectra of *Synechocystis* sp. PCC 6803 cells. A. Spectra were recorded for the wild type (dotted line), Δ*sll1906* (solid line), Δ*chlL* (dashed line), and Δ*chlL*/Δ*sll1906* (dashed and dotted line) strains grown at a light intensity of 40 μmol photons m^{-2} s^{-1}. The spectra were normalized to 100 at 725 nm, where PSI emits maximally. B. Spectra were recorded for the *chlL*⁻ strain after growth at 40 μmol photons m^{-2} s^{-1} for 0 h (solid line), 9 h (X), and 24 h (short dashed line), and the Δ*chlL*/Δ*sll1906* strain after growth at this light intensity for 0 h (○), 9 h (long dashed line), and 24 h (dotted line) after a week of culturing under LAHG conditions. The spectra were normalized to 100 at 683 nm, where phycobilisomes and some chlorophylls emit maximally. The excitation wavelength was 435 nm. a.u., arbitrary units.

biogenesis upon chlorophyll synthesis. The results show that deletion of Sll1906 did not appear to alter the delivery of chlorophyll to chlorophyll-binding proteins or aiding photosystem assembly.

Discussion

The putative BCD family was introduced in an earlier study (Saier *et al.*, 1999), and the BCD proteins in different organisms have been named as PucC or bacteriochlorophyll synthase. The function of the BCD family has been examined in *Rhodobacter capsulatus*, which contains three members of the BCD family, PucC, LhaA, and ORF428. The LhaA and PucC proteins were reported to enhance correct LH complex assembly (Young *et al.*, 1998; Jaschke et al, 2008). The Sll1906 protein in *Synechocystis* has a 24-27% amino acid sequence identity with *Rhodobacter* BCD members and has a hydropathy profile similar to that of the LhaA/PucC proteins. The BCD family proteins sequences of purple bacteria (*Rhodobacter capsulatus* and *Rhodopseudomonas palustris*) and cyanobacteria (*Synechocystis* sp. PCC 6803, *Prochlorococcus marinus* 9211, and *Synechococcus* sp. CC9902) were analyzed. Transmembrane segments (TMSs) 1 and 2, and TMSs 7 and 8 as well as their connecting loop regions are well conserved, and the loop region between TMSs 4 and 5 as well as TMS5 is also well conserved. These results are consistent with an earlier study (Saier *et al.*, 1999). Interestingly, the rest of the protein sequence (over 50%) has low or no similarity between BCD family of purple bacteria and cyanobacteria but is highly conserved within purple bacteria and moderately conserved within cyanobacteria.

Sll1906 was suggested to be involved in tetrapyrrole delivery for assembly of chlorophyll-binding complexes (Young and Beatty, 1998). However, *Synechocystis* cells

Table V-2. Protein sequence alignments and possible chlorophyll-binding amino acid residues in Sll1906 relative to PucC from *Rhodobacter capsulatus* and *Synechocystis psbB*. Underlined residues represent possible chlorophyll binding sites. Sll1906 protein sequences 1 and 2 represent residues 22-49 and 76-87. CP47 protein sequence 2 represents residues 13-25.

Organisms	Protein sequence 1	Protein sequence 2
Rb capsulatus PucC	RLSLFQITVGMTLTLLAGTLNRVMIVEL	KSDTHKSALGLRR
Syn 6803 Sll1906	RLGLFQMGLGIMSLLTLGVLNRVLIDEL	LSDSQRLWGYH-R
PsbB (CP47)		LNDPGRLISVHLM

lacking *sll1906* have normal chlorophyll content and chlorophyll synthesis (Table V-1 and Figure V-3), whereas also the tetrapyrrole biosynthesis pathway was not disrupted in the mutant (no accumulation in chlorophyll precursors) (Figure V-2A). Also, judging from the 77 K fluorescence emission spectra, lack of Sll1906 did not impair PSII and PSI assembly (Figure V-4).

In order to examine if Sll1906 possibly binds chlorophyll, Table V-2 shows examples of the Sll1906 protein sequences that contain possible chlorophyll-binding amino acid residues (underlined). Protein sequence 1 is highly conserved in all organisms possessing BCD proteins and contain a few amino acid residues that could bind chlorophyll. Protein sequence 2 is conserved in cyanobacteria only but aligns well with part of PsbB containing a histidine that binds chlorophyll (Muh *et al.*, 2008). Therefore, Sll1906 may have chlorophyll-binding ability.

In conclusion, the Δ*sll1906* mutant did not show significant effects on pigment content and photosystem assembly. However, this does not necessarily mean that Sll1906 is not involved in these processes as other (parallel) pathways may exist that may fully compensate for the lack of Sll1906.

CHAPTER VI. PERSPECTIVE AND OUTLOOK

A combination of stable-isotope labeling (^{15}N) and mass spectrometry is a powerful method to provide insights in the dynamics of photosystems in the membrane. In this study, the lifetimes of PSI and PSII proteins have been determined to range from 30-75 h and 1-33 h, respectively. The wide range of lifetimes indicates that the damaged photosynthetic proteins can be replaced independently, and the other proteins can be re-used and assembled into functional photosynthetic complexes. Indeed, *Synechocystis* cells have nascent photosynthetic proteins in the membrane for the replacement of damaged proteins or for photosystem biogenesis when photosynthetic complexes turn over. If there are changes in environment or growth conditions, cells may be able to response rapidly by utilizing these nascent proteins and retain a homeostasis of the photosystems. It would be interesting to examine the lifetimes of photosynthetic proteins and change in the pool of nascent photosynthetic proteins upon transition between different growth conditions. Also, the IsiA (CP43') protein, an iron-stress-induced protein, can form circular aggregates (rings) of up to 18 subunits around trimeric PSI in a first ring and possibly up to 25 subunits in a second ring under iron-deficient or some other stress conditions (Bibby *et al.*, 2001; Boekema *et al.*, 2001; Yeremenko *et al.*, 2004). IsiA proteins may serve as a light-harvesting antenna and as an energy dissipator for PSI (Bibby *et al.*, 2001; Berera *et al.*, 2009). By applying a combination of stable-isotope labeling and mass spectrometry on strains with and without IsiA proteins under iron-sufficient/deficient conditions, the effects of IsiA on lifetimes of PSI proteins and the dynamics of PSI complexes switching between monomeric and trimeric forms can be studied.

Chlorophyll is the most abundant cofactor in the photosystems. A total of 131 chlorophyll molecules are in PSII and PSI combined, and synthesis of one chlorophyll molecule from glutamate requires 9 ATP and 13 NADPH. It is a significant investment just on cofactors for cyanobacteria to practice photosynthesis. *Synechocystis* cells have evolved an efficient way of reutilizing chlorophyll from the damaged chlorophyll-binding proteins in the PSI and PSII complexes. As known from this study, SCPs play an important role in PSII chlorophyll recycling. However, what factors function in the recycling of PSI chlorophyll still needs to be investigated. Although chlorophyll can be utilized, highly active chlorophyll synthesis is required as there is always a significant amount of chlorophyll-binding proteins synthesized for both photosystem repair and biogenesis to retain a homeostasis of photosystems and cell growth.

As chlorophyll is a strong photo-oxidizer, free chlorophyll is very dangerous for cells by rapidly producing reactive oxygen species in the presence of light and oxygen, and cellular damage may happen as quick as in a few seconds. However, chlorophyll in chlorophyll-binding proteins is relatively safe as efficient quenchers, such as carotenoids, are nearby, as demonstrated by the long half-lives of chlorophyll-binding proteins that do not turn over on a timescale of up to 40 h. Therefore, cooperation between chlorophyll biosynthesis and synthesis of chlorophyll-binding proteins is important. This study shows that SCPs are possible candidates as bridges in communication between chlorophyll and PSII proteins as upon removal of SCPs the rate of chlorophyll synthesis and the amount of chlorophyll molecules are reduced while the amount of PSII proteins decrease and the accumulation of nascent PSII proteins in membranes disappears. Interestingly, the phenotype is exhibited only in the absence of PSI. However, PSI possesses about 90% of chlorophyll in the *Synechocystis* cells. The deletion of SCPs in the PSI-containing strain can not inhibit ALA synthesis significantly because chlorophyll synthesis needs to meet

the demand of chlorophyll from PSI. It is as yet unknown which protein(s), if any, that function like SCPs serve PSI, and whether such protein(s) can function like SCPs for PSII. The Sll1906 protein, a member of putative bacteriochlorophyll delivery family, may possibly function as a bridge between chlorophyll and chlorophyll-binding proteins. However, deletion of Sll1906 does not show any phenotype in either chlorophyll biosynthesis/degradation or photosystem assembly. In order to understand how the synthesis of chlorophyll and chlorophyll-binding proteins is coordinated and chlorophyll is delivered to the chlorophyll-binding proteins, a continuous search for factor(s) that function like the SCPs in PSII but, for example, work in PSI is critical.

References

Adamska, I., Roobol-Boza, M., Lindahl, M., and Andersson, B. (1999) Isolation of pigment-binding early light-inducible proteins from pea. *Eur. J. Biochem.* **260,** 453–460

Adamska, I. (2001) The Elip family of stress proteins in the thylakoid membranes of pro- and eukaryota. *Advances in Photosynthesis and Respiration: Regulation of Photosynthesis* (Aro, E. M., and Andersson, B., eds) **Vol. 11,** pp. 487–505, Kluwer Academic Publishers, Dordrecht, The Netherlands

Adhikari, N. D., Orler, R., Chory, J., Froehlich, J. E., and Larkin, R. M. (2009) Porphyrins promote the association of GENOMES UNCOUPLED 4 and a Mg-chelatase subunit with chloroplast membranes. *J. Biol. Chem.* **284,** 24783-24796

Amunts, A., Drory, O., and Nelson, N. (2007) The structure of a plant photosystem I supercomplex at 3.4 Å resolution. *Nature* **447**, 58-63

Anbudurai, P. R., Mor, T. S., Ohad, I., Shestakov, S. V., and Pakrasi, H. B. (1994) The *ctpA* gene encodes the C-terminal processing protease for the D1 protein of the photosystem-II reaction-center complex. *Proc. Natl. Acad. Sci. USA* **91,** 8082-8086

Aro, E. M., Virgin, I., and Andersson, B. (1993) Photoinhibition of photosystem II – inactivation, protein damage and turnover. *Biochim. Biophys. Acta* **1143,** 113-134

Aro, E. M., Suorsa, M., Rokka, A., Allahverdiyeva, Y., Paakkarinen, V., Saleem, A., Battchikova, N., and Rintamaki, E. (2005) Dynamics of photosystem II: a proteomic approach to thylakoid protein complexes. *J. Exp. Bot.* **56,** 347–356

Bailey, S., Thompson, E., and Nixon, P. J. (2002) A critical role for the Var2 FtsH homologue of *Arabidopsis thaliana* in the photosystem II repair cycle *in vivo*. *J. Biol. Chem.* **277,** 2006-2011

Barber, J. (2002) P680: what is it and where is it? *Bioelectrochemistry* **55,** 135-138

Beale, S. I. (1990) Biosynthesis of the tetrapyrrole pigment precursor, aminolevulinic acid, from glutamate. *Plant Physiol.* **93,** 1273-1279

Beale, S. I. (1999) Enzymes of chlorophyll biosynthesis. *Photosyn. Res.* **60,** 43-73

Beck, C. F. and Grimm, B. (2006) *Involvement of Tetrapyrroles in Cellular Regulation* in *Advances in Photosynthesis and Respiration: Chlorophylls and bacteriochlorophylls,* Vol. 25 (Grimm, B., Porra, R. J., Rudiger, W., and Scheer, H. eds.) pp. 223-235, Springer, Dordrecht

Berera, R., van Stokkum, I. H. M., D'Haene, S., Kennis, J. T. M., van Grondelle, R., and Dekker, J. P. (2009) A mechanism of energy dissipation in cyanobacteria. *Biophys. J.* **96,** 2261-2267

Bhaya, D., Dufresne, A., Vaulot, D., and Grossman, A. (2002) Analysis of the *hli* gene family in marine and freshwater cyanobacteria. *FEMS Microbiol. Lett.* **215,** 209–219

Bibby, T. S., Nield, J., and Barber, J. (2001) A photosystem II-like protein, induced under iron-stress, forms an antenna ring around the photosystem I trimer in cyanobacteria. *Nature* **412,** 743-745

Bjellqvist, B., Pasquali, C., Ravier, F., Sanchez, J. C., and Hochstrasser, D. (1993) A nonlinear wide-range immobilized pH gradient for 2-dimensional electrophoresis and its definition in a relevant pH scale. *Electrophoresis* **14,** 1357–1365

Blankenship, R. E. (2002) *Molecular Mechanisms of Photosynthesis*. Blackwell Science, Malden

Boekema, E. J., Hifney, A., Yakushevska, A. E., Piotrowski, M., Keegstra, W., Berry, S., Michel, K. P., Pistorius, E. K., and Kruip, J. (2001) A giant chlorophyll-protein complex induced by iron deficiency in cyanobacteria. *Nature* **412,** 745-748

Bricker, T. M., Morvant, J., Masri, N., Sutton, H. M., and Frankel, L. K. (1998) Isolation of a highly active photosystem II preparation from *Synechocystis* 6803 using a histidine-tagged mutant of CP47. *Biochim. Biophys. Acta* **1409,** 50–57

Bryant, D. A. (1994) *The Molecular Biology of Cyanobacteria.* Kluwer Academic Press, Dordrecht

Burke, D. H., Hearst, J. E., and Sidow, A. (1993) Early evolution of photosynthesis: clues from nitrogenase and chlorophyll iron proteins. *Proc. Natl. Acad. Sci. USA*. **90,** 7134-7138

Carpenter, S. D., Charité, J., Eggers, B., and Vermaas, W. F. J. (1990) The *psbC* start codon in *Synechocystis* sp. PCC 6803. *FEBS Lett.* **260,** 135-137

Chitnis, V. P. and Chitnis, P. R. (1993) PsaL subunit is required for the formation of photosystem I trimers in the cyanobacterium *Synechocystis* sp. PCC 6803. *FEBS Lett.* **336,** 330 –334

Cormann, K. U., Bangert, J. A., Ikeuchi, M., Rögner, M., Stoll, R., and Nowaczyk, M. M. (2009) Structure of Psb27 in solution: Implications for transient binding to photosystem II during biogenesis and repair. *Biochemistry* **48,** 8768-8770

Dobakova, M., Tichy, M., and Komenda, J. (2007) Role of the PsbI protein in photosystem II assembly and repair in the cyanobacterium *Synechocystis* sp. PCC 6803. *Plant Physiol.* **145,** 1681-1691

Dobakova, M., Sobotka, R., Tichy, M., and Komenda, J. (2009) Psb28 protein is involved in the biogenesis of the photosystem II inner antenna CP47 (PsbB) in the cyanobacterium *Synechocystis* sp PCC 6803. *Plant Physiol.* **149,** 1076-1086

Dolganov, N. A. M., Bhaya, D., and Grossman, A. R. (1995) Cyanobacterial protein with similarity to the chlorophyll *a/b* binding proteins of higher plants: Evolution and regulation. *Proc. Natl. Acad. Sci. USA* **92,** 636-640

Durnford, D. G., Deane, J. A., Tan, S., McFadden, G. I., Gantt, E., and Green, B. R. (1999) A phylogenetic assessment of the eukaryotic light-harvesting antenna proteins, with implications for plastid evolution. *J. Mol. Evol.* **48,** 59–68

Eckhardt, U., Grimm, B., and Hortensteiner, S. (2004) Recent advances in chlorophyll biosynthesis and breakdown in higher plants. *Plant Mol. Biol.* **56,** 1-14

Ermakova-Gerdes, S., Shestakov, S., and Vermaas, W. (1996) Targeted random mutagenesis in the D2 protein of photosystem II: Identification of functionally important residues at the lumenal side of the thylakoid. *Plant Mol. Biol.* **30,** 243-254

Ferreira, K. N., Iverson, T. M., Maghlaoui, K., Barber, J., and Iwata, S. (2004) Architecture of the photosynthetic oxygen-evolving center. *Science* **303,** 1831–1838

Fischer, N., Hippler, M., Setif, P., Jacquot, J. P., and Rochaix, J. D. (1998) The PsaC subunit of photosystem I provides an essential lysine residue for fast electron transfer to ferredoxin. *EMBO J.* **17,** 849-858

Funk, C., Schroder, W. P., Green, B. R., Renger, G., and Andersson, B. (1994) The intrinsic 22 kDa protein is a chlorophyll-binding subunit of photosystem II. *FEBS Lett.* **342,** 261–266

Funk, C. and Vermaas, W. (1999) A cyanobacterial gene family coding for single-helix proteins resembling part of the light-harvesting proteins from higher plants. *Biochemistry* **38,** 9397–9404

Funk, C. (2001) *The PsbS protein: A Cab-protein with a Function of its Own* in *Advances in Photosynthesis and Respiration: Regulation of Photosynthesis* (Aro, E. M., and Andersson, B., eds) **Vol. 11,** pp. 453–467, Kluwer Academic Publishers, Dordrecht, The Netherlands

Gharahdaghi, F., Weinberg, C. R., Meagher, D. A., Imai, B. S., and Mische, S. M. (1999) Mass spectrometric identification of proteins from silver-stained polyacrylamide gel: A method for the removal of silver ions to enhance sensitivity. *Electrophoresis* **20,** 601–605

Griffiths, W. T. (1975) Characterization of of the terminal stages of chlorophyll(ide) synthesis in etioplast membrane preparations. *Biochem. J.* **152,** 623-635

Grimm, B. (1999) *The Metabolic Pathway of Tetrapyrrole Biosynthesis* in *Peroxidizing Herbicides* (Böger, P. and Wakabayashi, K. eds), pp 213-244, Springer-Verlag, Berlin

Guskov, A., Kern, J., Gabdulkhakov, A., Broser, M., Zouni, A., and Saenger, W. (2009) Cyanobacterial photosystem II at 2.9 Å resolution and the role of quinones, lipids, channels and chloride. *Nat. Struct. Biol.* **16**, 334-342

Hao, L. M., Schmidt, K., Paulsen, H., and Funk, C. (2001) Isolation and reconstitution of hypothetical pigment carrier proteins. *Proceedings of the 12th International Congress on Photosynthesis* (Larkum, T., and Critchley, C., eds) pp. S31–005, Commonwealth Scientific and Industrial Research Organisation Publishing, Melbourne, Australia

Havaux, M., Guedeney, G., He, Q., and Grossman, A. R. (2003) Elimination of high-light-inducible polypeptides related to eukaryotic chlorophyll a/b-binding proteins results in aberrant photoacclimation in *Synechocystis* PCC6803. *Biochim. Biophys. Acta* **1557,** 21–33

He, Q. and Vermaas, W. (1998) Chlorophyll *a* availability affects *psbA* translation and D1 precursor processing *in vivo* in *Synechocystis* sp. PCC 6803. *Proc. Natl. Acad. Sci. USA* **95,** 5830-5835

He, Q., Dolganov, N., Bjorkman, O., and Grossman, A. R. (2001) The high light-inducible polypeptides in *Synechocystis* PCC6803 – expression and function in high light. *J. Biol. Chem.* **276,** 306–314

Heddad, M. and Adamska, I. (2000) Light stress-regulated two-helix proteins in *Arabidopsis thaliana* related to the chlorophyll *a/b*-binding gene family. *Proc. Natl. Acad. Sci. U. S. A.* **97,** 3741–3746

Heddad, M. and Adamska, I. (2002) The evolution of light stress proteins in photosynthetic organisms. *Comp. Funct. Genom.* **3,** 504–510

Herranen, M., Battchikova, N., Zhang, P., Graf, A., Sirpio, S., Paakkarinen, V., and Aro, E. M. (2004) Towards functional proteomics of membrane protein complexes in *Synechocystis* sp. PCC 6803. *Plant Physiol.* **134,** 470-481

Inagaki, N., Yamamoto, Y., and Satoh, K. (2001) A sequential two-step proteolytic process in the carboxyl-terminal truncation of precursor D1 protein in *Synechocystis* sp PCC 6803. *FEBS Lett.* **509,** 197-201

Jansson, S. (1994) The light-harvesting chlorophyll *a/b* binding proteins. *Biochim. Biophys. Acta* **1184,** 1-19

Jansson, S. (1999) A guide to the Lhc genes and their relatives in Arabidopsis. *Trends Plant Sci.* **4,** 236–240

Jansson, S., Andersson, J., Kim, S. J., and Jackowski, G. (2000) An Arabidopsis thaliana protein homologous to cyanobacterial high-light-inducible proteins. *Plant Mol. Biol.* **42,** 345–351

Jansson, S. (2005) *A Protein Family Saga: From Photoprotection to Light-Harvesting* in *Photoprotection, Photoinhibition, Gene Regulation and Environment* (Demmig-Adams, B., ed) pp. 145–153, Springer, Dordrecht, The Netherlands

Jaschke, P., LeBlanc, H., Lang, A., and Beatty, J. (2008) The PucC protein of *Rhodobacter capsulatus* mitigates an inhibitory effect of light-harvesting 2 α and β proteins on light-harvesting complex 1. *Photosynth. Res.* **95,** 279-284

Jensen, P. E., Haldrup, A., Rosgaard, L., and Scheller, H. V. (2003) Molecular dissection of photosystem I in higher plants: topology, structure and function. *Physiol. Plant.* **119,** 313-321

Jordan, P., Fromme, P., Witt, H. P., Klukas, O., Saenger, W., and Krauss, N. (2001) Three-dimensional structure of cyanobacterial photosystem I at 2.5 Å resolution. *Nature* **411**, 909-917

Joyard, J., Ferro, M., Masselon, C., Seigneurin-Berny, D., Salvi, D., Garin, J., and Rolland, N. (2009) Chloroplast proteomics and the compartmentation of plastidial isoprenoid biosynthetic pathway. *Mol. Plant* **2,** 1154-1180

Kaneko, T., Sato, S., Kotani, H., Tanaka, A., Asamizu, E., Nakamura, Y., Miyajima, N., Hirosama, M., Sugiura, M., Sasamoto, S., Kimura, T., Hosouchi, T., Matsuno, A., Muraki, A., Nakazaki, N., Naruo, K., Okumura, S., Shimpo, S., Takeuchi, C., Wada, T., Watanabe, A., Yamada, M., Yasuda, M., and Tabata, S. (1996) Sequence analysis of the genome of the unicellular cyanobacterium *Synechocystis* sp. PCC 6803. II. Sequence determintation of the entire genome and assignment of potential protein-coding regions. *DNA Res.* **3,** 109-136

Karapetyan, N. V., Holzwarth, A. R., and Rogner, M. (1999) The photosystem I trimer of cyanobacteria: molecular organization, excitation dynamics and physiological significance. *FEBS Lett.* **460,** 395–400

Kashino, Y., Lauber, W. M., Carroll, J. A., Wang, Q., Whitmarsh, J., Satoh, K., and Pakrasi, H. B. (2002) Proteomic analysis of a highly active photosystem II preparation from the cyanobacterium *Synechocystis* sp PCC 6803 reveals the presence of novel polypeptides. *Biochemistry* **41,** 8004–8012

Kato, Y., Miura, E., Ido, K., Ifuku, K., and Sakamoto, W. (2009) The variegated mutants lacking chloroplastic FtsHs are defective in D1 degradation and accumulate reactive oxygen species. *Plant Physiol.* **151,** 1790-1801

Keren, N., Ohkawa, H., Welsh, E. A., Liberton, M., and Pakrasi, H. B. (2005) Psb29, a conserved 22-kD protein, functions in the biogenesis of photosystem II complexes in *Synechocystis* and *Arabidopsis*. *Plant Cell* **17,** 2768-2781

Kern, J., Loll, B., Zouni, A., Saenger, W., Irrgang, K. D., and Biesiadka, J. (2005) Cyanobacterial photosystem II at 3.2 angstrom resolution – the plastoquinone binding pockets. *Photosynth. Res.* **84,** 153–159

Klimmek, F., Sjödin, A., Noutsos, C., Leister, D., and Jansson, S. (2006) Abundantly and rarely expressed Lhc protein genes exhit distinct regulation patterns in plants. *Plant Physiol.* **140,** 793–804

Komenda, J., Lupinkova, L., and Kopecky, J. (2002) Absence of the psbH gene product destabilizes photosystem II complex and bicarbonate binding on its acceptor side in *Synechocystis* PCC 6803. *Eur. J. Biochem.* **269,** 610–619

Komenda, J., Reisinger, V., Muller, B. C., Dobakova, M., Granvogl, B., and Eichacker, L. A. (2004) Accumulation of the D2 protein is a key regulatory step for assembly of the photosystem II reaction center complex in *Synechocystis* PCC 6803. *J. Biol. Chem.* **279,** 48620–48629

Komenda, J., Barker, M., and Kuvikova, S. (2006) The FtsH protease Slr0228 is important for quality control of photosystem II in the thylakoid membrane of *Synechocystis* sp PCC 6803. *Plant Cell Physiol.* **46,** 1477-1483

Komenda, J., Kuvikova, S., Granvogl, B., Eichacker, L. A., Diner, B. A., and Nixon, P. J. (2007) Cleavage after residue Ala352 in the C-terminal extension is an early step in the maturation of the D1 subunit of photosystem II in *Synechocystis* PCC 6803. *Plant Cell* **19,** 2839-2854

Komenda, J., Nickelsen, J., Tichy, M., Prasil, O., Eichacker L. A., and Nixon, P. J. (2008) The cyanobacterial homologue of HCF136/YCF48 is a component of an early photosystem II assembly complex and is important for both the efficient assembly and repair of photosystem II in *Synechocystis* sp. PCC 6803. *J. Biol. Chem.* **283,** 22390-22399

Kouril, R., Arteni, A. A., Lax, J., Yeremenko, N., D'Haene, S., Rogner, M., Matthijs, H. C., Dekker, J. P., and Boekema, E. J. (2005) Structure and functional role of supercomplexes of IsiA and photosystem I in cyanobacterial photosynthesis. *FEBS Lett.* **579,** 3253–3257

Krieger-Liszkay, A. (2005) Singlet oxygen production in photosynthesis. *J. Exp. Bot.* **56,** 337-346

Krieger-Liszkay, A., Fufezan, C., and Trebst, A. (2008) Singlet oxygen production in photosystem II and related protection mechanism. *Photosynth. Res.* **98,** 551-564

Kufryk, G., Hernandez-Prieto, M. A., Kieselbach, T., Miranda, H., Vermaas, W., and Funk, C. (2008) Association of small CAB-like proteins (SCPs) of *Synechocystis* sp. PCC 6803 with photosystem II. *Photosynth. Res.* **95,** 135-145

Kühlbrandt, W., Wang, D. N., and Fujiyoshi, Y. (1994) Atomic model of plant light-harvesting complex by electron crystallography. *Nature* **367,** 614–621

Kussmann, M., Nordhoff, E., Rahbek-Nielsen, H., Haebel, S., Rossel- Larsen, M., Jakobsen, L., Gobom, J., Mirgorodskaya, E., Kroll-Kristensen, A., Palm, L., and Roepstorff, P. (1997) Matrix-assisted laser desorption/ionization mass spectrometry

sample preparation techniques designed for various peptide and protein analysis. *J. Mass Spectrom.* **32,** 593–601

Kuttkat, A., Edhofer, I., Eichacker, L. A., and Paulsen, H. (1997) Light-harvesting chlorophyll *a/b*-binding protein stably inserts into etioplast membranes supplemented with Zn-pheophytin *a/b*. *J. Biol. Chem.* **272,** 20451-20455

Lagarde, D., Beuf, L., and Vermaas, W. (2000) Increased production of zeaxanthin and other pigments by application of genetic engineering techniques to *Synechocystis* sp strain PCC 6803. *Appl. Environ. Microbiol.* **66,** 64–72

LeBlanc, H. N. and Beatty, J. T. (1996) Topological analysis of the *Rhodobacter capsulatus* PucC protein and effects of C-terminal deletions on light-harvesting complex II. *J. Bacteriol.* **178,** 4801-4806

Li, X. P., Bjorkman, O., Shih, C., Grossman, A. R., Rosenquist, M., Jansson, S., and Niyogi, K. K. (2000) A pigment-binding protein essential for regulation of photosynthetic light harvesting. *Nature* **403,** 391–395

Lindell, D., Sullivan, M. B., Johnson, Z. I., Tolonen, A. C., Rohwer, F., and Chisholm, S. W. (2004) Transfer of photosynthesis genes to and from *Prochlorococcus* viruses. *Proc. Natl. Acad. Sci. U. S. A.* **101,** 11013–11018

Liu, Z., Yan, H., Wang, K., Kuang, T., Zhang, J., Gui, L., An, X., and Chang, W. (2004) Crystal structure of spinach major light-harvesting complex at 2.72 angstrom resolution. *Nature* **428,** 287–292

Loll, B., Kern, J., Saenger, W., Zouni, A., and Biesiadka, J. (2005) Towards complete cofactor arrangement in the 3.0 Å resolution structure of photosystem II. *Nature* **438**, 1040-1044

Loll, B., Kern, J., Saenger, W., Zouni, A., and Biesiadka, J. (2007) Lipids in photosystem II: Interaction with protein and cofactors. *Biochim. Biophys. Acta* **1767,** 509-519

MacPherson, A. N., Telfer, A., Barber, J., and Truscott, T. G. (1993) Direct detection of singlet oxygen from isolated photosystem II reaction centres. *Biochim. Biophys. Acta* **1143,** 301-309

Mann, M. and Wilm, M. (1994) Error tolerant identification of peptides in sequence databases by peptide sequence tags. *Anal. Chem.* **66,** 4390–4399

Mattoo, A. K., Hoffman-Falk, H., Marder, J. B., and Edelman, M. (1984) Regulation of protein metabolism: coupling of photosynthetic electron transport to *in vivo* degradation of the rapidly metabolized 32-kilodalton protein of the chloroplast membranes. *Proc. Natl. Acad. Sci. USA* **81,** 1380-1384

Mattoo, A. K., Giardi, M. T., Raskind, A., and Edelman, M. (1999) Dynamic metabolism of photosystem II reaction center proteins and pigments. *Physiol. Plant.* **107,** 454-461

Mayer, S. and Beale, S. (1992) Succinyl-coenzyme A synthetase and its role in aminolevulinic acid biosynthesis in *Euglena gracilis*. *Plant Physiol.* **99,** 482-487

Meskauskiene, R., Nater, M., Goslings, D., Kessler, F., Op den Camp, R., and Apel, K. (2001) FLU: A negative regulator of chlorophyll biosynthesis in *Arabidopsis thaliana*. *Proc. Natl. Acad. Sci. USA* **98,** 12826-12831

Mikami, K., Kanesaki, Y., Suzuki, I., and Murata, N. (2002) The histidine kinase Hik33 perceives osmotic stress and cold stress in *Synechocystis* sp PCC 6803. *Mol. Microbiol.* **46,** 905–915

Mochizuki, N., Tanaka, R., Grimm, B., Masuda, T., Moulin, M., Smith, A. G., Tanaka, A., and Terry, M. J. (2010) The cell biology of tetrapyrroles: a life and death struggle. *Trends Plant Sci.* **15,** 488-498

Muh, F., Renger, T., and Zouni, A. (2008) Crystal structure of cyanobacterial photosystem II at 3.0 Å resolution: A closer look at the antenna system and the small membrane-intrinsic subunits. *Plant Physiol. Biochem.* **46,** 238-264

Mullet, J., Gamble-Klein, P., and Klein, R. (1990) Chlorophyll regulates accumulation of the plastid-encoded chlorophyll apoproteins CP43 and D1 by increasing apoprotein stability. *Proc. Natl. Acad. Sci. USA* **87,** 4038-4042

Mullineaux, C. W., and Emlyn-Jones, D. (2005) State transitions: an example of acclimation to low-light stress. *J. Exp. Bot.* **56,** 389–393

Muraki, N., Nomata, J., Ebata, K., Mizogucho, T., Shiba, T., Tamiaki, H., Kurisu, G., and Fujita, Y. (2010) X-ray crystal structure of the light-independent protochlorophyllide reductase. *Nature* **465,** 110-114

Nixon, P. J., Trost, J. T., and Diner, B. A. (1992) Role of the carboxyl terminus of polypeptide D1 in the assembly of a function water-oxidizing manganese cluster in photosystem II of the cyanobacterium *Synechocystis* sp PCC 6803 – assembly requires a free carboxyl group at C-terminal position 344. *Biochemistry* **31,** 10859-10871

Nixon, P. J., Barker, M., Boehm, M., de Vries, R., and Komenda, J. (2005) FtsH-mediated repair of the photosystem II complex in response to light stress. *J. Exp. Bot.* **56,** 357–363

Nixon, P., Michoux, F., Yu, J., Boehm, M., and Komenda, J. (2010) Recent advances in understanding the assembly and repair of photosystem II. *Ann. Bot.* **106,** 1-16

Norling, B., Zak, E., Andersson, B., and Pakrasi, H. (1998) 2D-isolation of pure plasma and thylakoid mebranes from the cyanobacterium *Synechocystis* sp. PCC 6803. *FEBS Lett.* **436,** 189–192

Nowaczyk, M. M., Hebeler, R., Schlodder, E., Meyer, H. E., Warscheid, B., and Rögner, M. (2006) Psb27, a cyanobacterial lipoprotein, is involved in the repair cycle of photosystem II. *Plant Cell* **18,** 3121-3131

Ohad, I., Kyle, D. J., and Arntzen, C. J. (1984) Membrane-protein damage and repair – removal and replacement of activated 32-kilodalton polypeptide in chloroplast membranes. *J. Cell Biol.* **99,** 481-485

Ohta, N., Matsuzaki, M., Misumi, O., Miyagishima, S. Y., Nozaki, H., Tanaka, K., Shin, I. T., Kohara, Y., and Kuroiwa, T. (2003) Complete sequence and analysis of the plastid genome of the unicellular red alga *cyanidioschyzon merolae*. *DNA Res.* **10,** 67–77

Perkins, D. N., Pappin, D. J., Creasy, D. M., and Cottrell, J. S. (1999) Probability-based protein identification by searching sequence databases using mass spectrometry data. *Electrophoresis* **20,** 3551–3567

Peter, E. and Grimm, B. (2009) GUN4 is required for posttranslational comtrol plant tetrapyrrole biosynthesis. *Mol. Plant* **2,** 1198-1210

Plucken, H., Muller, B., Grohmann, D., Westhoff, P., and Eichacker, L. A. (2002) The HCF136 protein is essential for assembly of the photosystem II reaction center in *Arabidopsis thaliana*. *FEBS Lett.* **532,** 85-90

Porra, R. J., Thompson, W. A., and Kriedemann, P. E. (1989) Determination of accurate extinction coefficients and simultaneous-equations for assaying chlorophyll-*a* and chlorophyll-*b* extracted with 4 different solvents – verification of the concentration of chlorophyll standards by atomic-absorption spectroscopy. *Biochim. Biophys. Acta* **975,** 385–394

Powles, S. B. (1984) Photoinhibition of photosynthesis induced by visible light. *Ann. Rev. Plant Physiol.* **35,** 15-44

Prasil, O., Adir, N., and Ohad, I. (1992) *Mechanisms of photoinhibition and recovery processes* in *Topics in Photosynthesis: Dynamics of photosystem II*. Vol. II (Barber, J. ed) pp. 293-348, Elsevier, Amsterdam

Prentki, P. and Krisch, H. M. (1984) In vitro insertional mutagenesis with a selectable DNA fragment. *Gene* **29,** 303–313

Promnares, K., Komenda, J., Bumba, L., Nebesarova, J., Vacha, F., and Tichy, M. (2006) Cyanobacterial small chlorophyll binding protein ScpD (HliB) is located on the periphery of photosystem II in the vicinity of PsbH and CP47 subunits. *J. Biol. Chem.* **281**, 32705-32713

Rakhimberdieva, M. G., Stadnichuk, I. N., Elanskaya, I. V., and Karapetyan, N. V. (2004) Carotenoid-induced quenching of the phycobilisome fluorescence in photosystem II-deficient mutant of *Synechocystis* sp. *FEBS Lett.* **574,** 85–88

Rappsilber, J., Ishihama, Y., and Mann, M. (2003) Stop and go extraction tips for matrix-assisted laser desorption/ionization, nanoelectrospray, and LC/MS sample pretreatment in proteomics. *Anal. Chem.* **75,** 663–670

Reinbothe, C., Bartsch, S., Eggink, L. L., Hoober, J. K., Brusslan, J., Andrade-Paz, R., Monnet, J., and Reinbothe, S. (2006) A role for chlorophyllide *a* oxygenase in the regulated import and stabilization of light-harvesting chlorophyll *a/b* proteins. *Proc. Natl. Acad. Sci. USA* **103,** 4777-4782

Richter, A., Peter, E., Pors, Y., Lorenzen, S., Grimm, B., and Czarnecki, O. (2010) Rapid dark repression of 5-aminolevulinic acid synthesis in green Barley leaves. *Plant Cell Physiol.* **51,** 670-681

Rieble, S. and Beale, S. I. (1991) Purification of glutamyl-tRNA reductase from *Synechocystis* sp. PCC 6803. *J. Biol. Chem.* **266,** 9740-9744

Ried, J. L. and Collmer, A. (1987) An NPTI-SACB-SACR cartridge for constructing directed, unmarked mutations in gram-negative bacteria by marker exchange-eviction mutagenesis. *Gene* **57,** 239–246

Rippka, R., Deruelles, J., Waterbury, J. B., Herdman, M., and Stanier, R. T. (1979) Generic assignments, strain histories and properties of pure cultures of cyanobacteria. *J. Gen. Microbiol.* **111,** 1–61

Saier, M., Beatty, J., Goffeau. A., Harley, K., Heijne, W., Huang, S., Jack, D., Jahn, P., Lew, K., Liu, J., Pao, S., Paulsen, I., Tseng, T., and Virk, P. (1999). The major facilitator superfamily. *J. Mol. Microbiol. Biotechnol.* **1,** 257-279

Sarma, R., Barney, B. M., Hamilton, T. L., Jones, A., Seefeldt, L. C., and Peters, J. W. (2008) Crystal structure of the L protein of *Rhodobacter sphaeroides* light-independent protochlorophyllide reductase with MgADP bound: a homologue of the nitrogenase Fe protein. *Biochemistry* **47,** 13004-13015

Schagger, H., and von Jagow, G. (1991) Blue native electrophoresis for isolation of membrane-protein complexes in enzymatically active form. *Anal. Biochem.* **199,** 223–231

Schuster, G., Timberg, R., and Ohad, I. (1988) Turnover of thylakoid photosystem II proteins during photoinhibition of *Chlamydomonas reinhardtii. Eur. J. Biochem.* **177,** 403-410

Shalygo N., Czarnecki, O., Peter, E., and Grimm, B. (2009) Expression of chlorophyll synthase is also involved in feedback-control of chlorophyll biosynthesis. *Plant Mol. Biol.* **71,** 425-436

Shen, G., Boussiba, S., and Vermaas, W. F. J. (1993) *Synechocystis* sp PCC 6803 strains lacking photosystem I and phycobilisomes function. *Plant Cell* **5,** 1853–1863

Shevchenko, A., Wilm, M., Vorm, O., and Mann, M. (1996) Mass spectrometric sequencing of proteins from silver stained polyacrylamide gels. *Anal. Chem.* **68,** 850–858

Silva, P., Thompson, E., and Bailey, S. (2003) FtsH is involved in the early stages of repair of photosystem II in *Synechocystis* sp. PCC 6803. *Plant Cell* **15,** 2152-2164

Smith, D. and Howe, C. J. (1993) The distribution of photosystem-I and photosystem-II polypeptides between the cytoplasmic and thylakoid membranes of cyanobacteria. *FEMS Microbiol. Lett.* **110,** 341-347

Sobotka, R., Komenda, J., Bumba, L., and Tichy, M. (2005) Photosystem II assembly in CP47 mutant of *Synechocystis* sp PCC 6803 is dependent on the level of chlorophyll precursors regulated by ferrochelatase. *J. Biol. Chem.* **280,** 31595–31602

Sobotka, R., McLean, S., Zuberova, M., Hunter, C. N., and Tichy, M. (2008) The C-terminal extension of ferrochelatase is critical for enzyme activity and for functioning of the tetrapyrrole pathway in *Synechocystis* strain PCC 6803. *J. Bacteriol.* **190,** 2086-2095

Sonoike, K. (2006) *Photoinhibition and protection of photosystem I* in *Advances in Photosynthesis and Respiration: The Light-driven Plastocyanin - Ferredoxin Oxidoreductase*, Vol. 24 (Golbeck, J. ed.) pp. 657-668, Springer, Dordrecht

Srivastava, A. and Beale, S. I. (2005) Glutamyl-tRNA reductase of *Chlorobium vibrioforme* is a dissociable homodimer that contains one tightly bound heme per subunit. *J. Bacteriol.* **187,** 4444-4450

Staehelin, L. A. (1976) Reversible particle movements associated with unstacking and restacking of chloroplast membranes *in vitro*. *J. Cell Biol.* **71,** 136-158

Staehelin, L. A. (2003) Chloroplast structure: from chlorophyll granules to supra-molecular architecture of thylakoid membranes. *Photosynth. Res.* **76,** 185-196

Standfuss, J., Terwisscha van Scheltinga, A. C., Lamborghini, M., and Kuhlbrandt, W. (2005) Mechanisms of photoprotection and nonphotochemical quenching in pea light-harvesting complex at 2.5A resolution. *EMBO J.* **24,** 919–928

Stewart, D. H. and Brudvig, G. W. (1998) Cytochrome *b559* of photosystem II. *Biochim. Biophys. Acta* **1367,** 63-87

Storm, P., Hernandez-Prieto, M., Eggink, L. L., Hoober, J. K., and Funk, C. (2008) The small CAB-like proteins of *Synechocystis* sp. PCC 6803 bind chlorophyll. *Photosynth. Res.* **98,** 479-488

Sullivan, M. B., Coleman, M. L., Weigele, P., Rohwer, F., and Chisholm, S. W. (2005) Three *Prochlorococcus* cyanophage genomes: Signature features and ecological interpretations. *PLoS Biol.* **3,** e144

Tanaka, R. and Tanaka, T. (2007) Tetrapyrrole biosynthesis in higher plants. *Annu. Rev. Plant Biol.* **58,** 321-346

Teramoto, H., Itoh, T., and Ono, T. A. (2004) High-light inducible Lhc-like genes newly identified in *Chamydomonas reinhartii*. *Plant Cell Physiol.* **45,** 1221–1232

Thidholm, E., Lindstrom, V., Tissier, C., Robinson, C., Schroder, W. P., and Funk, C. (2002) Novel approach reveals localisation and assembly pathway of the PsbS and PsbW proteins into the photosystem II dimer. *FEBS Lett.* **513,** 217–222

Towbin, H., Staehelin, T., and Gordon, J. (1979) Electrophoretic transfer of proteins from polyacrylamide gels to nitrocellulose sheets – procedure and some applications. *Proc. Natl. Acad. Sci. U. S. A.* **76,** 4350–4354

Triantaphylides, C. and Havaux, M. (2009) Singlet oxygen in plants: production, detoxification and signaling. *Trends Plant Sci.* **14,** 219-228

Vass, I., Styring, S., Hundal, T., Koivuniemi, A., Aro, E. M., and Andersson, B. (1992) Reversible and irreversible intermediates during photoinhibition of photosystem II: Stable reduced Q_A species promote chlorophyll triplet formation. *Proc. Natl. Acad. Sci. USA* **89,** 1408-1412

Vavilin, D. and Vermaas, W. (2002) Regulation of the tetrapyrrole biosynthetic pathway leading to heme and chlorophyll in plants and cyanobacteria. *Physiol. Plant.* **115,** 9-24

Vavilin, D., Brune, D. C., and Vermaas, W. (2005) ^{15}N labeling to determine chlorophyll synthesis and degradation in *Synechocystis* sp PCC 6803 strains lacking one or both photosystems. *Biochim. Biophys. Acta* **1708,** 91–101

Vavilin, D., Yao, D., and Vermaas, W. (2007) Small Cab-like proteins retard degradtion of photosystem II-associated chlorophyll in *Synechocystis* sp. PCC 6803 – kinetic analysis of pigment labeling with N-15 and C-13. *J. Biol. Chem.* **282**, 37660-37668

Wang, Q., Jantaro, S., Lu, B., Majeed, W., Bailey, M., and He, Q. (2008) The high light-inducible polypeptides stabilize trimeric photosystem I complex under high light conditions in *Synechocystis* PCC 6803. *Plant Physiol.* **147,** 1239-1250

Wilson, A., Ajlani, G., Verbavatz, J. M., Vass, I., Kerfeld, C. A., and Kirilovsky, D. (2006) A soluble carotenoid protein involved in phycobilisome-related energy dissipation in cyanobacteria. *Plant Cell* **18,** 992–1007

Wu, Q. and Vermaas, W. F. J. (1995) Light-dependent chlorophyll *a* biosynthesis upon *chlL* deletion in wild-type and photosystem I-less strains of the cyanobacterium *Synechocystis* sp PCC 6803. *Plant Mol. Biol.* **29,** 933-945

Xu, H., Vavilin, D., Funk, C., and Vermaas, W. (2002) Small Cab-like proteins regulating tetrapyrrole biosynthesis in the cyanobacterium *Synechocystis* sp PCC 6803. *Plant Mol. Biol.* **49,** 149–160

Xu, H., Vavilin, D., Funk, C., and Vermaas, W. (2004) Multiple deletions of small cab-like proteins in the cyanobacterium *Synechocystis* sp PCC 6803 – Consequences for pigment biosynthesis and accumulation. *J. Biol. Chem.* **279,** 27971–27979

Yao, D., Kieselbach, T., Komenda, J., Promnares, K., Prieto, M. A., Tichy, M., Vermaas, W., and Funk, C. (2007) Localization of the small CAB-like proteins in photosystem II. *J. Biol. Chem.* **282**, 267-276

Yeremenko, N., Kouril, R., Ihalainen, S., D'Haene, S., van Oosterwijk, N., Andrizhiyevskaya, E. G. Keegstra, W., Dekker, H. L., Hagemann, M., Boekema, E. J., Matthijs, H. C. P., and Dekker, J. P. (2004) Supramolecular organization and dual function of the IsiA chlorophyll-binding protein in cyanobacteria. *Biochemistry* **43,** 10308-10313

Young, C. S. and Beatty, J. T. (1998) Topological model of the *Rhodobacter capsulatus* light-harvesting complex I assembly protein LhaA. *J. Bacteriol.* **180,** 4742-4745

Young, C. S., Reyes, R. C., and Beatty, J. T. (1998) Genetic complementation and kinetic analyses of *Rhodobacter capsulatus ORF1696* mutants indicate that the ORF1696 protein enhances assembly of the light-harvesting I complex. *J. Bacteriol.* **180,** 1759-1765

Zak, E., Norling, B., Maitra, R., Huang, F., Andersson, B., and Pakrasi, H. B. (2001) The initial steps of biogenesis of cyanobacterial photosystems occur in plasma membranes. *Proc. Natl. Acad. Sci. USA* **98,** 13443-13448

Zhang, L. X., Paakkarinen, V., van Wijk, K. J., and Aro, E. M. (1999) Co-translational assembly of the D1 protein into photosystem II. *J. Biol. Chem.* **274,** 16062-16067

Zhang, L. and Aro, E. M. (2002) Synthesis, membrane insertion and assembly of the chloroplast-encoded D1 protein into photosystem II. *FEBS Lett.* **512,** 13-18

Zouni, A., Witt, H. T., Kern, J., Fromme, P., Krauss, N., Saenger, W., and Orth, P. (2001) Crystal structure of photosystem II from *Synechococcus* elongates at 3.8 angstrom resolution. *Nature* **409,** 739–743